ABSTRACT

Title of Document: MOLECULAR MECHANISMS OF PLANT RESPONSES TO COLD, HEAT AND SALT STRESSES IN *ARABIDOPSIS*

Qingmei Guan, Doctor of Philosophy, 2013

Directed By: Dr. Jianhua Zhu, Assistant Professor, Department of Plant Science and Landscape Architecture

Abiotic stresses, such as temperature extremes and salinity adversely affect plant productivity and distribution worldwide. Resistant or susceptible to stresses is a complex trait because more than one stress may occur simultaneously, for example, salinity is accompanied with ion toxicity and water deficit. To survive in a fixed environment, plants have to adjust their metabolisms and developmental programs to adapt to the stress or acclimate to the transitory stress. The responses of plants to different abiotic stresses are extremely complex, involving stress perception, signaling transduction, and response induction. We took a forward genetic analysis approach and identified three novel proteins in the reference plant *Arabidopsis thaliana*, Regulator of CBF Gene Expression 1 (RCF1), Regulator of CBF Gene Expression 3 (RCF3), and Short Root in Salt Medium 3 (RSA3), which are critical for plant tolerance to cold, heat and salinity, respectively. RCF1 is a cold-inducible DEAD box RNA helicase protein which is localized in the nucleus. RCF1 is a

positive regulator for chilling and freezing tolerance. RCF1 functions to maintain proper splicing of pre-mRNAs because many cold-responsive genes are mis-spliced in *rcf1-1* mutant plants under cold stress. RCF3 encodes a KH-domain containing putative RNA-binding protein. RCF3 is a negative regulator of most heat stress transcription factors (*HSFs*). Consistent with the overall increased accumulation of heat-responsive genes, the *rcf3* mutants are heat-tolerant. RSA3, a xylogluscan galactosyltransferase, is essential for salt stress tolerance. *rsa3-1* mutant plants are hypersensitive to NaCl and LiCl but not to CsCl or to general osmotic stress. RSA3 controls expression of many genes including genes encoding proteins for reactive oxygen species (ROS) detoxification under salt stress. RSA3 functions to maintaining the proper organization of actin microfilaments in order to minimize damage caused by excessive ROS.

miRNAs play important regulatory roles in plants by targeting messenger RNAs (mRNAs) for cleavage or translational repression. We determined role of the heat-inducible *miR398* in plant heat stress tolerance. Our results suggest that plants use a previously unrecognized strategy to achieve thermotolerance, especially for the protection of reproductive tissues. This strategy involves the down-regulation of two copper/zinc superoxide dismutase (*CSDs*) and their copper chaperone *CCS* through the heat-inducible *miR398*.

MOLECULAR MECHANISMS OF PLANT RESPONSES TO COLD, HEAT AND SALT STRESSES IN *ARABIDOPSIS*

By

Qingmei Guan

Dissertation submitted to the Faculty of the Graduate School of the
University of Maryland, College Park, in partial fulfillment
of the requirements for the degree of
Doctor of Philosophy
2013

Advisory Committee:
Professor. Caren Chang
Associate Prof. Gary D. Coleman
Associate Prof. June M. Kwak, Dean's Rep.
Associate Prof. Shunyuan Xiao
Assistant Prof. Jianhua Zhu, Chair

Preface

This dissertation is composed of an overview, four chapters, a conclusion and 19 appendices. Each chapter is structured in manuscript format with an abstract, introduction, results, discussion, and materials and methods. As such, descriptions of some methods are repeated. Ideas and facts presented in introduction sections may be expressed in a similar manner for chapter 2 and chapter 3. Supplemental materials are presented in the corresponding appendices and indicated with syntax for each appendix (i.e. supplemental materials in chapter 1 are designated as Appendix A). A comprehensive bibliography is located at the end of document.

Dedication

This work was dedicated to my parents because of all the great things they have been doing for me; this work was dedicated to my closest friend and husband, Xinke Xue, for his entire understanding, tolerance and support; this work was dedicated to my lovely little girl, Jiner, who is the most important person for me in the world.

Acknowledgements

I would like to thank my supervisor Dr. Jianhua Zhu, for his great and continued support. Without him, this work would never have been done. His thoughtful advice, encouragement, and knowledgeable ideas guided me to be a plant scientist whom I am today. I would also appreciate for his help in improving my writing skills.

I would like to thank my committee members for their great suggestions and encouragement. They always have good ideas and they are a great source for critical thinking.

I am very grateful to Chinese Scholarship Council (CSC) which partially provided my stipend. Without this scholarship, I would not have such a chance to study at UMD.

I want to express my thanks to the following co-authors, Jianmin Wu, Xiaoyan Lu, Changlong Wen, Renyi Liu, Chenglin Chai, Haitao Zeng, Changhua Jiang, Yanyan Zhang, Wenbo Li and Zhenyu Wang for their contribution to this work. I also want to thank my lab mates who helped me: Lixin Li, Ozlem Cekic, Xiule Yue, Xiaohui Hu, Rongrong Wang, and Zhengpei Yao.

I would like to express my special thanks to Dr. Gary Coleman, Dr. Heven Sze, Dr. Anne Simon and Dr. Priscila Chaverri and their lab members as we used their lab equipment.

Table of Contents

List of Figures

List of Abbreviations

RCF1: Regulator of CBF gene expression 1

RSA3: Short root in salt medium 3

RCF3: Regulator of CBF gene expression 3

HSF: Heat stress transcription factor

HSP: Heat shock protein

HS: Heat stress

CBF/DREB: CRT/DRE binding factor

SPFH: SPFH/PHB domain-containing membrane-associated protein

CIR1: MYB family transcription factor circadian 1

PRR5: Pseudo-response Regulator 5

SK12: Shaggy-like serine/threonine kinase 12

ZAT12: Zn transporter of *Arabidopsis thaliana* 12

ROS: Reactive oxygen species

ICE1: Inducer of CBF Expression 1

LOS4: Low expression of osmotically responsive genes 4

SOS: Salt-Overly-Sensitive

CSD: copper-zinc SOD

CCS: copper chaperone of CSD1 and CSD2

MV: methyl viologen

H_2O_2: Hydrogen peroxide

SPL7: SQUAMOSA promoter binding protein–like7

Overview

Abiotic stresses, such as cold, heat, drought, salt, and oxidative stress, are serious threats to agriculture worldwide. Based on a FAO (Food and Agriculture Organization of the United Nations) report in 2007, 96.5% of the global rural land area is affected by environmental stresses. In particular, 26% of the global rural land is affected by temperature stress and 6% is affected by salinity (Cramer et al., 2011). Abiotic stresses adversely affect plant growth and account for 50% of the total crop yield loss in many regions (Bray et al, 2000). Resistant or susceptible to stresses is a complex trait because more than one stress may occur simultaneously. For example, salinity is accompanied with ion toxicity and water deficient, and drought is frequently accompanied with heat stress (Chinnusamy et al., 2003). In consequence, drought, cold, heat and oxidative stress may cause similar cellular damage.

To survive in a fixed environment, plants have to adjust their metabolisms and developmental programs to adapt to the stress or acclimate to the transitory stress. Responses of plants to abiotic stresses are extremely complex, involving stress perception, signal transduction, and response induction. Under salt stress, plants have evolved a Salt-Overly-Sensitive (SOS) pathway to cope with the damage by salinity. In the SOS pathway, a salt-stress induced calcium signal is perceived by a calcium sensor SOS3. SOS3 then activates SOS2, a protein serine/threonine protein kinase. The SOS3-SOS2 protein complex phosphorylates SOS1, a Na+/H+ antiporter in the plasma membrane and thus activates SOS1. The SOS3-SOS2 protein complex also regulates the activity of other ion transporters such as NHX1, a vacuolar Na^+/H^+ exchanger (Chinnusamy et al., 2003). Under cold stress, *CBF* genes serve as major

regulatory hubs and control the expression of other cold-responsive genes including *COR* (*cold- regulated*), *KIN* (*cold- induced*), *LT1* (*low- temperature-induced*), and *RD* (*responsive to dehydration*) genes. The upstream components of *CBF* genes include positive regulators (ICE1 [inducer of CBF expression 1] and CAMTA [Calmodulin-binding transcription activator] and negative regulators (MYB15 [a R2R3 MYB family protein] and ZAT12 [Zn transpoter of *Arabidopsis thaliana* 12]). Genetic analysis reveals that low temperature appears to initiate a cycle of activation and inactivation of ICE1 by SIZ1 (an E3 ligase) mediated sumoylation and HOS1 (a Really Interesting New Gene (RING)-finger protein) mediated ubiquitination and degradation (Thomashow, 1999; Chinnusamy et al., 2006; Chinnusamy et al., 2007; Zhu et al., 2007; Thomashow, 2010). In response to heat stress, plants evolved a signaling pathway with the hub of heat stress transcription factors (HSFs) mediated heat shock proteins (HSPs) synthesis. Plant genome contains multi-member HSFs. *Arabidopsis thaliana* has 21 HSFs while tomato and rice have 18 and 23 HSFs, respectively. The HSFs are divided into three major classes (A, B and C) based on their characteristic structure in the functional domain (Nover et al., 2001; Baniwal et al., 2004). It is clear that the HSFA1 members are master regulators of other HSFs. So far, little is known about the upstream components of HSFs in plants.

Research findings in the last decade showed that microRNAs (miRNAs) play important roles in plant abiotic stress responses (Khraiwesh et al., 2012). Abiotic stress can regulate the levels of miRNAs and their target genes and thus the research about miRNAs can promote understanding the role of miRNAs in stress responses (Sunkar et al., 2007).

Thus far, many components involved in abiotic stresses have been identified although only few of them have been shown to be useful in improving abiotic stress tolerance in crops. The reason behind this is the complexity of the mechanisms of abiotic stress tolerance. Therefore, a combination of forward and reverse genetics to identify more components critical for plant abiotic stress tolerance is essential. We took a forward genetic analysis approach and identified three novel proteins critical for plant tolerance to salt stress and temperature extremes in the reference plant *Arabidopsis thaliana.* These proteins are: RCF1 (Regulator of CBF gene expression 1), RCF3, and RSA3 (Short root in salt medium 3). We also defined the role of a heat-inducible miR398 in plant heat stress tolerance.

Chapter 1: A DEAD Box RNA Helicase Is Critical for Pre-mRNA Splicing, Cold-Responsive Gene Regulation, and Cold Tolerance in *Arabidopsis*

Abstract

Cold stress resulting from chilling and freezing temperatures substantially reduces crop production worldwide. To identify genes critical for cold tolerance in plants, we screened *Arabidopsis* mutants for de-regulated expression of a firefly *luciferase* reporter gene under the control of a cold-inducible *CBF2* (C-repeat binding factor 2) promoter (*CBF2:LUC*). An *rcf1-1* (*regulator of CBF gene expression 1*) mutant that is hypersensitive to cold stress was chosen for in-depth characterization. *RCF1* encodes a cold-inducible DEAD box RNA helicase. Unlike a previously reported DEAD box RNA helicase (LOS4) that controls mRNA export, RCF1 does not play a role in mRNA export. Instead, RCF1 functions to maintain proper splicing of pre-mRNAs because many cold-responsive genes are mis-spliced in *rcf1-1* mutant plants under cold stress. Functional characterization of four genes (*Pseudo-response regulator 5* [*PRR5*], *Shaggy-like serine/threonine kinase* [*AtSK12*], *MYB family transcription factor circadian 1* [*CIR1*], and *SPFH/PHB domain-containing membrane-associated protein* [*SPFH*]) that are mis-spliced in *rcf1-1* revealed that these genes are cold-inducible, positive (*CIR1* and *SPFH*) and negative (*PRR5* and *AtSK12*) regulators of cold-responsive genes and cold tolerance. Together, our results suggest that the cold-inducible RNA helicase RCF1 is essential for pre-mRNA

splicing and is important for cold-responsive gene regulation and cold tolerance in plants.

Keywords: RCF1, RNA helicase, pre-mRNA splicing, cold stress, gene regulation

Introduction

Adaptation is the way of life for sessile and poikilothermic land plants, which must endure environmental stresses including those caused by low/high temperatures, water deficit, and salinity. These abiotic stresses not only limit the geographical distribution of plants but also reduce the global productivity and quality of important agricultural crops. Although plant temperature changes with the ambient temperature, most temperate plants can acquire tolerance to freezing temperatures by a prior exposure to low non-freezing temperatures, a process termed cold acclimation (Guy, 1990; Thomashow, 1999; Ruelland et al., 2009). Freezing tolerance is essential for temperate crops like winter wheat and canola, but tropical and subtropical plants are incapable of cold acclimation. Thus, the productivity and quality of tropical crops (like rice, maize, soybean, cotton, and tomato) are reduced even by non-freezing low temperatures (i.e., chilling). Therefore, the engineering or breeding of chilling- and freezing- tolerant crop plants is an important goal in agriculture. Such engineering or breeding requires a thorough understanding of the molecular mechanisms of the cold stress signal perception and transduction in plant cells that lead to chilling tolerance and/or cold acclimation.

The expression of many genes in plants is regulated by low temperature (Dhindsa and Monroy, 1994; Guy et al., 1994; Palva et al., 1994; Thomashow, 1994). Most of these genes maintain high levels of expression throughout cold treatment but

their expression decreases rapidly upon return from cold to normal growth temperatures (Thomashow, 1994). The cold-responsive genes encode a diverse array of proteins including enzymes involved in respiration and in the metabolism of carbohydrates, lipids, phenylpropanoids and antioxidants; molecular chaperones; anti-freezing proteins; and many other proteins of unknown function (Guy et al., 1994).

Differential screening and cloning studies in plants have identified a core set of robustly cold-regulated genes (Thomashow, 1999). The promoters of many of these genes contain one or several copies of the dehydration-responsive-element *(DRE)/*C-repeat (*CRT) cis*-element, which has the core sequence CCGAC (Yamaguchi-Shinozaki and Shinozaki, 1994; Stockinger et al., 1997). CRT-binding factors (CBFs), also known as DRE-binding proteins (DREBs), are upstream transcription factors in the APETALA2 (AP2)/ETHYLENE RESPONSE FACTOR (ERF) family that bind to the promoter *cis*-element and activate the expression of these cold-responsive genes (Stockinger et al., 1997; Liu et al., 1998). The *CBF* genes themselves are induced by low temperatures, and this induction is transient and precedes that of downstream cold-responsive genes with the *DRE/CRT cis*-element (Medina et al., 1999). Transgenic *Arabidopsis* plants ectopically expressing *CBF3* contain elevated levels of proline and soluble sugars, which correlate with increased freezing tolerance (Gilmour et al., 2000). Inducer of *CBF* Expression 1 (ICE1), a bHLH (basic helix–loop–helix) protein, is an upstream transcription factor that binds to the *CBF3* promoter and is required for activation of *CBF3* expression upon cold stress (Chinnusamy et al., 2003). An R2R3-type MYB transcription factor, AtMYB15, interacts with ICE1 and negatively regulates the expression of *CBF* genes

under cold stress (Agarwal et al., 2006). HOS1, a negative regulator of the *CBF2* and *CBF3* genes, was identified from a genetic screen for mutants with enhanced expression of *CBF* target genes (Ishitani et al., 1998; Lee et al., 2001). *HOS1* encodes a Really Interesting New Gene (RING)-finger protein that has ubiquitin E3 ligase activity (Lee et al., 2001; Dong et al., 2006). Both *in vitro* and *in vivo* ubiquitination assays showed that HOS1 mediates the polyubiquitination of ICE1 under cold (Dong et al., 2006). *Sensitive* to *Freezing 6* (*SFR6*) plays a role in cold acclimation via the CBF pathway after CBF translation (Knight et al., 2009). Recently, Shi et al. (2012) reported that proteins in the ethylene signaling pathway negatively control freezing tolerance by down-regulation of *CBF* and type-A *Arabidopsis response regulators* (*ARR*) genes in *Arabidopsis*.

CBF2 negatively regulates CBF1 and CBF3 (Novillo et al., 2004), and ZAT12 negatively regulates the expression of the *CBF* genes (Vogel et al., 2005). Novillo et al. (2007) reported that CBF1 and CBF3 function additively in cold acclimation and differently from CBF2; CBF2 defines different gene classes in the CBF regulon. Doherty et al. (2009) showed that members of calmodulin-binding proteins of the CAMTA family of transcription factors can bind to one of the *cis*-elements in the *CBF2* promoter *in vitro* and are important for freezing tolerance. Additional molecular factors modulating *CBF2* expression remain to be identified.

To identify additional molecular factors that are critical for cold tolerance and cold-responsive gene regulation, we fused the *CBF2* promoter to a firefly *luciferase* reporter gene (*CBF2:LUC*) and introduced this cold-inducible gene cassette into *Arabidopsis thaliana* plants. Screening of the ethyl methanesulfonate (EMS)-

mutagenized M_2 plants led to the isolation of mutants with altered *CBF* gene expression and/or cold stress tolerance. We designated these mutants as *regulator of CBF gene expression* (*rcf*). We report the in-depth characterization of one such mutant, *rcf1-1*. The *rcf1-1* mutant plants are hypersensitive to chilling and freezing temperatures. Map-based cloning revealed that *RCF1* encodes a cold-inducible DEAD box RNA helicase. Unlike a previously reported DEAD box RNA helicase (LOS4) that controls mRNA export, RCF1 maintains proper splicing of pre-mRNAs of nuclear-encoded genes. Loss-of-function and gain-of-function characterization of four genes that are mis-spliced in *rcf1-1* under cold stress revealed that they are important regulators of cold-responsive genes and cold tolerance. Together, our results indicate that a cold-inducible nuclear-localized RNA helicase RCF1 is critical for pre-mRNA splicing and for cold-responsive gene regulation and cold tolerance in plants.

Results

Isolation of the *rcf1-1* Mutant

To identify novel molecular factors that control expression of cold-responsive transcription factors and that have an essential role in cold tolerance, we generated transgenic *Arabidopsis* plants that express a firefly *luciferase* reporter gene under the control of the cold-responsive *CBF2* promoter (*CBF2:LUC*, referred to as wild type) and subsequently screened the EMS-mutagenized M_2 population for mutants with de-regulated *CBF2:LUC* expression. We designated these mutants as *regulator of CBF gene expression* (*rcf*). The *rcf1-1* mutant was chosen for in-depth characterization. Compared to wild-type plants, *rcf1-1* plants have a much higher level of *CBF2:LUC*

expression under cold stress (Figure1-1), suggesting that RCF1 might be a negative regulator of *CBF2* gene expression.

We backcrossed *rcf1-1* with the wild type. All F_1 plants showed a wild-type phenotype in response to cold stress, and F_2 plants segregated at approximately 3:1 (wild type vs. *rcf1-1*). These results suggested that *rcf1-1* is a recessive mutation in a single nuclear gene.

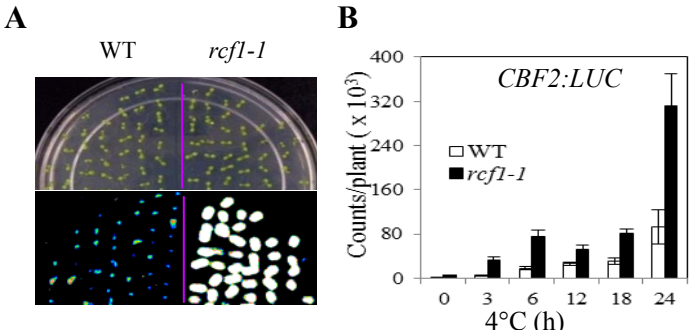

Figure 1-1. *LUC* Expression in *rcf1-1* Under Cold Stress. (A) *CBF2:LUC* expression in 7-d-old wild-type (WT) and *rcf1-1* seedlings treated at 4°C for 24 h. (B) Quantification of luminescence intensity in (A). *CBF2:LUC* expression was quantitatively measured as luminescence intensity (counts/plant). Data are also included for non-stressed and cold-treated seedlings at different time points. Error bars represent the standard deviation (n = 20-40).

RCF1 Is Required for Plant Tolerance to Chilling and Freezing Stresses

We investigated the effect of the *rcf1-1* mutation on plant sensitivity to chilling and freezing stresses. Chilling tolerance was assessed based on hypocotyl elongation in the dark. As shown in Figure 1-2, hypocotyl elongation was similar for *rcf1-1* and the wild type at 21°C but was dramatically less for *rcf1-1* than for the wild type at 4°C, indicating that normal function of RCF1 is required for chilling stress tolerance. We subsequently determined the freezing tolerance of *rcf1-1* by two methods: an electrolyte leakage assay (Sukumaran and Weiser, 1972; Ishitani et al., 1998) and a

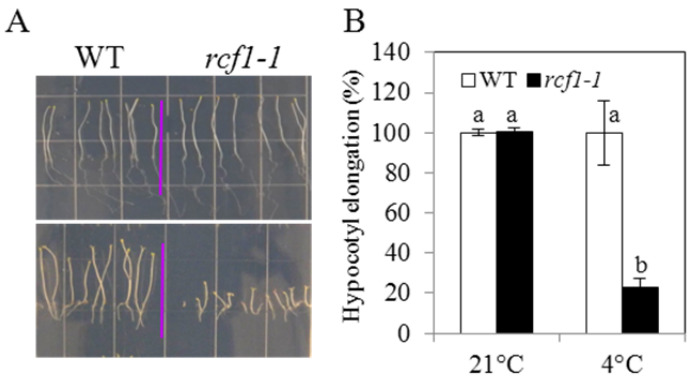

Figure 1-2. Chilling Sensitivity of Wild Type and *rcf1-1* at 4°C in Darkness. (A) Top panel, 21°C for 15 d; bottom panel, 4°C for 52 d. (B) Quantification of hypocotyl elongation of plants shown in (A). Error bars represent the standard deviation (n = 60-100). One-way ANOVA (Tukey-Kramer test) was performed and statistically significant differences are indicated by different lowercase letters (p <0.003).

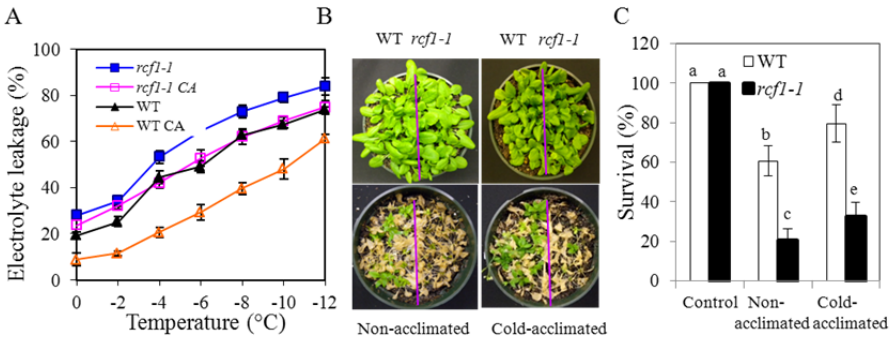

Figure 1-3. Freezing Tolerance of Wild type and *rcf1-1* Mutant Plants. (A) Leakage of electrolytes from excised leaflets of *rcf1-1* and wild-type plants when treated at temperatures below freezing. *rcf1-1* CA, cold-acclimated *rcf1-1* plants. WT CA, cold-acclimated wild-type plants. (B) Whole-plant freezing tolerance of the wild type and *rcf1-1*. Plants were photographed 10 d after freezing treatments. (C) Survival rates of *rcf1-1* and the wild type in (B). Error bars represent the standard deviation (n = 8-16 in [A], and 100–140 in [C]). One-way ANOVA (Tukey-Kramer test) was performed and statistically significant differences are indicated by different lowercase letters (p <0.003).

whole-plant freezing assay (Warren et al., 1996; Xin and Browse, 1998; Jaglo-Ottosen et al., 1998; Zhu et al., 2008). The *rcf1-1* plants were hypersensitive to freezing temperatures before and after cold acclimation (Figure 1-3), indicating that the ability to be fully acclimated is substantially reduced in *rcf1-1*. Together, these results suggest that RCF1 is a positive regulator of chilling and freezing tolerance in plants.

RCF1 Controls Gene Expression under Cold Stress

To gain insight into the molecular function of RCF1 in the cold stress-tolerance pathway, we examined its role in gene regulation with real-time RT-PCR (qRT-PCR) analysis and whole-genome microarray analysis. Consistent with the increased *CBF2:LUC* expression in *rcf1-1*, qRT-PCR analysis revealed that transcripts of *luciferase* and endogenous *CBF2* were more abundant in *rcf1-1* at all time points after cold treatment (Figure 1-4A and B). We then determined whether the *rcf1-1* mutation affects other members in the *CBF* gene family. Expression of *CBF1* and *CBF3* was dramatically elevated in *rcf1-1* compared to the wild type throughout cold treatment (Figure 1-4C). CBF members are known to control the expression of downstream genes that have the DRE/C-repeat *cis* element in their promoters. Therefore, we examined whether *rcf1-1* affects the expression of known *CBF* downstream genes such as *RD29A* and *COR15A*. Cold induction of *RD29A* and *COR15A* was substantially greater in *rcf1-1* than in wild-type plants (Figure 1-4D). These results, which sharply contrast with the reduced cold tolerance of the *rcf1-1* mutant (Figure 1-2 and 1-3), indicate that RCF1 is a negative regulator for expression of *CBF* genes and their downstream target genes under cold stress. These results also

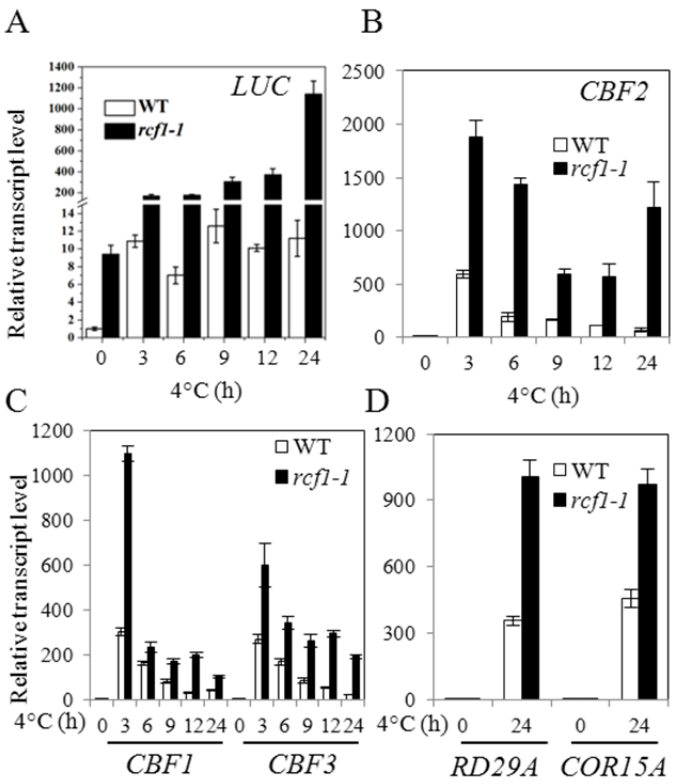

Figure 1-4. The *rcf1-1* Mutation Causes Higher Induction of the *LUC* Gene and Endogenous Cold-Responsive Genes under Cold Stress. (A)–(D) Transcript levels of *luciferase* gene (*LUC*), and of endogenous *CBF2*, *CBF1*, *CBF3*, *RD29A*, and *COR15A* in 14-d-old wild-type and *rcf1-1* seedlings treated at 4°C for the indicated time points. Error bars represent the standard deviation (n = 4).

suggest that CBF-independent factors may not function properly in the *rcf1-1* mutant plants. Alternatively, increased expression of *CBF* genes in *rcf1-1* may be a compensatory response to the severely reduced cold tolerance of *rcf1-1*.

To detect changes in global gene expression in the *rcf1-1* mutant plants, we performed a whole-genome microarray analysis with Affymetrix *Arabidopsis* ATH1 GeneChips. RNA was extracted from both wild-type and *rcf1-1* seedlings that had been treated at 4°C for 0, 12, or 24 h. Analyses of the ATH1 microarray data indicated that, compared to their expression in wild-type seedlings, 35 genes were up-regulated by at least 3-fold and five genes were down-regulated by at least 3-fold in the *rcf1-1* mutant under control conditions (Appendix A1). Among the 35 up-regulated genes in *rcf1-1*, most encode proteins that are predicted to function in response to stress (Appendix A1A). The ATH1 microarray data also showed that after a 12-h cold treatment and compared to the wild type, *rcf1-1* contains 49 genes whose expression is significantly increased by at least 3-fold and 32 genes whose expression is significantly reduced by at least 3-fold (Appendix A2). After a 24-h cold treatment and compared to the wild type, expression in *rcf1-1* was increased by at least 3-fold for 95 genes and decreased by at least 3-fold for 73 genes (Appendix A3). Compared to their expression in the wild type, the expression of five genes was significantly increased in *rcf1-1* by at least 3-fold at all time points after cold treatment while expression of one gene was significantly reduced in *rcf1-1* by at least 3-fold at all time points after cold treatment (Appendix A4A and A4B). Microarray data analysis also revealed that transcripts of 20 genes were significantly increased in *rcf1-1* by at least 3-fold after 12-h and 24-h cold treatment while transcripts of six genes were

dramatically reduced in *rcf1-1* by at least 3-fold after 12-h and 24-h cold treatment (Appendix A4C and A4D). Although the genes in *rcf1-1* that are differentially expressed in response to cold stress encode proteins involved in diverse biological processes, a relatively large proportion of the up-regulated genes and some of the down-regulated genes encode proteins that are predicted to function in biotic or abiotic stress-response pathways (Appendix A2 – A4). Relative to publically available data concerning gene expression in response to cold stress in wild-type plants, gene expression substantially differs in *rcf1-1* (Appendix A5 – A9).

In our ATH1 microarray analysis, transcripts of *CBF1*, *CBF2*, and *CBF3* were significantly increased in *rcf1-1* after 12 h or 24 h of cold stress, suggesting that our microarray data are reliable. Our microarray analysis was confirmed by qRT-PCR analysis of seven genes that showed altered expression patterns in *rcf1-1* (Figure 1-4D and Figure 1-5). For example, both microarray analysis and qRT-PCR indicated that *ZAT12* in *rcf1-1* is up-regulated after 12 h and 24 h of cold treatment (Figure 1-5A). Similarly, the detection of up-regulation and down-regulation was consistent for ATH1 microarray analysis and qRT-PCR for *At5g59950*, *Stabilized 1*, and *At2g42270*, which encode an RNA-binding protein, a pre-mRNA splicing factor (STA1) (Lee et al., 2006), and a U5 small nuclear ribonucleoprotein helicase (Brr2b), respectively (Figure 1-5B and C). Both ATH1 microarray and qRT-PCR analyses also indicated that one of the upstream transcriptional activators of *CBF2*, the CAMTA family protein *CAMTA1*, is down-regulated in *rcf1-1* (Appendix A2B and Figure 1-5D). These results suggest that elevated-accumulation of the *CBF2* gene in *rcf1-1* is not due to the increased activity of *CAMTA1*. Together, these data indicate

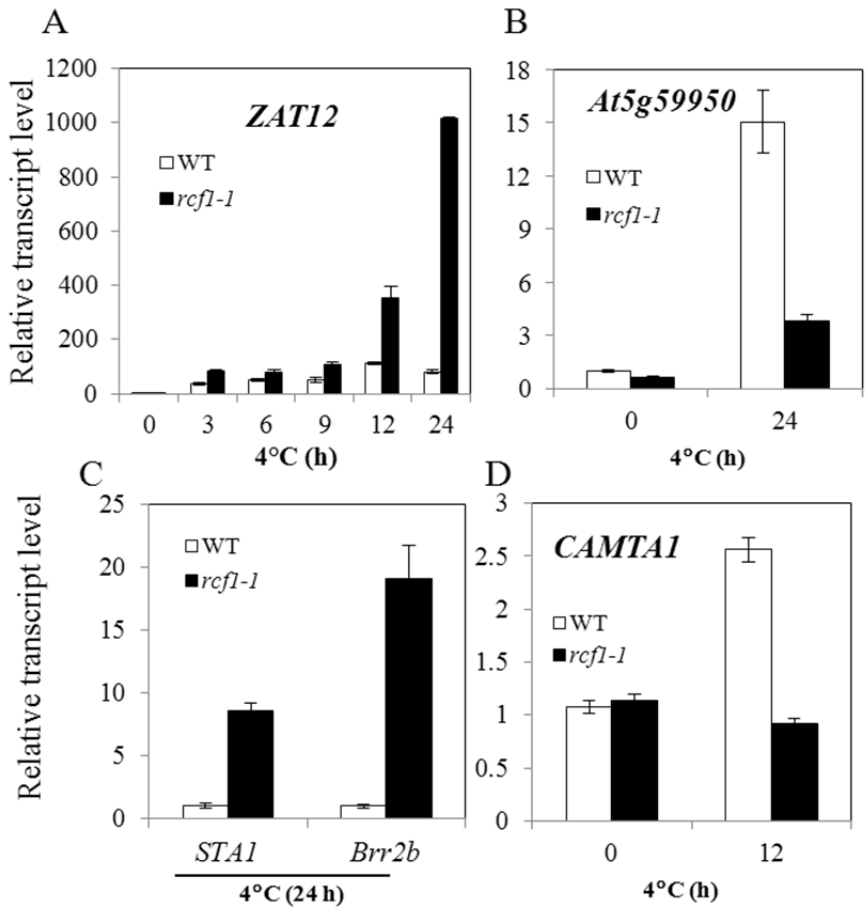

Figure 1-5. Validation of the Microarray Data by qRT-PCR Analysis. *At5g59950* encodes an RNA-binding (RRM/RBD/RNP) family protein. Error bars represent the standard deviation (n = 4). WT, wild type.

that RCF1 plays an important role in gene regulation under both normal and cold stress conditions.

RCF1 Encodes a Cold-Inducible DEAD Box RNA Helicase

The *rcf1-1* phenotypes indicate that RCF1 has an essential role in chilling and freezing tolerance and in the regulation of cold-responsive gene expression. We used a map-based cloning strategy to identify the *RCF1* gene (Figure 1-6). A segregating F_2 population was generated from a cross between *rcf1-1* (in the Columbia background) and the wild type Landsberg *erecta*. A total of 1414 homozygous *rcf1-1* mutant plants were selected from the F_2 population, and genomic DNA was extracted from each plant for genetic mapping. The *RCF1* locus is in the lower arm of chromosome 1 between bacterial artificial chromosomes (BACs) T20H2 and T22I11. The *RCF1* locus was narrowed to BAC clone F9H16, and the candidate genes were sequenced. A single-nucleotide mutation from G to A at position 2650 from the transcription start site was found in *At1g20920* of the *rcf1-1* mutant. This mutation would change the amino acid Gly to Arg at position 808 of the decoded At1g20920 polypeptide. The *At1g20920* gene encodes a putative DEAD box RNA helicase. We confirmed the identity of *RCF1* with a gene complementation test using the wild-type *RCF1* gene, including its own promoter and coding sequences (Figure 1-7A). We made an RCF1-GFP fusion protein in transgenic tobacco and *Arabidopsis* plants to determine the RCF1 subcellular localization, and confocal microscopy indicated that RCF1 is predominantly localized in the nucleus (Figure 1-7B and C). The RCF1-GFP fusion protein is able to fully restore the *rcf1-1* mutant phenotype (Figure 1-7D), indicating that the RCF1-GFP fusion protein is functional *in planta*. The expression

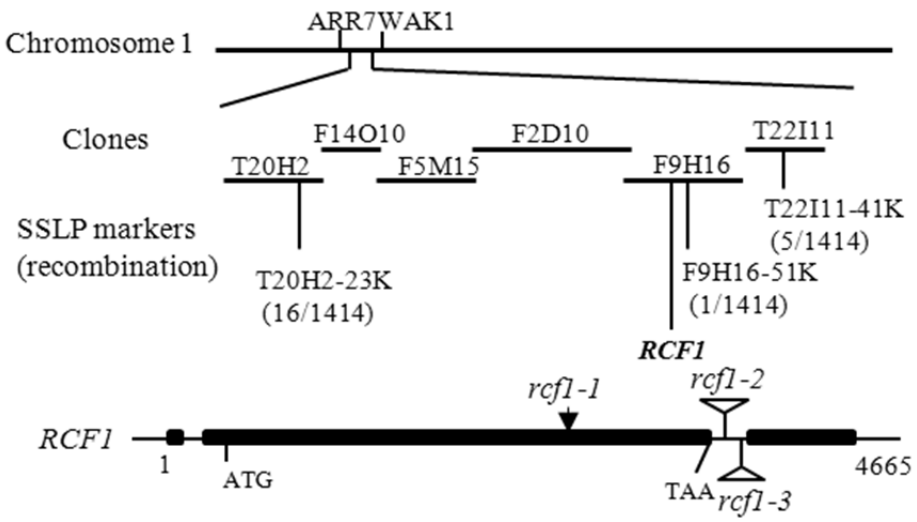

Figure 1-6. Positional Cloning of *RCF1*. Numbers of recombination are from 1414 F_2 progeny seedlings that are homozygous for *rcf1-1* phenotypes. The *rcf1-1* mutation is caused by a single-nucleotide substitution (from G to A at position 2650, relative to transcription start site), and this mutation changes amino acid Gly808 to Arg. Structure of the *RCF1* gene and positions of *rcf1-1*, *rcf1-2*, and *rcf1-3* mutations are indicated. Filled boxes indicate exons, and lines between boxes indicate introns.

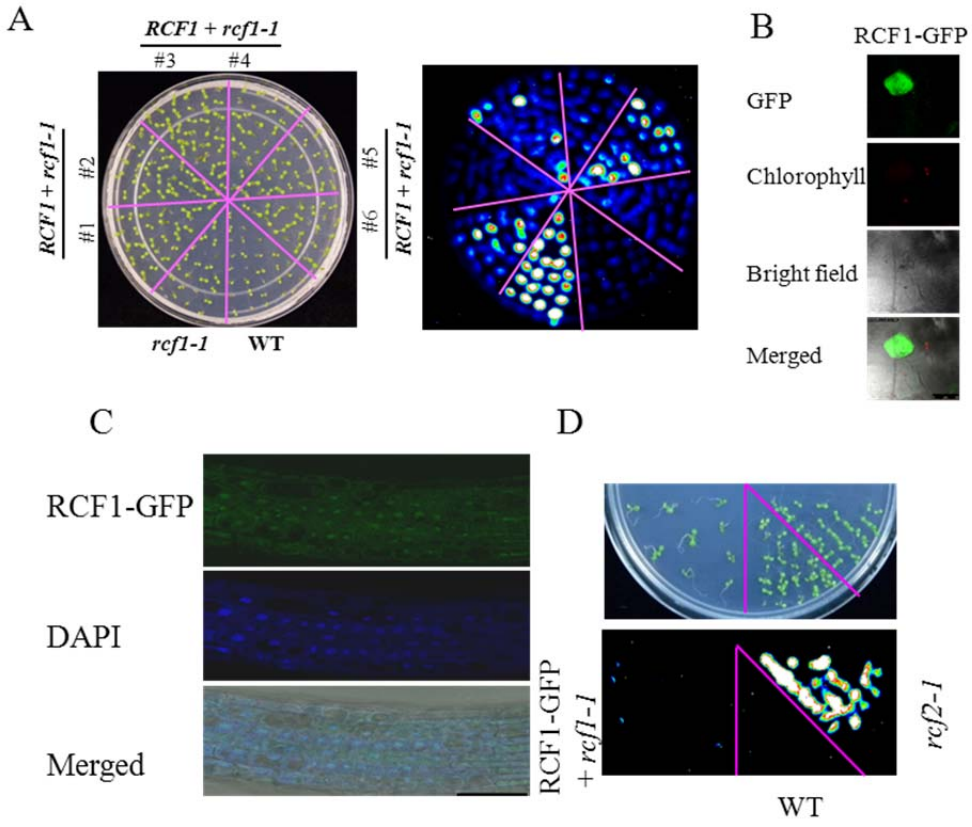

Figure 1-7.Complementation Test of *rcf1-1* and Localization of RCF1. (A) Molecular complementation of the *rcf1-1* mutant by the wild-type *RCF1* gene. Shown are seedlings on an MS agar plate (left) and the corresponding luminescence image after 4°C treatment for 24 h (right). (B) RCF1-GFP is localized in the nucleus of tobacco leaf epidermal cells. Bars = 25 µm. (C) Confocal image of *Arabidopsis* root cells expressing the RCF1-GFP fusion protein. Cells were stained with DAPI to indicate the nuclei. Bars = 25 µm. (D) Complementation of *rcf1-1*with the RCF1-GFP gene. Shown are seedlings on an MS agar plate (top) and the corresponding luminescence image after 4°C treatment for 24 h (bottom).

of *RCF1* appears to be up-regulated by cold stress and reaches its peak level after 12 h of cold treatment (Figure 1-8A). qRT-PCR analysis indicated that *rcf1-2* and *rcf1-3* are null alleles of *RCF1* and that the *rcf1-2* and *rcf1-3* mutations have the same effect as the *rcf1-1* mutation on the expression of *CBF* genes (Figure 1-8B and C).

RNA helicases are a class of enzymes that use energy derived from the hydrolysis of ATP to unwind double-stranded RNAs (de la Cruz et al., 1999). We produced recombinant RCF1 protein and tested its RNA helicase activity by measuring its ATPase activity. RCF1 indeed exhibits RNA-dependent ATPase activity (Figure 1-9A and B). When the DEAD box domain (core amino acid sequence Asp-Glu-Ala-Asp (D-E-A-D)) is altered to DAAD, the RCF1 ATPase activity is abolished (Figure 1-9B). We also found that *RCF1* carrying this DAAD mutation under the control of the *RCF1* native promoter failed to complement the *rcf1-1* mutant (Figure 1-9C), indicating that the DEAD box domain of RCF1 is critical for its function *in planta*.

RCF1 Is Not Involved in mRNA Export

The DEAD box RNA helicase LOS4 was previously identified through a genetic screen of de-regulated expression of *RD29A:LUC* (Gong et al., 2005). LOS4 is localized in the cytoplasm in a nuclear rim-enriched pattern and is important for mRNA export at cold temperature (Gong et al., 2005). We used the poly(A) *in situ* hybridization assay to determine whether RCF1 is also involved in mRNA export. As shown in Figure 1-9D, the different responses of *los4-1* vs. C24 (background of *los4-1*) to the presence and absence of cold stress suggest that our experimental conditions were similar to those reported by Gong et al. (2005), but differences were not

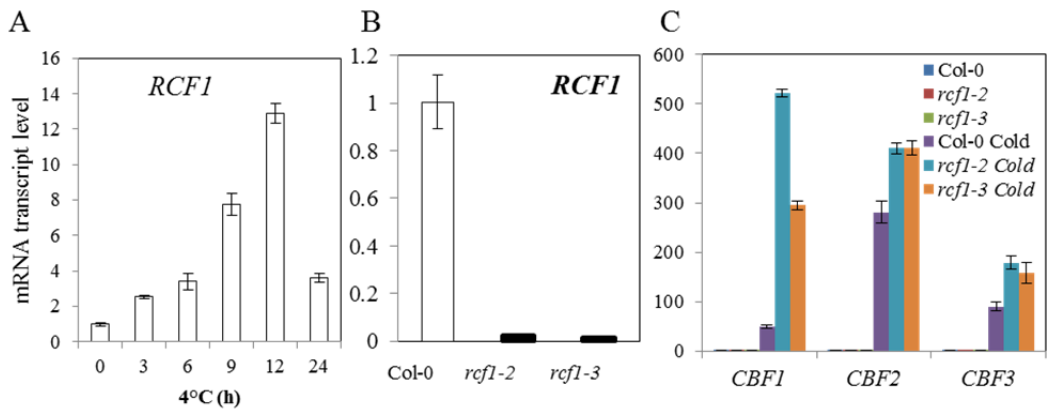

Figure 1-8. *RCF1* Is Cold-Inducible and Expression of *CBF* Genes Is Elevated in *rcf1-2* and *rcf1-3* Mutant Plants. (A) Time-course expression of *RCF1* in 14-d-old wild-type seedlings. (B) Expression of *RCF1* in *rcf1-2 and rcf1-3* plants determined by qRT-PCR analysis. (C) Transcript levels of *CBF1*, *CBF2*, and *CBF3* in Col-0, *rcf1-2*, and *rcf1-3* seedlings subjected to 0 or 12 h at 4°C. Error bars in (D) and (E) indicate the standard deviation (n = 4).)

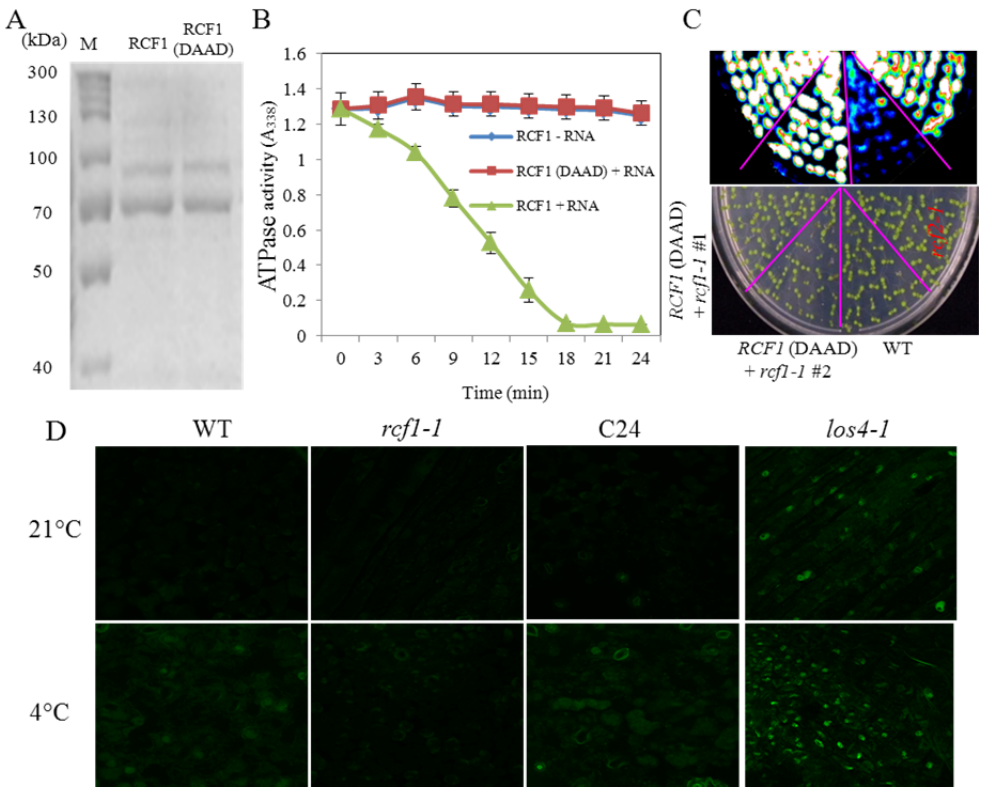

Figure 1-9. RCF1 Is an RNA-Dependent RNA Helicase That Is Not Involved in mRNA Export.

(A) Recombinant GST-RCF1 and GST-RCF1 (DAAD) proteins purified by column affinity chromatography, separated by SDS-PAGE, and stained by coomassie blue. M, protein ladder. (B) ATPase activity of RCF1 and mutant RCF1(DAAD). ATPase activity was measured spectrophotometrically in the presence or absence of plant total RNA. Error bars represent the standard deviation (n = 4). (C) RCF1 (DAAD) driven by the RCF1 native promoter is unable to complement the *rcf1-1* phenotype. Shown in (C) is *CBF2:LUC* expression in 7-d-old seedlings subjected to 4°C for 24 h. (D) poly(A) *in situ* hybridization assays of 2-week-old seedlings subjected to 0 or 24 h 4°C treatment to test the potential role of RCF1 in mRNA export. WT, wild type.

detected in the responses of the wild type vs. *rcf1-1*. These data indicate that RCF1 is not involved in mRNA export.

RCF1 Is Required for Proper Splicing of Pre-mRNAs for Cold-Responsive Genes Including Positive and Negative Regulators of *CBF*s and for Cold Tolerance

Database searches revealed that *RCF1* co-expresses with a pre-mRNA splicing factor, *STA1*, and a U5 small nucleoprotein helicase, *Brr2b*. We isolated a knockdown mutant of *Brr2b* (Figure 1-10A). We found that, like RCF1, STA1 and Brr2b also negatively regulate the expression of *CBF2* (Figure 1-10B). Double mutants of *rcf1-1 sta1-2* and *rcf1-1 brr2b* did not show any additive effect on *CBF2* expression (Figure 1-10B), suggesting that RCF1, STA1, and Brr2b function in a common pathway to control *CBF2* gene expression. We observed that *Brr2b* is cold-inducible (Figure 1-10C). Plants of *sta1* and *brr2b* mutants were hypersensitive to chilling stress as indicated by reduced hypocotyl growth (Figure 1-10D-G; Lee et al., 2006). Both *sta1-2* and *brr2b* mutant plants were more sensitive to freezing stress than wild-type plants before and after cold acclimation as determined by an electrolyte leakage assay that indicated increased damage in the membranes of the mutant plants (Figure 1-10H). Together, these data suggest that, like RCF1, STA1 and Brr2b are positive regulators of cold tolerance.

Because database searches suggested that RCF1, STA1, and Brr2b are part of a splicesome containing more than 100 proteins (The *Arabidopsis* Initiative Resources) and because STA1 is involved in pre-mRNA splicing (Lee et al., 2006), we determined the potential role of RCF1 in pre-mRNA splicing. To identify

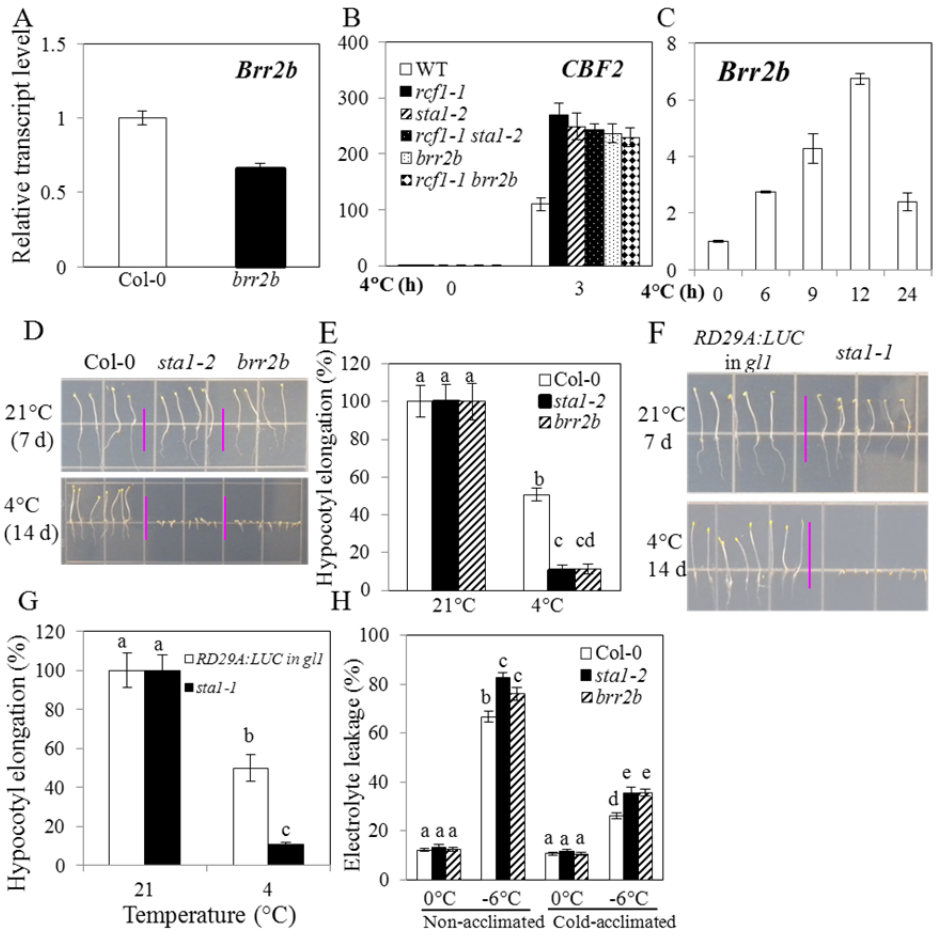

Figure 1-10. STA1 and Brr2b Negatively Control *CBF2* Expression and Are Positive Regulators of Cold Tolerance. (A) *Brr2b* expression in the Col-0 and *brr2b* (knockdown mutant of *Brr2b*) plants. (B) *CBF2* expression in *rcf1-1*, *rcf1-1 sta1-2*, and *rcf1-1 brr2b*. RNA was extracted from 14-d-old seedlings treated with 4°C for 0 or 3 h. WT, wild type. (C) *Brr2b* expression in the wild type at the indicated time. (D) Chilling tolerance of *sta1-2* and *brr2b* plants. (E) Quantification of hypocotyl elongation of plants shown in (D). (F) Chilling tolerance of *sta1-1* mutant plants. (G) Quantification of hypocotyl elongation of plants shown in (F). (H) Freezing tolerance of *sta1-2* and *brr2b* plants. Error bars represent the standard deviation (n = 4 in [A]-[C]; n = 30-50 in [E]; n = 30-40 in [G]; n = 12-20 in [H]). WT, wild type. One-way ANOVA (Tukey-Kramer test) was performed in (E), (G) and (H) to display statistically significant differences indicated by different lowercase letters ($p < 0.01$).

candidate genes whose splicing events may be affected by the *rcf1-1* mutation, we performed full-genome tiling arrays with Affymetrix *Arabidopsis* tiling array GeneChips (1.0R) with wild-type and *rcf1-1* plants that had been treated at 4°C for 0 or 12 h. Statistical analysis of the 1.0R tiling array data detected intron retention events (false discovery rate < 0.05) for 204 unique genes in the *rcf1-1* mutant plants subjected to cold treatment for 12 h, which is when *RCF1* reaches its peak expression level (Appendix A10A). These mis-spliced genes in *rcf1-1* encode proteins with diverse functions in many biological processes, and the predicted roles of more than one-third (77 of 204) of these genes involve responses to abiotic or biotic stresses (Appendix A10A). We designed primers and probes unique to the introns of genes that are retained in the *rcf1-1* mutant, and we carried out semi-quantitative RT-PCR and Northern hybridization analyses to validate the 1.0R tiling array data. Six genes that displayed mis-spliced transcripts in *rcf1-1* as revealed in the 1.0R tiling array experiments with cold-treated plants were selected for validation: *At5g37260*, *At5g54100, At5g24470*, *At3g05840*, *At5g25350*, and *At1g27910*. These genes encode MYB family transcription factor circadian 1 (CIR1), SPFH/PHB domain-containing membrane-associated protein (SPFH), pseudo-response regulator 5 (PRR5), a Shaggy-like serine/threonine kinase (AtSK12), EIN3-binding F box protein 2 (EBF2), and plant U-box 45 (PUB45), respectively. Transcripts of the six genes were found to contain at least one intron in the *rcf1-1* mutant under cold (Figure 1-11A-C). The retained introns were not detected in *rcf1-1* plants without cold treatment (Figure 1-11B-D). The *sta1-2* and *brr2b* mutations do not seem to suppress the mis-splicing

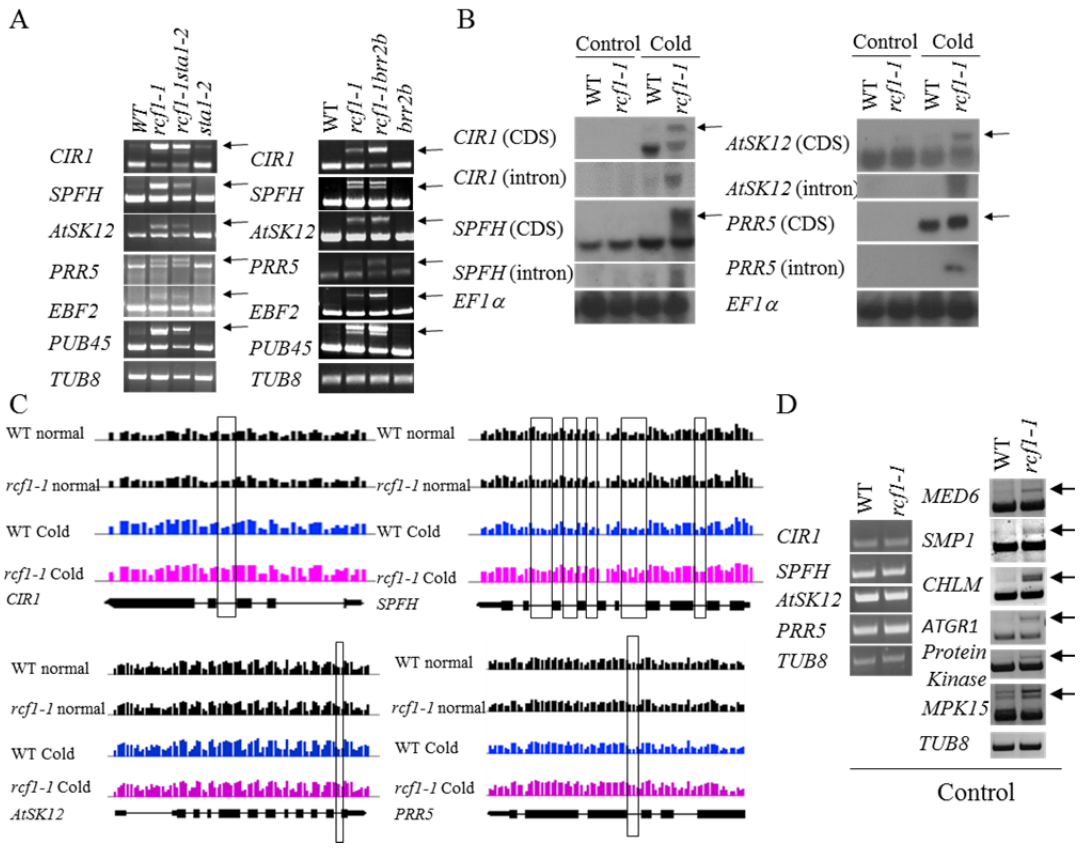

Figure 1-11. RCF1 Functions in Pre-mRNA Splicing under Cold. (A) Mis-spliced transcripts of *CIR1*, *SPFH*, *AtSK12*, *PRR5*, *EBF2*, *and PUB45* in *rcf1-1*, *rcf1-1sta1-2*, and *rcf1-1brr2b* but not in *sta1-2* or *brr2b* under cold stress (4°C for 12 h) as determined by semi-quantitative RT-PCR analysis. (B) Northern hybridization analysis of *CIR1*, *SPFH*, *AtSK12*, and *PRR5* genes in *rcf1-1*. Membranes were also hybridized with introns specific to *CIR1*, *SPFH*, *AtSK12*, and *PRR5*. (C) Visualization of intron retention of *CIR1*, *SPFH*, *AtSK12*, *PRR5*, *EBF2* and *PUB45* in *rcf1-1* with the integrated genome browser. Vertical bars represent averaged log2 expression values of unique probes in the gene region; introns that were retained in *rcf1-1* under cold treatment are indicated with black boxes; gene structures on the bottom of each panel are based on TAIR10 annotation. (D) Transcripts of genes tested in (A) and *MED6* (*At3g21350*), SMP1 (*At1g65660*), *CHLM* (*At4g25080*), *ATGR1* (*At3g52115*), *protein kinase* (*At1g21590*), and *MPK15* (*At1g73670*) under unstressed condition. WT, wild type. *TUB8* and *EF1α* were used as loading controls. Arrows indicate intron-retained transcripts.

effect of *rcf1-1* on these six loci (Figure 1-11A), suggesting that RCF1 may function in a different pathway than STA1 and Brr2b for pre-mRNA splicing under cold stress.

Statistical analysis of the 1.0R tiling array data generated with RNA samples extracted from wild-type and *rcf1-1* plants grown under normal conditions did not detect any genes with significant intron retention events (false discovery rate < 0.05) in *rcf1-1* (GEO accession number GSE41377). Although the 1.0R tiling array data produced from the unstressed wild-type and *rcf1-1* plants did not pass the thresholds in our statistical analysis, we were able to confirm the intron retention events through semi-quantitative RT-PCR analysis for the following six genes: *At3g21350*, *At1g65660*, *At4g25080*, *At3g52115*, *At1g21590*, and *At1g73670*. *At3g21350* encodes mediator 6 (MED6), which is an important component of the mediator complex in the regulation of RNA polymerase II transcription activity. *At1g65660* encodes SWELLMAP 1 (SMP1), which is a CCHC zinc finger protein that may function as a step II splicing factor. *At4g25080* encodes a protein with methyltransferase activity responsible for the methylation of magnesium protoporphyrin IX (CHLM). *At3g52115* encodes GAMMA RESPONSE GENE 1 (ATGR1), which is induced in response to ionizing radiation and may be involved in DNA damage-induced growth arrest. *At1g21590* encodes a protein kinase with an adenine nucleotide alpha hydrolases-like domain. *At1g73670* encodes MAP kinase 15 (MPK15) (Appendix A10B; Figure 1-11D; Figure 1-12). These encoded proteins have diverse functions in cellular processes including signal transduction (MPK15), gene regulation (SMP1 and MED6), and stress responses (ATGR1 and At1g21590) (Appendix A10B).

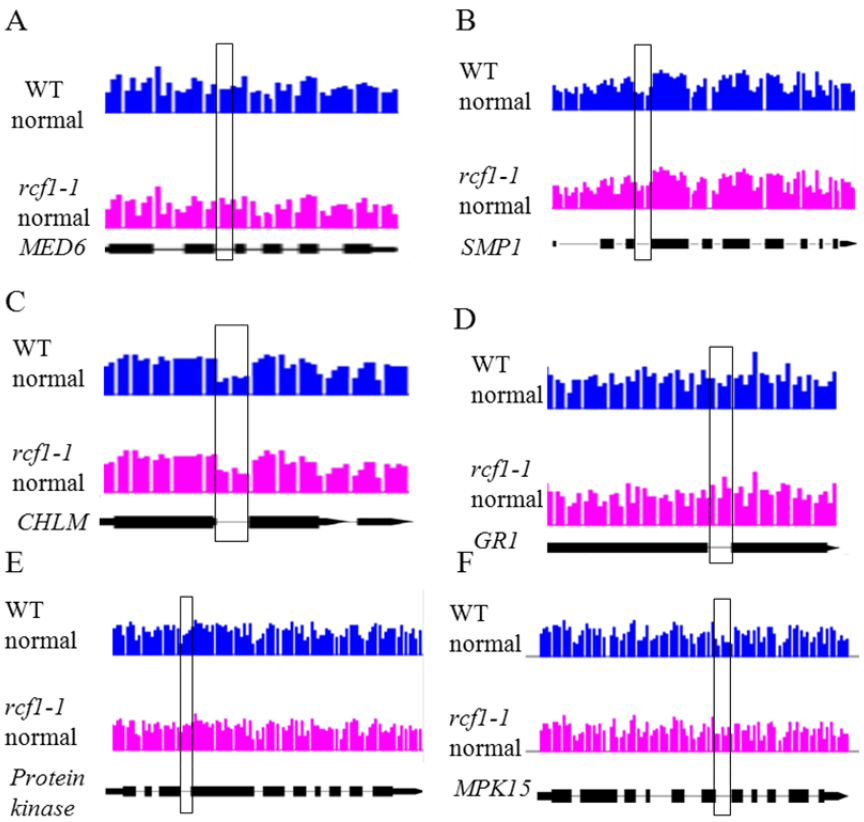

Figure 1-12. Visualization of Intron Retention of *MED6* (*At3g21350*), *SMP1* (*At1g65660*), *CHLM* (*At4g25080*), *GR1* (*At3g52115*), *Protein Kinase* (*At1g21590*), and *MPK15* (*At1g73670*) under Unstressed Condition in *rcf1-1* with the Integrated Genome Browser. Vertical bars represent averaged log2 expression values of unique probes in the gene region; introns that were retained in *rcf1-1* under normal condition were indicated with black boxes; gene structures on the bottom of each panel are based on TAIR10 annotation.

Searches of the publically available microarray databases revealed that many of the mis-spliced genes in *rcf1-1* under cold stress are cold-responsive in wild-type plants, suggesting that they play a role in the cold stress-tolerance pathway (Appendix A11). Indeed, *CIR1, SPFH*, *AtSK12*, and *PRR5* are cold-inducible (Figure 1-13A). To investigate possible functions of these four genes in cold stress responses, we isolated their T-DNA knockouts (Figure 1-14A-D). As shown in Figure 1-13B–D, expression of *CBFs* and *RD29A* is substantially reduced in *cir1* and *spfh* plants under cold stress, and these mutant plants are hypersensitive to freezing stress before and after cold acclimation. Furthermore, transgenic plants that overexpress *CIR1* (*CIR1 OE*) and *SPFH* (*SPFH OE*) display increased expression of *CBF* genes and increased tolerance to freezing stress before and after cold acclimation (Figure 1-13E and F; Figure 1-14E). These results indicate that CIR1 and SPFH are positive regulators for cold-responsive gene expression and cold tolerance. In contrast, *atsk12* and *prr5* plants displayed elevated expression of *CBFs* and *RD29A* under cold and increased tolerance to freezing temperatures (Figure 1-13B-D). In addition, transgenic plants that overexpress *AtSK12* (*AtSK12 OE*) and *PRR5* (*PRR5 OE*) showed reduced expression of *CBF* genes and decreased tolerance to freezing stress (Figure 1-13E and F; Figure 1-14F). These results suggest that *AtSK12* and *PRR5* are negative regulators of cold-responsive gene expression and cold tolerance.

Overexpression of *RCF1* in *Arabidopsis* Increases Tolerance to Chilling and Freezing Stresses

Because RCF1 is required for cold stress tolerance and is important for cold-responsive gene regulation, we investigated whether over-production of RCF1 would

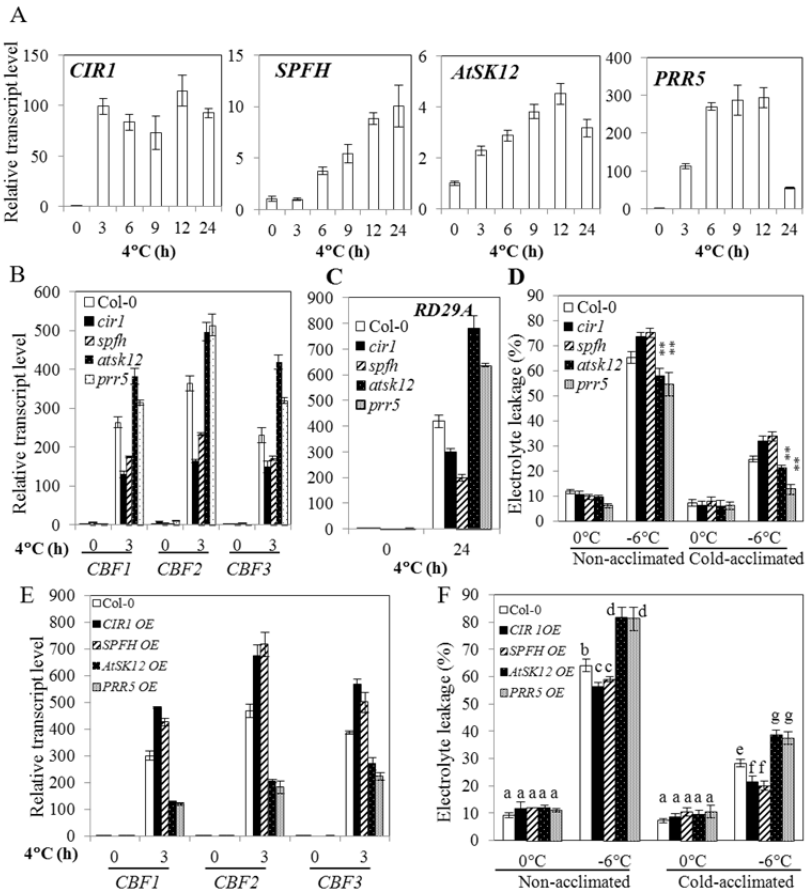

Figure 1-13. *CIR1*, *SPFH*, *AtSK12*, and *PRR5* Regulate Expression of *CBF* Genes and Cold Tolerance. (A) *CIR1*, *SPFH*, *AtSK12*, and *PRR5* are cold-inducible in the wild type. (B) and (C) Relative transcript levels of *CBF1*, *CBF2*, *CBF3*, and *RD29A* in *cir1*, *spfh*, *atsk12*, and *prr5* mutant plants. (D) Freezing tolerance of *cir1*, *spfh*, *atsk12*, and *prr5* mutant plants determined by electrolyte leakage assays. ** denotes $P < 0.01$, as determined by Student's *t*-test. (E) Relative transcript levels of *CBF1*, *CBF2*, and *CBF3* in overexpression plants of *CIR1* (*CIR1 OE*), *SPFH* (*SPFH OE*), *AtSK12* (*AtSK12 OE*), and *PRR5* (*PRR5 OE*). (F) Freezing tolerance of *CIR1 OE*, *SPFH OE*, *AtSK12 OE*, and *PRR5 OE* plants. Cold acclimation in (D) and (F) was achieved by incubating plants at 4°C for 1 week. Data in (E) and (F) are from one representative transgenic line of two independent transgenic lines of *CIR1 OE*, *SPFH OE*, *AtSK12 OE*, and *PRR5 OE* plants (Figure 1-14E and F). Error bars indicate the standard deviation (n = 4 in [B], [C], and [E]; n = 12-15 in [D] and [F]). One-way ANOVA (Tukey-Kramer test) was performed for data in (F), and statistically significant differences are indicated by different lowercase letters ($p < 0.01$).

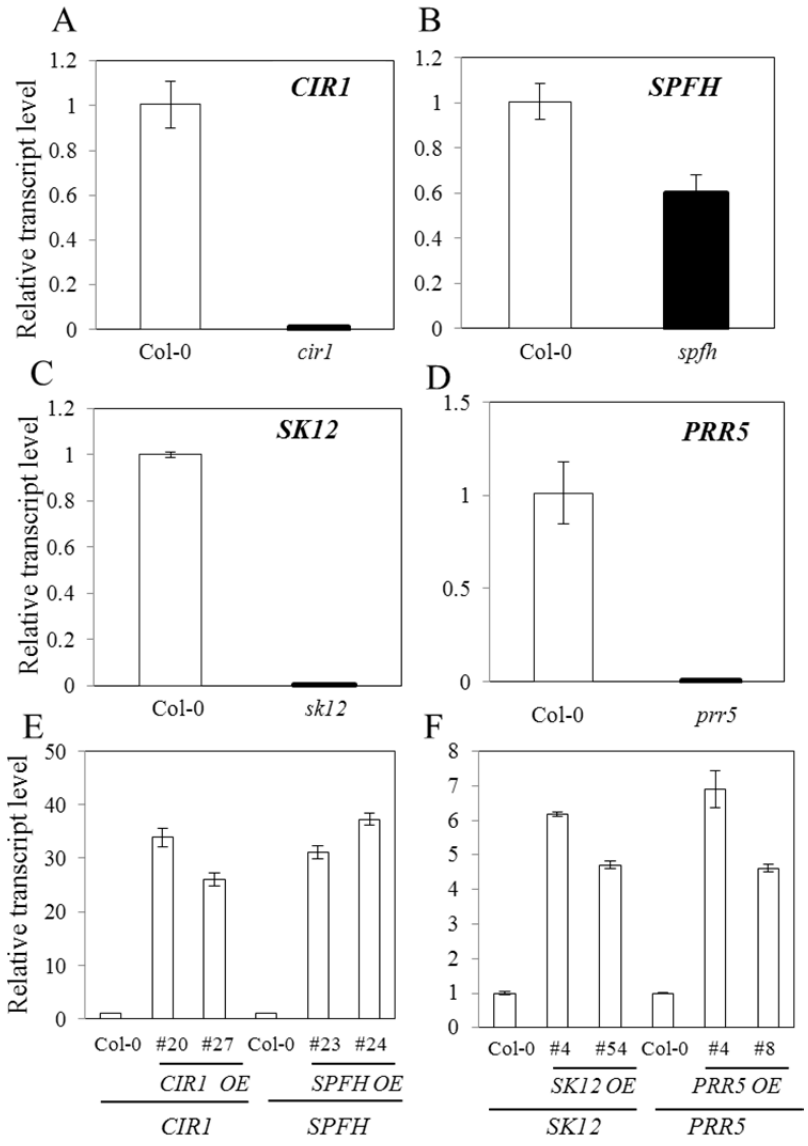

Figure 1-14. **Expression of *CIR1*, *SPFH*, *SK12*, and *PRR5* in T-DNA knockouts of *CIR1*, *SPFH*, *SK12*, and *PRR5 (cir1*, *spfh*, *prr5*, and *sk12*), *CIR1* Overexpression (*CIR1 OE*), *SPFH* Overexpression (*SPFH OE*), *SK12* Overexpression (*SK12 OE*), and *PRR5* Overexpression (*PRR5OE)* Seedlings Determined by qRT-PCR Analysis.** qRT-PCR analysis was performed with 14-d-old seedlings grown under control conditions. Error bars indicate the standard deviation (n = 4).

improve the performance of plants under cold stress. We generated transgenic *Arabidopsis* plants that overexpress *RCF1* under the control of the 35S promoter, and we selected two independent *RCF1* overexpression lines (Figure 1-15A). The *RCF1* overexpression lines developed longer hypocotyls than the wild type under chilling stress, indicating an increased resistance to chilling stress (Figure 1-15B and C). Expression of *CBF* genes is repressed in the *RCF1* overexpression lines (Figure 1-15D). These results further support our conclusion that RCF1 is a negative regulator for these cold-responsive transcriptional activators. In an electrolyte leakage assay, the RCF1 overexpression lines displayed significantly increased tolerance to freezing temperature with or without cold acclimation (Figure 1-15E). Together, these results further support our conclusion that RCF1 is required for cold tolerance in plants.

Discussion

We identified the cold-inducible DEAD box-containing RNA helicase RCF1 through a forward genetic screen for genes critical for cold tolerance. We confirmed that recombinant RCF1 protein produced in *E. coli* has RNA helicase activity and that changing the functional DEAD box to DAAD abolishes its helicase activity (Figure 1-9). Similarly, the *RCF1* gene carrying the DAAD mutation in the DEAD box failed to complement the *rcf1-1* mutant, suggesting that the DEAD domain or the RNA helicase activity of RCF1 is essential for its biological function.

The RCF1 protein differs from a previously identified DEAD box RNA helicase, LOS4, in subcellular localization and function. Although both proteins are localized in the nucleus, LOS4 is enriched in the nuclear rims (Gong et al., 2005) but RCF1 is not (Figure 1-7). The subcellular localization of LOS4 is correlated with its

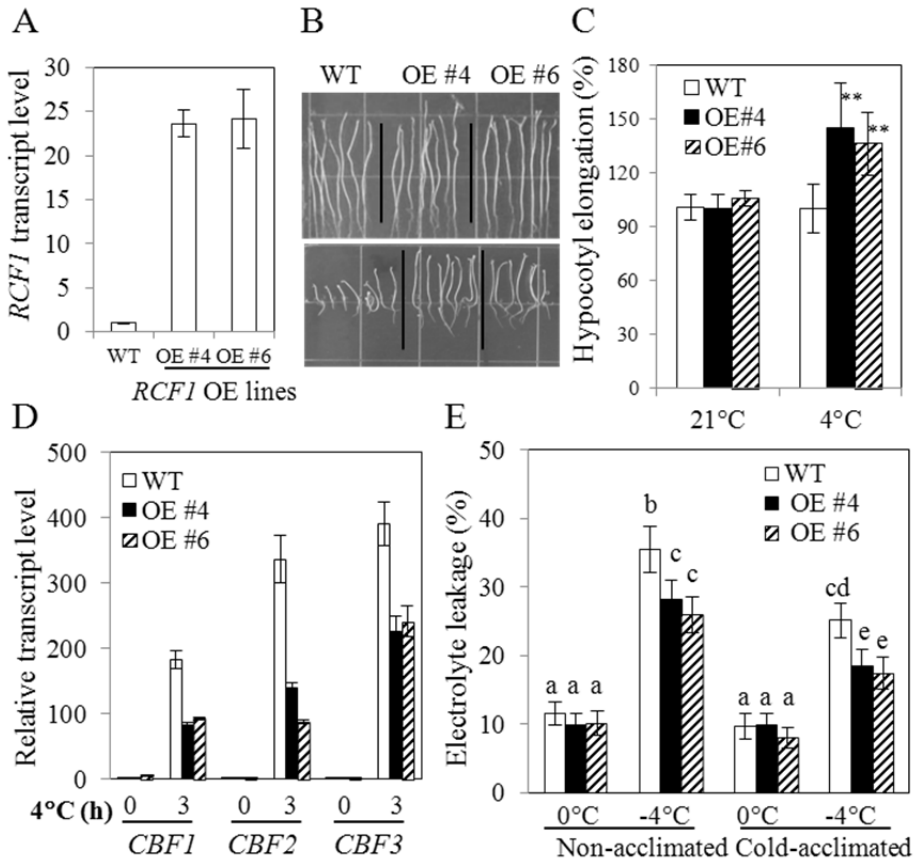

Figure 1-15. Overexpression of RCF1 Increases Cold Stress Tolerance. (A) RCF1 expression levels in the wild type and two transgenic lines overexpressing RCF1 (OE). (B) Chilling stress tolerance of wild-type and RCF1 OE plants. Top panel, 21°C for 13 d; bottom panel, 4°C in the dark for 32 d. (C) Quantification of hypocotyl elongation of plants shown in (B). Hypocotyl elongation of the wild type (at 21°C or 4°C) was considered to be 100%. ** denotes P <0.01, as determined by Student's t-test. (D) Expression of CBF1, CBF2, and CBF3 in wild-type and RCF1 OE plants subjected to 0 or 3 h at 4°C. (E) Freezing tolerance of RCF1 OE plants determined by electrolyte leakage assays. CA, cold acclimation (4°C for 1 week). Error bars indicate the standard deviation (n = 4 in [A] and [D]; n = 20 in [C]; n = 12 in [E]). WT, wild type. One-way ANOVA (Tukey-Kramer test) was performed for data in (E), and statistically significant differences are indicated by different lowercase letters ($p < 0.005$).

important role in mRNA export at cold temperatures (Gong et al., 2005), and the different location for RCF1 indicates that it is probably not involved in mRNA export. A role of RCF1 in mRNA export was ruled out by the poly(A) *in situ* hybridization assays (Figure 1-9D).

DEAD box RNA helicases contribute to all aspects of RNA metabolism, including nuclear gene transcription, pre-mRNA splicing, nucleo-cytoplasmic transport, and gene expression (Rocak and Linder, 2004; Cordin et al., 2006). In the current study, three lines of evidence demonstrate a role of RCF1 in pre-mRNA splicing. First, RCF1 co-expresses with another RNA helicase, Brr2b, and a pre-mRNA splicing factor, STA1. Second, database searches indicated that RCF1, STA1, and Brr2b are part of the spliceosome composed of over 100 proteins. Although there is no experimental evidence that Brr2b is involved in pre-mRNA splicing in *Arabidopsis*, a Brr2b homologue in yeast is involved in pre-mRNA splicing (Hahn et al., 2012). We therefore reasoned that RCF1 may function in some aspects of splicing. Third, full-genome tiling array analyses indicated that RCF1 controls pre-mRNA splicing of six genes without cold stress and 204 unique genes under cold stress (Appendix A10). Because the mis-spliced genes in *rcf1-1* under cold stress are not affected in *sta1-2* or *brr2b* mutants, RCF1 seems to function in the pre-mRNA splicing pathway independently of STA1 and Brr2b. Based on our results, we believe that RCF1, Brr2b, and STA1 may be components of different pre-mRNA splicing complexes that regulate the pre-mRNA splicing of different genes. That our 1.0R tiling array experiments detected only a relatively small number of mis-spliced genes in *rcf1-1* under normal growth condition (Figure 1-11D; Figure 1-12; GEO accession

number GSE41377) may be explained by the fact that the 1.0R tiling arrays used in the current study may be insufficiently sensitive to detect all mis-splicing events.

Our data indicate that *rcf1-1* mutant plants are defective in basal freezing tolerance (Figure 1-3) and that the reduced basal freezing tolerance may be due to mis-splicing of the six genes in *rcf1-1* under normal condition (Figure 1-11D). Two of the six mis-spliced genes (ATGR1 and a protein kinase) in *rcf1-1* under normal condition have predicted roles in stress responses (Appendix A10B). Mis-splicing of these two genes in *rcf1-1* under normal condition may reduce the ability of *rcf1-1* to cope with freezing temperatures without cold acclimation. Two additional genes whose transcripts are mis-spliced in *rcf1-1* under normal condition (*SMP1* and *MED6*) are involved in gene regulation. *SMP1* encodes a CCHC zinc finger protein with step II splicing factor activity. The spliceosome catalyzes pre-mRNA splicing in two steps. After catalytic step I, a major remodeling of the spliceosome occurs to establish the active site for step II. Step II splicing factors are responsible for the correct selection of 3′ splicing sites (Chua and Reed, 1999). SMP1 is functionally redundant with SMP2. One of the functional targets of SMP1 and SMP2 is the transcript of *STRUWWELPETER* (*SWP*) that resembles the subunits of the mediator complex required for transcriptional activation (Clay and Nelson, 2005). MED6 is one of the mediators of RNA polymerase II (Pol II). The mediator of Pol II is required for diverse aspects of the transcription process including activation, repression, basal transcription, and phosphorylation of the C-terminal domain (CTD) of the largest subunit of Pol II (Kim et al., 1994; Björklund and Kim, 1996). MED6 homologs in *Drosophila* and yeast play important roles as transcriptional co-

activators (Lee and Kim, 1998; Gim et al., 2001). The MED6 in *Arabidopsis* may function similarly to its homologs in yeast and *Drosophila*. Furthermore, splicing of *MPK15* is defective in *rcf1-1* under normal condition, and MPK15 is likely involved in activation of gene expression. As mentioned above, MPK15, SMP1, and MED6 are involved in gene regulation, and mis-splicing of these three genes in *rcf1-1* may alter expression of genes, for example, those genes that are differentially expressed in *rcf1-1* under non-stressed conditions (Appendix A1). The altered gene expression in *rcf1-1* may contribute to reduced basal freezing tolerance.

Although *rcf1-1* plants should theoretically display enhanced freezing tolerance when transcripts of cold-responsive genes accumulate to a higher level, the opposite phenotype was observed (Figure 1-3). Our results show that RCF1 is required for tolerance to chilling and freezing stresses in plants because *rcf1-1* mutant plants are hypersensitive to cold stress and overexpression of *RCF1* increases cold tolerance (Figure 1-2, 1-3, and 1-15). These results suggest that an essential regulator (s) of cold tolerance is defective in *rcf1-1*. *CIR1* and *SPFH* are two good candidates of such essential regulators of cold tolerance, and transcripts of these two genes were mis-spliced in *rcf1-1* under cold stress (Figure 1-11). CIR1 is involved in circadian-regulated developmental processes, and circadian rhythmic expression of *CIR1* is regulated by the central oscillators CIRCADIAN CLOCK-ASSOCIATED 1 (CCA1) and LATE ELONGATED HYPOCOTYL (LHY), two MYB transcription factors that have partially redundant functions (Wang and Tobin, 1998; Schaffer et al., 1998; Mizoguchi et al., 2002; Zhang et al., 2007). The functions of CCA1 and LHY in the regulation of *CBF* expression have been reported (Dong et al., 2011), but the function

of CIR1 in cold stress response has not been determined. SPFH is one of the SPFH/PHB (stomatin-prohibtin-flotillin-HflC/K) domain-containing superfamily proteins, and members of the SPFH protein superfamily are generally associated with plasma or mitochondrial membranes and are involved in many cellular processes including protein turnover or oligomerization, cell proliferation, and ion channel regulation (Tavernarakis et al., 1999; Nadimpalli et al., 2000; Rivera-Milla et al., 2006). According to our investigation of the loss-of-function and gain-of-function of *CIR1* and *SPFH* genes, CIR1 and SPFH positively control expression of cold-responsive genes including *CBFs* and are required for cold tolerance (Figure 1-13B–F). *CIR1* and *SPFH* appear to function in the cold stress-tolerance pathway in a *CBF*-dependent manner. In addition, the list of RCF1 target genes as revealed by the ATH1 microarray and 1.0R tiling array analyses might include other positive and negative regulators that are essential for cold stress tolerance (for example, factors functioning in CBF-independent pathways). The molecular function of these positive and negative regulators for cold tolerance requires further study but indications about these regulators were provided by the gene expression data generated in our microarray and tiling array analyses. Although the differentially expressed genes in *rcf1-1* with or without cold stress encode proteins that are involved in diverse biological processes, many of the up-regulated genes and some of the down-regulated genes in *rcf1-1* encode proteins that are predicted to function in the biotic or abiotic stress-response pathways (Appendix A1- A3). Gene expression data in *rcf1-1* with and without cold treatment were quite different from publically available gene expression data from wild-type plants (Appendix A5 – A9). In the latter case, genes

are normally up-regulated in wild-type plants after cold stress, but these genes failed to increase in *rcf1-1* in response to cold (Appendix A6, A8). Similarly, genes that are repressed by cold stress in the wild type are turned on in *rcf1-1* (Appendix A7, A9). Aberrant expression of these genes in *rcf1-1* under cold stress potentially compromises the mutant's ability to cope with freezing temperatures. Furthermore, many of the mis-spliced genes in *rcf1-1* revealed by the 1.0R tiling array analyses are responsive to cold stress in wild-type plants, suggesting that they are involved in cold stress responses (Appendix A11). The mis-splicing and resulting disruption of functions of some of these genes in *rcf1-1* plants may contribute to the increased cold sensitivity of *rcf1-1*.

The increased accumulation of *CBF* genes and their downstream targets in *rcf1-1* may be explained by the action of RCF1 target genes as revealed in the 1.0R tilling array experiments. PRR5 and AtSK12 appear to be negative regulators of *CBFs* and *RD29A* (Figure 1-13B and C). *PRR5* is strongly induced by cold, and *AtSK12* is moderately up-regulated by cold (Figure 1-13A). PRR5 is a negative regulator of *CBF* genes and is partially redundant with PRR7 and PRR9 (Nakamichi et al., 2009). The null allele of *prr5* used in this study (Figure 1-14D) differed from those reported previously (Nakamichi et al., 2009), and this single mutation was sufficient to display phenotypes such as altered expression of *CBF* genes and sensitivity to freezing temperatures. Mis-spliced transcripts of *PRR5* and *AtSK12* in *rcf1-1* presumably disrupt the normal function of these two genes, leading to increased induction of *CBF* genes in *rcf1-1* in a similar way as observed in the *prr5* and *atsk12* mutant plants. Overexpression of *PRR5* or *AtSK12* results in reduced

expression of *CBF* genes and reduced freezing tolerance (Figure 1-13E and F), confirming that PRR5 and AtSK12 are negative regulators of cold-responsive gene expression and cold tolerance.

There are additional examples of mutants that are more sensitive to cold stress than the wild type even though they accumulate higher levels of cold-responsive genes. The *sta1-1*, *sta1-2*, and *brr2b* mutant plants are hypersensitive to chilling and freezing stresses although *CBF2* gene is expressed to a higher level in these three mutants (Figure 1-10). Thus, STA1 and Brr2b are required for cold tolerance. Because the cold response of *rcf1-1* is similar to that of *sta1* and *brr2b*, it is possible that RCF1, STA1, and Brr2b share a common subset of target genes critical for cold tolerance. Identification of these common target genes controlled by RCF1, STA1, and Brr2b requires further investigation. Nevertheless, STA1 and Brr2b are two examples in addition to RCF1 of important proteins that are required for cold tolerance and that act as negative regulators of *CBF* gene expression. Increased expression of *CBF2* in *sta1-2* and *brr2b* can be a compensatory response to an increased sensitivity to cold stress, as was the case with *sta1-2* and *brr2b*, the over-accumulated transcripts of *CBF* genes in *rcf1-1* may be a compensatory response to the increased sensitivity of *rcf1-1* to cold stress. The underlying mechanism for this type of compensatory response has been a mystery. Our results show that the defective splicing of *AtSK12* and *PRR5* explains at least part of the compensatory response in the *rcf1-1* mutant. We have observed a similar phenomenon in *hos9-1* and *hos15* mutants, which accumulate higher levels of some cold-responsive genes but are

hypersensitive to cold stress (Zhu et al., 2004; Zhu et al., 2008). Unlike *rcf1-1*, however, *hos9-1* and *hos15* mutations do not affect cold-induction of *CBF* genes. The importance of RCF1 protein in cold stress responses is further supported by the consequences of *RCF1* overexpression in *Arabidopsis*. Overexpression of *RCF1* enhances the tolerance to chilling and freezing stresses (Figure 1-15), indicating that RCF1 and the splicing controlled by it are essential for cold tolerance. Furthermore, expression of *CBF* genes was down-regulated in *RCF1* overexpression lines, confirming that RCF1 is indeed a negative regulator of *CBF* genes. When *RCF1* is overexpressed, positive regulators for cold tolerance are presumably produced at a higher level and negative regulators are presumably suppressed to improve performance under cold stress. Although determining precisely how RCF1 functions in cold tolerance will require further investigation, our forward genetic analysis has demonstrated that by maintaining splicing of pre-mRNAs under cold, RCF1 is a crucial regulator of cold tolerance in plants.

Methods

Plant Materials and Growth Conditions

A firefly luciferase reporter gene driven by the cold stress-responsive *CBF2* promoter (-1500 bp to -1 bp upstream of the transcription start site) was introduced into *Arabidopsis* plants in the Columbia *glabrous1* (*gl1*) background. Seeds from one homozygous line expressing a single functional copy of the *CBF2:LUC* gene (referred to as the wild type) were mutagenized with ethyl methanesulfonate (EMS). The *rcf1-1* mutant with altered *CBF2:LUC* gene expression was isolated from M_2

seedlings with a charge-coupled device (CCD) camera imaging system (Ishitani et al. 1997).

Seeds of the following T-DNA insertion mutants were obtained from the Arabidopsis Biological Resource Center (ABRC, Columbus, OH): *rcf1-2* (SALK_138032), *rcf1-3* (SALK_062599), *sta1-2* (SAIL_262-C08), *brr2b* (SALK_048780), *prr5* (SALK_135000), *atsk12* (CS856017), *cir1* (SALK_051843), and *spfh* (SALK_090074). The *sta1-1* mutant was described previously (Lee et al., 2006). *Arabidopsis* seedlings on Murashige and Skoog (MS) medium agar plates (1x MS salts, 2% sucrose, 0.6% agar, pH 5.7) were routinely grown under cool, white light (~120 μmol m^{-2} s^{-1}) at 21 ± 1℃ with a 16-h-light/8-h-dark photoperiod. Soil-grown plants were kept under cool, white light (~100 μmol m^{-2} s^{-1}) with a 16-h-light/8-h-dark photoperiod at 21 ± 1℃ and with a 1:1 ratio of Metro Mix 360 and LC1 potting soil (Sun Gro Horticulture, Bellevue, WA).

Chilling- and Freezing-Tolerance Assays

For chilling-tolerance assays, seeds of relevant genotypes were sown side-by-side on agar plates containing MS medium (1x MS salts, 2% sucrose, 1.2% agar, pH 5.7). These agar plates were then wrapped with aluminum foil and kept vertically at 4°C or 21℃ in growth chambers for the desired time. Reduction in hypocotyl elongation at 4°C relative to that of the wild type at 21℃ was used as an indicator of sensitivity to chilling stress.

For evaluation of freezing tolerance with electrolyte leakage assays, 3-week-old wild-type and mutant or transgenic plants were grown in soil at room temperature or at 4°C under a long-day photoperiod (16-h-light/8-h-dark) for 1 week. Fully

developed rosette leaves were used for electrolyte leakage measurements as described (Sukumaran and Weiser, 1972; Ristic and Ashworth, 1993; Zhu et al., 2004). Whole-plant freezing tests were as described (Xiong et al., 2001) with modifications. Wild-type and *rcf1-1* plants were grown in soil under a long-day photoperiod (16-h-light/8-h-dark) in a growth chamber for 3 weeks at 21°C and then at 4°C for 1 week for cold acclimation. The plants were then placed in a low temperature chamber with the following freezing temperature regimen: from 4 to -1°C in 30 min, then hold at -1°C for 1 h (to initiate nucleation); then successive 2°C decreases at 30 min intervals to reach the next temperature (hold at the following temperatures for 3 h: -4, -6, -8, -10, and -12°C). Plant damage was scored 7 d later (Xiong et al., 2001).

Genetic Mapping and Complementation

The *rcf1-1* mutant was crossed with the Landsberg *erecta* accession, and 1414 mutant plants were chosen from the F_2 generation based on altered *CBF2:LUC* phenotype. Simple sequence length polymorphism (SSLP) markers were designed according to the information in the Cereon Arabidopsis Polymorphism Collection and were used to analyze recombination events (Jander et al., 2002). Initial mapping revealed that the *rcf1-1* mutation is located on the upper arm of chromosome 1 between T20H2 and T22I11. Fine mapping within this chromosomal interval narrowed the *RCF1* locus to the BAC clone F9H16. All candidate genes in this BAC were sequenced from the *rcf1-1* mutant and compared with those in GenBank to find the *rcf1-1* mutation.

For complementation of the *rcf1-1* mutant, a 6975-bp genomic fragment of *At1g20920* that included 2224 bp upstream of the translation initiation codon and 1251 bp downstream of the translation stop codon was amplified with F9H16 as a

template (see Appendix 12 for primer sequences). The amplified fragment was first cloned through Gateway technology (Invitrogen) into the pENTR4 vector, resulting in plasmid pENTR4-RCF1. The pENTR4-RCF1 plasmid was then subjected to site-directed mutagenesis to change the DEAD domain into the DAAD mutant version at the amino acid level with the primer pair listed in Appendix A12. The wild-type *RCF1* gene and mutated *RCF1* (DEAD to DAAD) were then introduced into the pMDC99. The constructs were transferred into *Agrobacterium tumefaciens* (strain GV3101), and *rcf1-1* plants were transformed by the floral dip method (Clough and Bent, 1998).

RCF1 Subcellular Localization and Overexpression of *RCF1*, *PRR5*, *AtSK12*, *CIR1*, and *SPFH*

The coding region of *RCF1* was amplified by PCR and cloned into the pMDC83 vector to make the RCF1-GFP fusion protein. This construct (pMDC83-RCF1) was then introduced into *Arabidopsis* wild-type (ecotype Columbia) and *rcf1-1* plants by floral dip transformation with *A. tumefaciens* strain GV3101. The pMDC83-RCF1 plasmid was also transformed into *A. tumefaciens* strain C58C1 and co-infiltrated with *35S:p19* (p19 is a RNA silencing repressor protein from tomato bushy stunt virus (Voinnet et al., 2003)) in *A. tumefaciens* strain C58C1 into the 3-week-old leaves of tobacco (*Nicotiana benthamiana*) plants. The infiltrated tobacco plants were allowed to grow for an additional 3 d in a growth chamber under a 16-h-light/8-h-dark photoperiod at 21℃. The subcellular localization of RCF1-GFP protein in tobacco leaves or in root tissues of *Arabidopsis* transgenic plants (T_2 generation) was determined with a Leica SP5X confocal microscope (Leica Microsystems). The *rcf1-*

1 mutant plants transformed with pMDC83-RCF1 in the T_2 generation were examined for *CBF2: LUC* expression to determine whether pMDC83-RCF1 fusion protein is functional *in planta*. Nuclear-localization of pMDC83-RCF3 fusion protein in tobacco leaves was used as a positive control. RCF3 protein was described previously (Guan et al., 2012).

For overexpression of *RCF1*, *PRR5*, *AtSK12*, *CIR1*, and *SPFH*, coding regions of these genes were amplified by PCR and cloned into the pMDC32 vector. The resulting plasmids (pMDC32-RCF1, pMDC32-PRR5, pMDC32-AtSK12, pMDC32-CIR1, and pMDC32-SPFH) were then transferred into *A. tumefaciens* (strain GV3101), and *Arabidopsis* wild-type plants (ecotype Columbia) were transformed by the floral dip method. Transgenic plants resistant to hygromycin (50 μg/ml) in the T_2 generation were tested for resistance to cold stress and for gene regulation under cold stress.

Microarray Analysis, Tilling Array Analysis, and Real-Time RT-PCR Analysis

Fourteen-d-old seedlings grown on MS medium (1x MS salts, 2% sucrose, 0.6% agar, pH 5.7) were used for RNA isolation. Total RNA was extracted from the wild type, different mutants, and/or transgenic plants with Trizol reagent (Invitrogen) and treated with DNase I (New England Biolabs) to remove any genomic DNA contaminants.

For GeneChip *Arabidopsis* Genome (ATH1, Affymetrix) array analysis, total RNA was used to prepare biotin-labeled complementary RNA targets. Microarray analysis was performed in the School of Medicine, University of Maryland at Baltimore, as described (Breitling et al., 2004). Two biological replicates were used

for each genotype. The data sets were subjected to the Robust Multiarray Averaging (RMA) normalization method. The RMA method for computing an expression measure is begun by computing background-corrected perfect match intensities for each perfect match cell on every GeneChip. The normalized data were further analyzed, and p-values were generated by the affylmGUI component of Bioconductor in statistics environment R with the default parameters (Irizarry et al., 2003; Gentleman et al., 2004). Genes with statistically significant differences in expression between the *rcf1-1* mutant and the wild type were selected by the RankProd method, which is a non-parametric method for identifying differentially expressed up- or down-regulated genes based on the estimated percentage of false discoveries ($p < 0.05$) (Hong et al., 2006). RankProd results were summarized with the script written in PERL.

For GeneChip *Arabidopsis* Tiling (1.0R, Affymetrix) array analysis, total RNA extracted from cold-treated (4°C for 12 h, which is when RCF1 is expressed at its peak level) wild-type and *rcf1-1* plants was used, and labeling, hybridization, and scanning were performed in the Genomics Core of the Institute for Integrative Genome Biology at the University of California at Riverside. Three biological replicates were used for each genotype. We first re-mapped the tiling array probes to the *Arabidopsis* genome (TAIR10) using SOAP2 (Li et al., 2009) and kept only probes that perfectly matched to a unique position in the genome for subsequent analyses. We then created a custom Chip Definition File (CDF) using the probe mapping result and used the aroma.affymetrix framework (Bengtsson et al., 2008) to quantile-normalize the raw tiling array data (three biological replicates each for the

rcf1-1 mutant and wild-type control). To identify retained introns, we first calculated the log2 signal intensity for each annotated intron (TAIR10) based on the trimmed-mean of signal intensities from all mapped probes. Introns with fewer than three mapped probes or with low expression (log2 expression value < 5 in all samples) were not further considered. We then used the SAM algorithm (Tusher et al., 2001) to identify introns with significantly elevated expression in the *rcf1-1* mutant samples relative to the wild type. A FDR (False Discovery Rate) of 0.05 was used as the significance cutoff. Intron retention in *rcf1-1* of selected genes under both normal and cold stress conditions was visualized with the integrated genome browser (IGB, http://bioviz.org/igb/; Nicol et al., 2009).

For real-time RT-PCR (qRT-PCR) analysis, 5 μg of total RNA was used for synthesis of the first-strand cDNA with the Maxima First-Strand cDNA Synthesis Kit (Fermentas) as described (Guan et al., 2012). Each experiment had three to five biological replicates (four technical replicates for each biological replicate), and each experiment was repeated at least three times. The comparative Ct method was applied, and *TUB8* was used as a reference gene.

Northern Hybridization Analysis

Fourteen-d-old seedlings grown on MS medium (1x MS salts, 2% sucrose, 0.6% agar, pH 5.7) and subjected to 0- or 12-h cold treatment at 4°C were used for RNA isolation. Total RNA was extracted with Trizol reagent (Invitrogen) and treated with DNase I (New England Biolabs) for potential genomic DNA contamination. Total RNA (30 μg) was then separated on a formaldehyde-containing agarose (1.2%, [wt/vol]) gel, transferred to a nylon transfer membrane (GE Healthcare) overnight,

and cross-linked. Blots were hybridized overnight (0.5 M phosphate buffer [pH 7.2], 7% [wt/vol] sodium dodecyl sulfate [SDS], 1 mM EDTA, and 2 mM bovine serum albumin) with ^{32}P-labeled probe at 60°C. Washes (20 min each at 60°C) were performed first in 2× SSC (1× SSC is 0.15 M NaCl plus 0.015 M sodium citrate) and 0.1% SDS; then in 1× SSC and 0.1% SDS; and finally in 0.5× SSC and 0.1% SDS. The elongation factor 1α (*EF1α*) gene was used as a loading control.

ATPase Activity Assay

A fragment of RCF1 cDNA (corresponding to amino acids 501–910 from the N-terminal region, spanning the ATPase motif) was amplified with the primer pair listed in Appendix A12 and cloned into pDEST15 to make a GST-tagged GST-RCF1 fusion protein. The resulting plasmid pDEST15-RCF1 was used as a template to make a mutant version of RCF1 (DEAD domain changed to DAAD) through site-directed mutagenesis (pDEST15-RCF1 (DAAD)). The pDEST15-RCF1 and pDEST15-RCF1 (DAAD) plasmids were transformed into *E. coli.* Rosetta (DE3)pLysS cells (EMD Millipore) and fusion proteins were purified with GST-affinity columns (GE Healthcare). The ATPase activities of RCF1 and its mutant version were determined as described by Iost et al. (1999) with minor modifications. This method uses pyruvate kinase and lactate dehydrogenase to link hydrolysis of ATP to oxidation of NADH, which results in a decrease in the absorbance at 338 nm. Briefly, assays were performed at 37°C in a reaction volume of 0.2 mL, in buffer containing 20 mM Tris-HCl, pH 8.0, 50 mM KCl, 5 mM $MgCl_2$, 1 mM dithiothreitol, 1 mM ATP, 300 μM NADH, 2 mM phosphoenolpyruvate, 73.5 nM RCF1 (or RCF1 (DAAD)), and 3

units/ml of pyruvate kinase and lactate dehydrogenase with or without 50 μg/ml *Arabidopsis* total RNA.

Poly(A) RNA in situ Hybridization Assay

Poly(A) RNA *in situ* hybridization was conducted essentially as described by Engler et al. (1994) and Gong et al. (2005). The samples were observed immediately using a Leica SP5X confocal microscope (Leica Microsystems) with a 488-nm excitation laser and a 522/DF35 emission filter. All samples were observed under the same conditions, including the use of the same 60x objective lens and the same laser strength.

Accession Numbers

Sequence data from this article can be found in the Arabidopsis Genome Initiative or GenBank/EMBL databases under the following accession numbers: *RCF1* (*At1g20920*), *STA1* (*At4g03430*), *Brr2b* (*At2g42270*), *CBF1* (*At4g25490*), *CBF2* (*At4g25470*), *CBF3* (*At4g25480*), *RD29A* (*At5g52310*), *PRR5* (*At5g24470*), *AtSK12* (*At3g05840*), *PUB45* (*At1g27910*), *EBF2* (*At5g25350*), *CIR1* (*At5g37260*), *SPFH* (*At5g54100*), *COR15A* (*At2g42540*), *MED6* (*At3g21350*), SMP1 (*At1g65660*), *CHLM* (*At4g25080*), *ATGR1* (*At3g52115*), *protein kinase* (*At1g21590*), *MPK15* (*At1g73670*), *TUB8* (*At5g23860*), and *EF1α* (*At1g07920*). The microarray and tiling array data discussed in this manuscript have been deposited in NCBI's Gene Expression Omnibus (Edgar et al., 2002) and can be accessed through GEO Series accession numbers GSE039090, GSE41377, and GSE41378.

Acknowledgements

I thank Jianmin Wu, Yanyan Zhang, Changhua Jiang, Chenglin Chai, Renyi Liu, and Jianhua Zhu for their contribution to this work. This work was supported by a USDA hatch fund (CA-R*-BPS-7754 H) to R.L. and by National Science Foundation Grants IOS0919745 and MCB0950242 to J.Z.

Chapter 2: A KH Domain-Containing Putative RNA-Binding Protein Is Critical for Heat Stress-Responsive Gene Regulation and Thermotolerance in *Arabidopsis*

Abstract

Heat stress is a severe environmental factor that significantly reduces plant growth and delays development. Heat stress factors (HSFs) are a class of transcription factors that are synthesized rapidly in response to elevations in temperature and are responsible for the transcription of many heat stress-responsive genes including those encoding heat shock proteins (HSPs). There are 21 HSFs in *Arabidopsis*, and recent studies have established that the HSFA1 family members are master regulators for the remaining HSFs. However, very little is known about upstream molecular factors that control the expression of *HSFA1s* genes and other *HSFs* genes under heat stress. Through a forward genetic analysis, we identified RCF3, a KH domain-containing nuclear-localized putative RNA-binding protein. RCF3 is a negative regulator of most *HSFs* including *HSFA1a*, *HSFA1b*, and *HSFA1d*. In contrast, RCF3 positively controls the expression of *HSFA1e*, *HSFA3*, *HSFA9*, *HSFB3*, and *DREB2C*. Consistent with the overall increased accumulation of heat-responsive genes, the *rcf3* mutant plants are more tolerant than the wild type to heat stress. Together, our results suggest that a KH domain-containing putative RNA-binding protein RCF3 is an important upstream regulator for heat stress-responsive gene expression and thermotolerance in *Arabidopsis*.

Key words: RNA-binding protein, RCF3, HSF, HSP

Introduction

As sessile organisms, plants are frequently challenged by environmental stresses including heat and drought and sometimes by the combination of heat and drought. Heat stress (HS) adversely affects crop production worldwide. Temperature increases of 5°C or more above the optimal temperature are generally experienced as HS by all living organisms including plants. HS disturbs normal cellular processes and can reduce plant growth and delay development. Exposure to HS for prolonged periods can even result in plant death.

In response to HS, plants have evolved signal transduction pathways in which HS transcription factors (HSFs) are important components. More than 20 HSFs are encoded by plant genomes, and these are grouped into three major classes (A, B, and C) based on structural characteristics and phylogenetic relationships (Nover et al., 2001; Baniwal et al., 2004). By recognizing and binding to HS elements (HSE: 5'-GAAnnTTC-3') conserved in promoters of HS-responsive genes, HSFs mediate the synthesis of heat shock proteins (HSPs) (Busch et al., 2005). HSPs are categorized into five classes based on their approximate molecular weights in kDa: HSP100, HSP90, HSP70, HSP60, and small heat shock proteins (sHSPs, 15–30 kDa) (Trent, 1996; Vierling, 1991). HSPs function as molecular chaperones and are essential for the maintenance and/or restoration of protein homeostasis.

Interplay among and complexity of the plant HSF members are currently being studied, and researchers have established that HSFA1 members act as master

regulators of other HSFs and therefore as master regulators of HS responses in tomato and *Arabidopsis* (Mishra et al., 2002; Liu et al., 2011; Nishizawa-Yokoi et al., 2011; Yoshida et al., 2011). However, very little is known about the more upstream regulators of these HSFA1s or the entire family of HSFs. In tomato, HSFB1 functions as a synergistic co-activator of HSFA1a (Bharti et al., 2004). Because of sequence differences in the C-terminus, the *Arabidopsis* HSFB1 is inactive as a co-activator of tomato HSFA1a (Bharti et al., 2004). In *Arabidopsis*, HSFB1 and HSFB2b act as it is s*HSFA7a* (Ikeda et al., 2011). All members of the DREB2 family (DREB2A, DREB2B, and DREB2C) are involved in the regulation of heat-responsive genes including *HSFA3* (Sakuma et al., 2006; Schramm et al., 2008; Chen et al., 2010). Liu et al. (2008) reported that a calmodulin-binding protein kinase 3 functions as an upstream activator for *HSFA1a* in *Arabidopsis*. AtCAM3 plays a role in the Ca^{2+}-CaM HS signal transduction pathway in *Arabidopsis* (Zhang et al., 2009). Furthermore, AtHSBP interacts with HSFA1a, HSFA1b, and HSFA2 and negatively regulates HSFA1b HSE-binding ability in vitro and functions as a negative regulator for HS responses in Arabidopsis (Hsu et al., 2010). Additional critical components in the signal transduction pathway for HS-responsive gene regulation remain to be identified.

In this study, we identified an *Arabidopsis* KH domain-containing putative RNA-binding protein, RCF3. RCF3 is localized in the nucleus and negatively regulates most *HSFs* genes including *HSFA1a*, *HSFA1b*, and *HSFA1d*. In contrast, RCF3 positively controls expression of *HSFA1e*, *HSFA3*, *HSFA9*, *HSFB3*, and *DREB2C*. Consistent with the overall increased accumulation of heat-responsive

genes, the *rcf3* mutant plants are more tolerant than the wild type to HS. Together, our results demonstrate that RCF3 is an important upstream molecular regulator for heat stress-responsive gene regulation and thermotolerance in *Arabidopsis*.

Results

Identification of the *rcf3-1* Mutant

We are interested in isolating and characterizing genes with essential functions in plant responses to temperature stresses (cold and/or heat). In the current study, we used a forward genetic analysis approach by screening an EMS-mutagenized *Arabidopsis* population for mutants with de-regulated expression of a *firefly luciferase* reporter gene under the control of the cold-inducible *CBF2* promoter (*ProCBF2::LUC*). We designated these mutants as *regulator of CBF gene expression* (*rcf*). The *rcf3-1* mutant was chosen for further characterization. Compared to wild-type plants, *rcf3-1* plants have a much higher level of *ProCBF2::LUC* expression under cold stress (Figure 2-1A). We backcrossed *rcf3-1* with the wild type. All F_1 plants showed a wild-type phenotype in response to cold stress, and F_2 plants segregated at approximately 3:1 (wild type vs. *rcf3-1*). These results suggested that *rcf3-1* is a recessive mutation in a single nuclear gene.

RCF3 Encodes a KH Domain-Containing Putative RNA-Binding Protein

Positional cloning revealed that the *rcf3-1* mutation is caused by a single nucleotide substitution from C to T at position 1600 from the transcription start site of gene *At5g53060* (Figure 2-1B). This mutation would change the amino acid Gln to a stop codon at position 344 of the decoded At5g53060 polypeptide. The *At5g53060* gene encodes a putative RNA-binding protein with five predicted KH domains (Figure 2-1

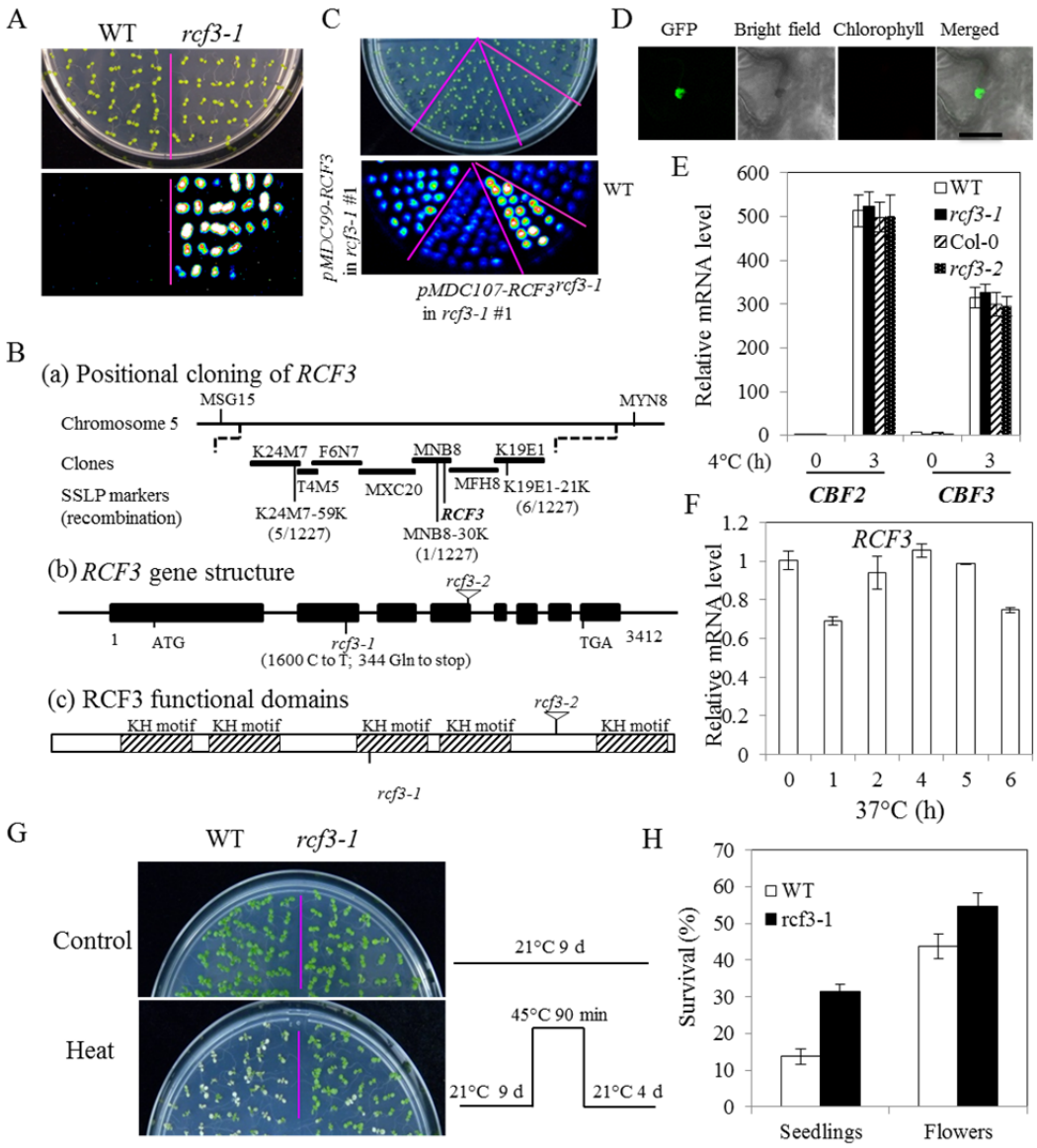

Figure 2-1. Molecular Cloning of *RCF3* and Thermotolerance of *rcf3-1* Mutant.

(A) *ProCBF2::LUC* expression in 7-d-old wild-type (WT) and *rcf3-1* seedlings treated at 4°C for 24 h. (B) Positional cloning of *RCF3*. (a) Map-based cloning of *RCF3*. Numbers of recombination are from 1227 F_2 progeny seedlings that were homozygous for the *rcf3-1* phenotype. (b) Structure of the *RCF3* gene and positions of *rcf3-1* and *rcf3-2* mutations are indicated. Filled boxes indicate exons, and lines between boxes indicate introns. (c) RCF3 functional domains and positions of *rcf3-1* and *rcf3-2* mutations. (C) Molecular complementation of the *rcf3-1* mutant by the wild-type *RCF3* gene. Shown are seedlings on an MS agar plate (upper panel) and the corresponding luminescence image after cold

treatment at 4°C for 24 h (lower panel). (D) RCF3-GFP is localized in the nucleus of tobacco leaf epidermal cells. (E) Expression of *CBF2* in *rcf3-1* and *rcf3-2* as determined by qRT-PCR analysis. (F) Expression of *RCF3* in the wild type in response to HS as determined by qRT-PCR analysis. Error bars in (E) and (F) represent the standard deviation (n = 6). (G) Thermotolerance of *rcf3-1*. There were 70-100 seedlings per genotype per MS agar plate. Pictures of plants for control experiment were taken before heat treatments.(H) Quantification of seedling survival rate shown in (G) and flowers of 1-month-old separate batches of WT and *rcf3-1* plants under heat stress (37°C for 4 d). Error bars represent the standard deviation (n = 20-30; n denotes the number of MS agar plates or number of pots).

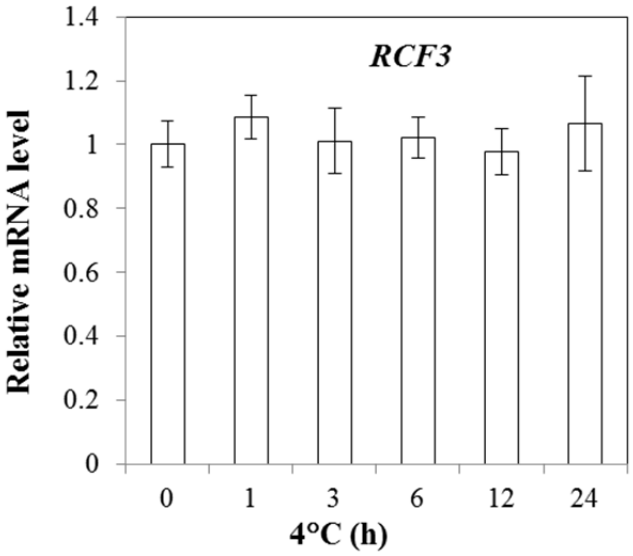

Figure 2-2. Expression of *RCF3* in Response to Cold Stress as Determined by qRT-PCR Analysis.

RCF3 expression in 14-d-old wild type seedlings subjected to cold treatment (4°C) was examined by qRT-PCR analysis. Error bars indicated the standard deviation (n = 6).

B). We confirmed the identity of *RCF3* with a gene complementation test using the wild-type *RCF3* gene, including its own promoter and coding sequences (Figure 2-1C). We made an RCF3-GFP fusion protein under the control of the *RCF3* native promoter in tobacco plants to determine the subcellular localization of RCF3, and confocal microscopy indicated that RCF3 is predominantly localized in the nucleus (Figure 2-1D). The RCF3-GFP transgene is biologically functional because it can restore the *rcf3-1* phenotype to the wild type (Figure 2-1C).

The *rcf3* Mutations Do not Alter Expression of Endogenous *CBF2* and *CBF3*, and the *rcf3-1* Mutant Plants Are Tolerant to HS

We performed real-time RT-PCR (qRT-PCR) analysis to determine the effect of the *rcf3-1* mutation on expression of the endogenous *CBF2* and *CBF3* genes. As shown in Figure 2-1E, the *rcf3-1* mutation does not alter cold-induction of *CBF2* or *CBF3*. We then isolated the *rcf3-2* allele, which is a T-DNA insertional line, and qRT-PCR analysis indicated that *rcf3-2* is a null allele of *RCF3* (Figure 2-5A). As was the case with *rcf3-1*, the expression level of *CBF2* and *CBF3* in *rcf3-2* is not significantly different from that in the wild type (Figure 2-1E). Under cold stress, the *rcf3-1* mutation apparently affects only the *ProCBF2::LUC* transgene, and neither the *rcf3-1* nor the *rcf3-2* mutation apparently alters the expression of endogenous *CBF2* or *CBF3*. In the future, we will explore at the whole-genome scale the effects of *rcf3* mutations on expression of other endogenous genes under cold stress.

RCF3 is transiently down-regulated by HS (Figure 2-1F), but it is not responsive to cold stress (Figure 2-2). These results suggest that RCF3 may be a negative regulator of plant responses to HS. We then determined whether the *rcf3-1* mutant has altered

responses to HS. To our surprise, the *rcf3-1* mutant seedlings showed substantial improvement in basal thermotolerance as indicated by a higher survival rate (Figure 2-1G and 2-1H).

The *rcf3-1* Mutation Affects Expression of *HSFs* under HS

Because tolerance to HS is greatly increased in *rcf3-1* mutant plants, we determined the expression levels of the master regulators of *HSFs*, the *HSFA1s*, in *rcf3-1*. Compared to their expression in the wild type, expression of *HSFA1a*, *HSFA1b*, and *HSFA1d* is elevated and expression of *HSFA1e* is reduced in *rcf3-1* under HS (Figure 2-3A and B). These results indicate that RCF3 is an important regulator of all four *HSFA1s*. We then expanded our gene expression study to the other 17 *HSFs* in *Arabidopsis*. Expression of *HSFA3* and *HSFA6b* is remarkably lower in *rcf3-1* than in the wild type under HS (Figure 2-3C and E). In contrast, transcript levels of *HSFA2*, *HSFA4a*, *HSFA5*, *HSFA6a*, *HSFA7a*, *HSFA7b*, and *HSFA8* are substantially higher in *rcf3-1* than in the wild type (Figure 2-3D-F). Except for *HSFB3*, which shows reduced expression in *rcf3-1*, all the remaining class B *HSFs* are negatively controlled by RCF3 (Figure 2-3G and H). *Arabidopsis* only has one member in HSF class C, *HSFC1*. *HSFC1* is down-regulated by HS in both the wild type and *rcf3-1*, but this down-regulation is less in *rcf3-1* (Figure 2-3H).

The *rcf3-1* Mutation Affects Expression of *DREB2s* under HS

Because transcript levels of *HSFA3* were reduced in *rcf3-1*, we determined expression levels of *DREB2s* in *rcf3-1* (DREB2A, DREB2B, and DREB2C are transcriptional activators for *HSFA3* and other HS-responsive genes). Heat-induction of both *DREB2A* and *DREB2B* is greatly enhanced in *rcf3-1* relative to the wild type (Figure

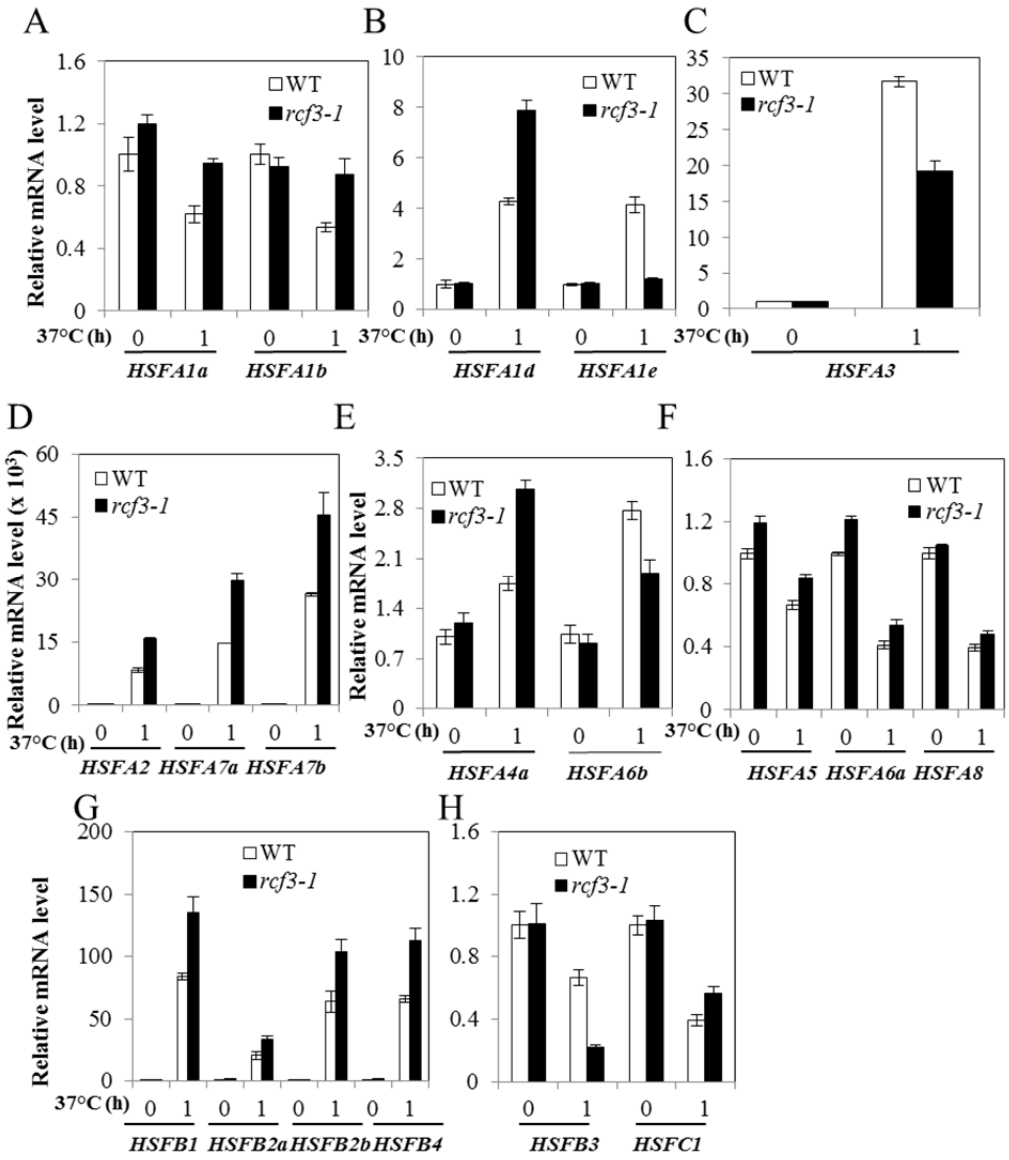

Figure 2-3. Expression of *HSFs* in *rcf3-1*. Expression of *HSFs* in wild-type and *rcf3-1* plants subjected to 0 or 1 h at 37°C. Error bars represent the standard deviation (n = 6).

2-4A and B). In contrast, the transcript level of *DREB2C* is dramatically lower in *rcf3-1* than in the wild type (Figure 2-4C).

RCF3 Negatively Regulates Expression of *HSPs* under HS

Previous sections revealed complex regulation of *HSFs* and *DREB2s* in *rcf3-1*. Because expression of *HSPs* is the most significant event in response to HS, we then measured the expression of *HSPs* in *rcf3-1*. In the absence of stress, expression of all tested *HSPs* was similar in *rcf3-1* and the wild type (Figure 2-4D and E). Under HS, however, transcript levels of three members of small *HSPs* (*HSP17.6*, *HSP18*, and *HSP25.3*) are substantially higher in *rcf3-1* than the wild type (Figure 2-4D and E). Expression of representative members of other classes of *HSPs* (*HSP70B*, *HSP90*, and *HSP101*) is significantly higher in *rcf3-1* than in the wild type under HS (Figure 2-4D and E).

Effect of *rcf3-1* Mutation on Expression of *CBK3*, *CaM3*, and *HSBP*

The camodulin-binding protein kinase 3 (CBK3) positively regulates *HSFA1a* (Liu et al., 2008). Because we observed increased expression of *HSA1a* in *rcf3-1*, we determined the *CBK3* transcript level in *rcf3-1*. Relative to its expression in the wild type, expression of *CBK3* is not altered in *rcf3-1* in the absence of HS but is moderately elevated in *rcf3-1* in the presence of HS (Figure 2-4F). We next examined the expression of another important regulator of HSPs, *Camodulin 3* (*CaM3*), and found no significant differences in *CaM3* expression in *rcf3-1* and the wild type in the presence or absence of HS (Figure 2-4F). Because AtHSBP is a negative regulator for HS responses in *Arabidopsis* (Hsu et al. 2010), we examined expression of *AtHSBP*

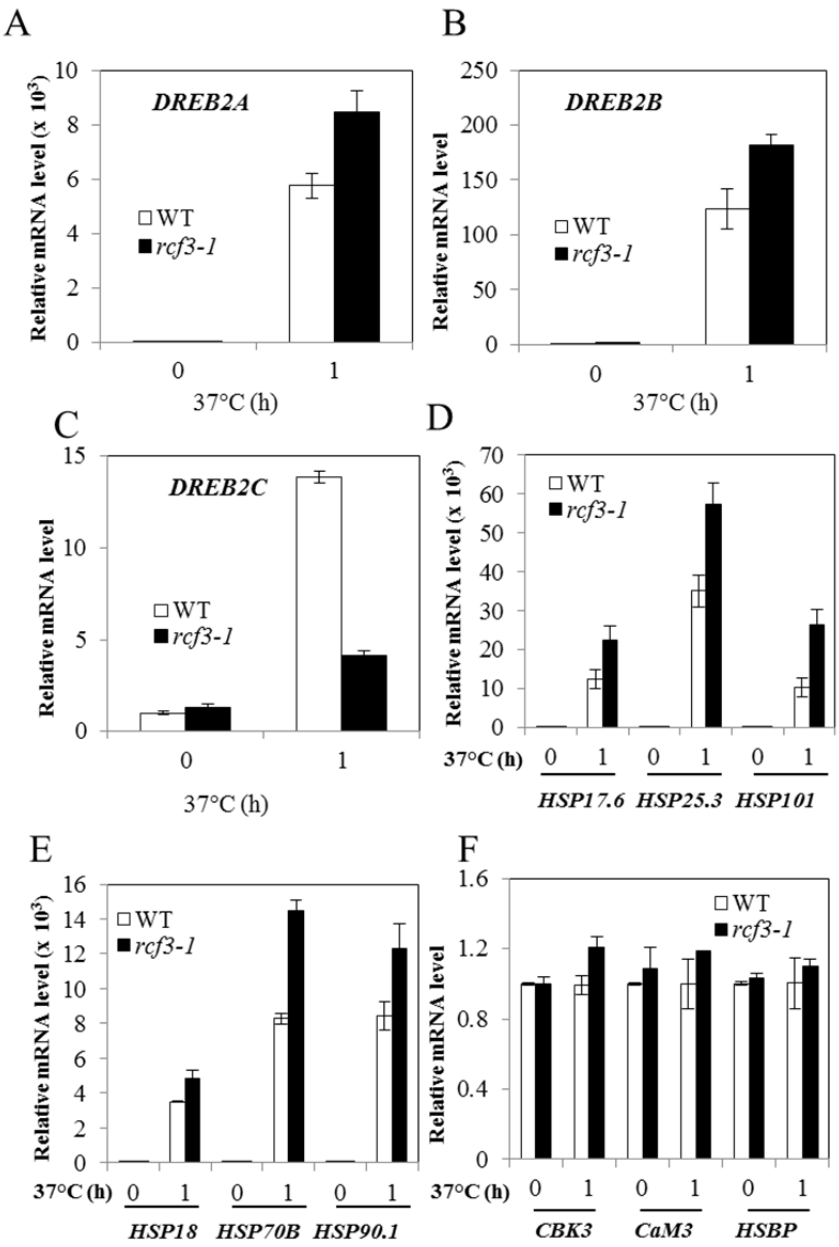

Figure 2-4. Expression of *DREB2s*, *HSPs*, *CBK3*, *CaM3*, and *HSBP* in *rcf3-1*. Expression of *DREB2s*, *HSPs*, *CBK3*, *CaM3*, and *HSBP* in wild-type and *rcf3-1* plants subjected to 0 or 1 h at 37°C. Error bars represent the standard deviation (n = 6).

in *rcf3-1*. As shown in Figure 2-4F, there are no significant differences in *AtHSBP* expression in *rcf3-1* and the wild type in the presence or absence of HS.

The *rcf3-2* Mutation Affects Expression of HS-Responsive Genes and *RCF3* Restores Effects of *rcf3-1* Mutation on Expression of *HSFA2* and *HSP17.6*

We also determined the effect of the *rcf3-2* mutation on the expression of HS-responsive genes. The *rcf3-2* mutation causes elevated accumulation of *HSFA2* and *HSFA7b* (Figure 2-5B and C). Consistent with increased transcripts of *HSFs* in *rcf3-2*, *HSP17.6* is expressed to a much higher level in *rcf3-2* under HS (Figure 2-5D). As was the case with *rcf3-1*, the *rcf3-2* seedlings are more tolerant to HS than wild type (Figure 2-5E). Wild type *RCF3* gene under the control of its native promoter is able to fully restore effects of *rcf3-1* mutation on thermotolerance and expression of *HSFA2* and *HSP17.*6 (Figure 2-5E- G). These data confirm that RCF3 controls expression of HS-responsive genes and is a negative regulator of thermotolerance.

Overexpression of *RCF3* Leads to Down-Regulation of HS-Responsive Genes

We produced transgenic Arabidopsis plants that overexpress *RCF3* (Figure 2-6A). Expression of *HSFA2* and *HSP17.6* under HS is substantially reduced in *RCF3* overexpression plants (Figure 2-6B). Consistently, RCF3 overexpression plants are more sensitive to heat stress (Figure 2-6C). These data further confirm that overall RCF3 is a negative regulator of HS-responsive gene expression.

Discussion

We identified the *RCF3* locus through a forward genetic analysis. The *rcf3-1* mutation appears to affect the expression of the *ProCBF2::LUC* transgene but not of the endogenous *CBF2* or *CBF3*. It is possible that the *rcf3-1* mutation promotes

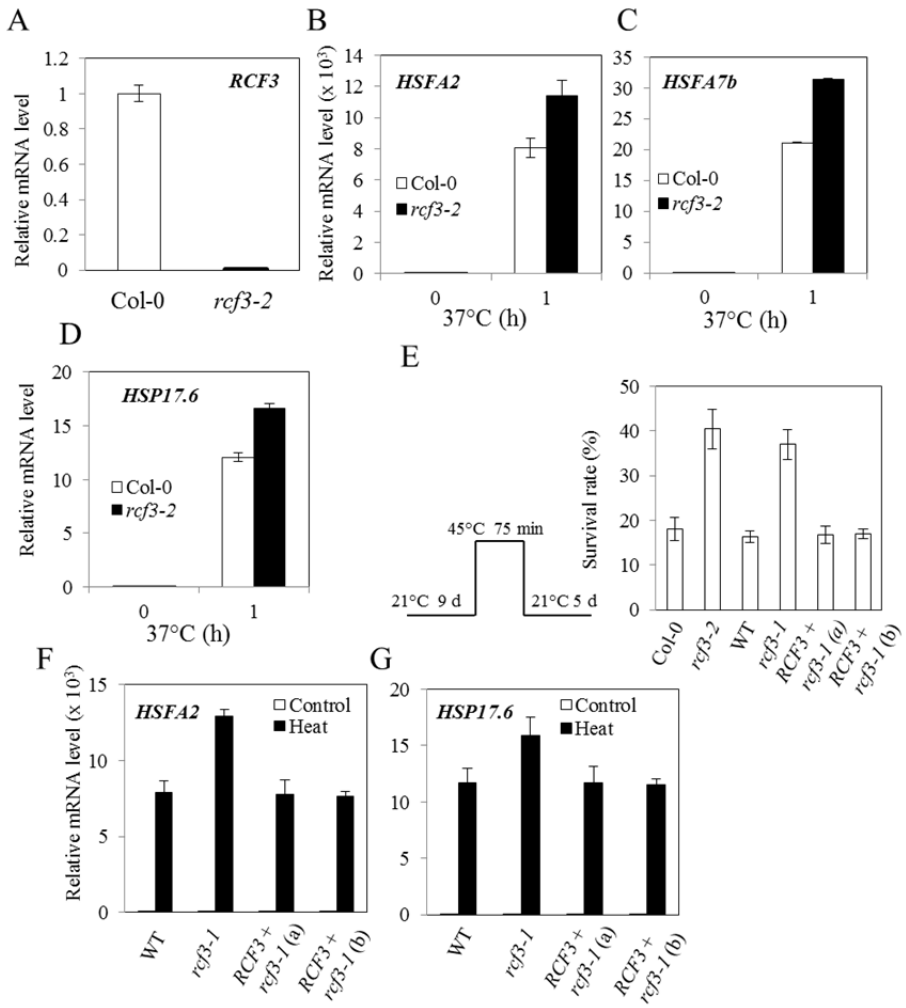

Figure 2-5. Expression of HS-Responsive Genes and Thermotolerance in *rcf3-2* and *rcf3-1* Complementation Lines. (A) Expression of *RCF3* in the wild type and *rcf3-2*. (B)–(D) Expression of HS-responsive genes in wild-type and *rcf3-2* plants subjected to 0 or 1 h at 37°C. (E) Thermotolerance of *rcf3-1*, *rcf3-2* , *RCF3*-pMDC99 in *rcf3-1* [*RCF3* + *rcf3-1* (a)] and *RCF3*-pMDC107 in *rcf3-1* [*RCF3* + *rcf3-1* (b)]. Seedlings (~30 per genotype) were grown on same 1/6 sections of MS agar medium plates. Error bars represent the standard deviation (n = 20; n denotes the number of MS agar medium plates). (F) and (G) Expression of HS-responsive genes in wild-type, *rcf3-1*, [*RCF3* + *rcf3-1* (a)] and [*RCF3* + *rcf3-1* (b)] plants subjected to 0 or 1 h at 37°C. Error bars represent the standard deviation (n = 6).

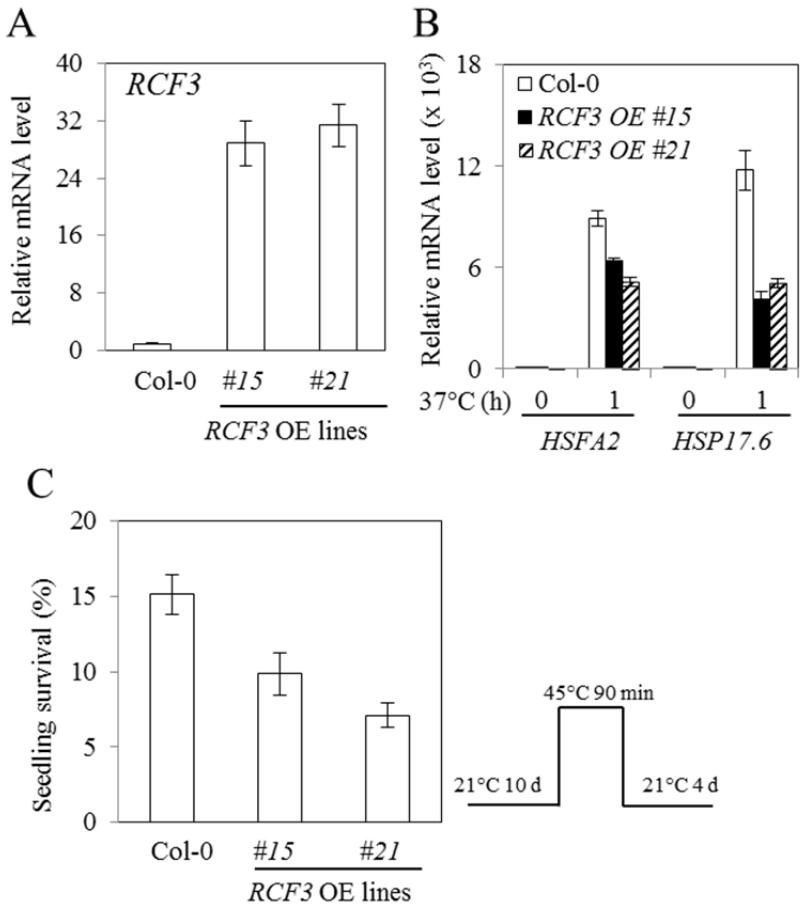

Figure 2-6. Expression of HS-Responsive Genes and Thermotolerance in *RCF3* Overexpression Plants.

(A) Expression levels of *RCF3* in *RCF3* overexpression (OE) plants. (B) Expression of *HSFA2* and *HSP17.6* in RCF3 OE plants. Error bars in (A-B) represent the standard deviation (n = 6). (C) Thermotolerance of *RCF3* OE seedlings. Seedlings of Col-0 and *RCF3* OE lines were grown on the same ¼ section of MS agar medium plate and there are 35-45 seedlings per MS agar medium plate per genotype. Error bars indicate the standard deviation (n = 20; n denotes number of MS agar medium plates).

transcription of *ProCBF2::LUC* or stabilizes its transcripts. Discrepancy between the *ProCBF2::LUC* transgene and the endogenous *CBF2* may be due to difference in *CBF2* promoter sequences. The DNA fragment used for the construction of *ProCBF2::LUC* is a minimal promoter, and it may lack some regulatory sequence present in the native promoter of endogenous *CBF2*. Similar discrepancies have been observed in other mutants such as *hos9* and *hos15*, which when stressed have greatly increased expression of *RD29A::LUC* but only moderately increased expression of endogenous *RD29A* (Zhu et al., 2004; Zhu et al., 2008).

Having determined that *RCF3* is responsive to HS, we investigated the function of RCF3 in HS responses. The nuclear-localized KH domain-containing putative RNA binding protein, RCF3, is an essential regulator of HS-responsive genes and is required for basal thermotolerance. First, we found that RCF3 negatively controls expression of most of the 21 *HSFs* in *Arabidopsis*. *HSFA1a*, *HSFA1b*, and *HSFA1d* are expressed to a much higher level in *rcf3-1* than in the wild type under HS. The increased transcripts of *CBK3* in *rcf3-1* may contribute to the observed higher heat-induction of *HSFA1a*. It seems that CaM3 activity in *rcf3-1* is not altered because there are no detectable changes in transcripts of *CaM3* in *rcf3-1* under HS. The increased activities of three of four HSFA1s may at least partially account for the hyper-accumulation of other *HSFs* and downstream *HSPs* in *rcf3-1* under HS. Second, RCF3 also positively controls expression of some HSFs. Expression of *HSFA1e, HSFA3*, *HSFA6b*, and *HSFB3* is significantly reduced in *rcf3-1* compared to the wild type. *HSFB1* and *HSFB2b* are negative regulators of other *HSFs* and *HSPs* (Ikeda et al., 2011). In *rcf3-1*, both *HSFB1* and *HSFB2b* are significantly up-

regulated. Increased activities of HSFB1 and HSFB2b in *rcf3-1* may lead to the observed less-accumulation of *HSFs* (*HSFA1e, HSFA3*, *HSFA6b*, and *HSFB3*) in *rcf3-1*. Reduction in activity of HSFA1e may also contribute to the overall lower expression of *HSFA3*, *HSFA6b*, and *HSFB3* in *rcf3-1*. Hsu et al. (2010) reported that *AtHSBP* negatively regulates *HSFA1b* and *HSPs*. We did not find significant differences in expression of *AtHSBP* in *rcf3-1* and the wild type in the presence or absence of HS. Therefore, increased heat-induction of *HSFs* and *HSPs* in *rcf3-1* does not result from changed AtHSBP activity. Third, RCF3 controls expression of *DREB2s* that are transcriptional activators of *HSFA3* and other HS-responsive genes. *DREB2A* and DREB2B are expressed to a higher level in *rcf3-1* while expression of *DREB2C* is decreased in *rcf3-1* relative to the wild type. Reduced activity of DREB2C may contribute to the observed decreased expression of *HSFA3* in *rcf3-1*. Fourth, the *rcf3-2* mutation has similar effects on HS-responsive gene expression and thermotolerance as seen in *rcf3-1*. In addition, wild type *RCF3* gene is able to fully restore the effects of *rcf3-1* mutation on HS-responsive gene expression and thermotolerance. Finally, as expected as being a largely negative regulator of HS responses, overexpression of *RCF3* in *Arabidopsis* results in lower heat-induction of HS-responsive genes and reduced thermotolerance. Together, these data indicate that RCF3 is critical for HS-responsive gene regulation and thermotolerance in *Arabidopsis*.

How RCF3 controls expression of *HSFs*, *DREB2s*, and *HSPs* remains to be investigated. We do not know the precise molecular function of RCF3 in the regulation of HS-responsive genes. *RCF3* encodes a nuclear-localized KH domain-

containing putative RNA-binding protein. *Arabidopsis* genome encodes at least 196 RNA recognition motif (RRM)-containing RNA binding proteins. They function in diverse cellular processes and members of glycine-rich RNA-binding proteins (GR-RBPs) are involved in salt, cold, dehydration, and ABA responses (Kim et al., 2005; Kwak et al., 2005; Kim and Kang, 2006; Kim et al., 2007a; Kim et al., 2007b; Kim et al., 2008; Lorković, 2009). Relative to RRM proteins, the K homology (KH) motif which was first discovered in the human hnRNP K protein, is the second most frequently identified RNA-binding domain (Burd and Dreyfuss, 1994). The KH domain is defined by approximately 60 amino acids with a typical pattern of hydrophobic residues and with the core consensus sequence of VIGXXGXXI residing in the middle of the domain (Burd and Dreyfuss, 1994). *Arabidopsis* genome contains at least 26 KH domain-containing proteins (Lorković and Barta, 2002). Except for a few of KH-domain proteins have been reported to play a role in controlling flowering time, vegetative development, and pre-mRNA processing of floral identity gene *AGAMOUS* (*AG*), the biological function of most of the *Arabidopsis* KH domain proteins remains unknown (Chekanova et al., 2002; Cheng et al., 2003; Lim et al., 2004; Mockler et al., 2004; Ripoll et al., 2006). In addition, a KH domain protein SPIN1 is involved in flowering time control in rice and it is negatively regulated and ubiquitinated by the E3 ubiquitin ligase SPL11 (Vega-Sánchez et al., 2008). SPIN1 can bind to both DNA and RNA in vitro assays (Vega-Sánchez et al., 2008). In the case of RCF3, it may need to recruit other critical factors (for example, transcription factors) involved in gene transcription. It is speculated that RCF3 may directly bind to RNAs of *HSFs* or indirectly regulate the binding property of *HSFs* by certain

transcription factors. Consistent with overall more accumulation of HS-responsive genes than the wild type, the *rcf3* mutants are more tolerant to HS. This conclusion is further supported by the observation that overexpression of *RCF3* results in reduced thermotolerance in *Arabidopsis* plants. Nevertheless, we have demonstrated through genetic analysis that RCF3 plays an essential role in gene regulation under HS and acts as a negative factor for basal thermotolerance in *Arabidopsis*.

Methods

Plant Materials and Growth Conditions

A firefly luciferase reporter gene driven by the cold stress-responsive *CBF2* promoter (-1500 bp to -1 bp upstream of the transcription start site) was introduced into *Arabidopsis* plants in the *Columbia glabrous1* (*gl1*) background. Seeds from one homozygous line expressing a single functional copy of the *ProCBF2::LUC* gene (referred to as the wild type) were mutagenized with ethyl methanesulfonate (EMS). The *rcf3-1* mutant with altered *ProCBF2::LUC* gene expression was isolated from M_2 seedlings with a charge-coupled device (CCD) camera imaging system (Ishitani et al. 1997).

Seeds of *rcf3-2* were obtained from the *Arabidopsis* Biological Resource Center (ABRC, Columbus, Ohio) with seed stock number SALK_143161. *Arabidopsis* seedlings on Murashige and Skoog (MS) medium agar plates (1x MS salts, 2% sucrose, 0.6% agar, pH 5.7) were routinely grown under cool, white light (~120 μmol m^{-2} s^{-1}) at 21℃ with a 16-h-light/8-h-dark photoperiod. Soil-grown plants were kept under cool, white light (~100 μmol m^{-2} s^{-1}) with a 16-h-light/8-h-dark

photoperiod at 21℃ with 1:1 ratio of potting soil Metro Mix 360 and LC1 (Sun Gro Horticulture, Bellevue, WA).

Thermotolerance Assays

Nine-d-old seedlings grown on MS agar medium plates were subjected to 21℃ or 45℃ for 75 or 90 min and allowed to grow for an additional 4 d. One-month-old of soil-grown wild type and *rcf3-1* plants were kept at 37℃ under white light (~120 μmol m^{-2} s^{-1}) with a 16-h-light/8-h-dark photoperiod for 4 d.

Genetic Mapping and Complementation

The *rcf3-1* mutant was crossed with the *Landsberg erecta* accession, and 1227 mutant plants were chosen from the F_2 generation based on altered *ProCBF2::LUC* phenotype. Simple sequence length polymorphism (SSLP) markers were designed according to the information in the Cereon *Arabidopsis* Polymorphism Collection and were used to analyze recombination events (Jander et al., 2002). Initial mapping revealed that the *rcf3-1* mutation is located on the lower arm of chromosome 5 between K24M7 and K19E1. Fine mapping within this chromosomal interval narrowed the *RCF3* locus to the BAC clone MNB8. All candidate genes in this BAC were sequenced from the *rcf3-1* mutant and compared with those in GenBank to find the *rcf3-1* mutation.

For complementation of the *rcf3-1* mutant, a 5840-bp genomic DNA fragment that included 2509 bp upstream of the translation initiation codon and 488 bp downstream of the translation stop codon of *At5g53060* was amplified with MNB8 as a template (see Appendix B1 for primer sequences). The amplified fragment was cloned into the pMDC99 binary vector through Gateway technology (Invitrogen).

This construct (pMDC99-RCF3) was then introduced into *rcf3-1* plants by floral dip transformation with *Agrobacterium tumefaciens* strain GV3101 (Clough and Bent, 1998).

Subcellular Localization of RCF3

A 5349-bp genomic DNA fragment that included 2509 bp upstream of the translation initiation codon of *At5g53060* was amplified by PCR and cloned into the pMDC107 vector to make the RCF3-GFP fusion protein. The resulting plasmid (pMDC107-RCF3) was transformed into *Agrobacterium tumefaciens* strain C58C1 and co-infiltrated with *35S:p19* (p19 is a RNA silencing repressor protein from tomato bushy stunt virus [Voinnet et al., 2003]) in *Agrobacterium tumefaciens* strain C58C1 into the leaves of 3-week-old tobacco (*Nicotiana benthamiana*) plants. The infiltrated tobacco plants were grown for an additional 3 d in a growth chamber under a 16-h-light/8-h-dark photoperiod at 21℃. The subcellular localization of RCF3-GFP protein in tobacco leaves was determined with a Leica SP5X confocal microscope (Leica Microsystems). The pMDC107-RCF3 construct was also introduced into *rcf3-1* plants by floral dip transformation with *Agrobacterium tumefaciens* strain GV3101 to test whether the RCF3-GFP protein is functional *in planta*.

Real-Time RT-PCR Analysis

Fourteen-d-old seedlings grown on MS medium (1x MS salts, 2% sucrose, 0.6% agar, pH 5.7) were used for RNA isolation. Total RNA was extracted from the wild type, mutants, and/or transgenic plants with Trizol reagent (Invitrogen) and treated with DNase I (New England Biolabs) for potential genomic DNA contaminations.

For real-time RT-PCR (qRT-PCR) analysis, 5 µg of total RNA was used for synthesis of the first-strand cDNA with the Maxima First-Strand cDNA Synthesis Kit in a total volume of 20 µL (Fermentas). The cDNA reaction mixture was diluted two times, and 5 µL was used as a template in a 20-µL PCR reaction. PCR reactions included a pre-incubation at 95°C for 2 min followed by 45 cycles of denaturation at 95°C for 15 s, annealing at 56°C for 40 s, and extension at 72°C for 45 s. All reactions were performed in the CFX96 Real-Time PCR Detection System (Bio-Rad) using Maxima® SYBR Green/Fluorescein qPCR Master Mix (Fermentas). Each experiment had six biological replicates (three technical replicates for each biological replicate). The comparative Ct method was applied. The primers used in this study are listed in Appendix B1.

ACCESSION NUMBERS

Sequence data from this article can be found in the Arabidopsis Genome Initiative or GenBank/EMBL databases under the following accession numbers: *RCF3* (*At5g53060*), *CBF2* (*At4g25470*), *CBF3* (*At4g25480*), *HSFA1a* (*At4g17750*), *HSFA1b* (*At5g16820*), *HSFA1d* (*At1g32330*), *HSFA1e* (*At3g02990*), *HSFA2* (*At2g26150*), *HSFA3* (*At5g03720*), *HSFA4a* (*At4g18880*), *HSFA5* (*At4g13980*), *HSFA6a* (*At5g43840*), *HSFA6b* (*At3g22830*), *HSFA7a* (*At3g51910*), *HSFA7b* (*At3g63350*), *HSFA8* (*At1g67970*), *HSFB1* (*At4g36990*), *HSFB2a* (*At5g62020*), *HSFB2b* (*At4g11660*), *HSFB3* (*At2g41690*), *HSFB4* (*At1g46264*), *HSFC1* (*At3g24520*), *DREB2A* (*At5g05410*), *DREB2B* (*At3g11020*), *DREB2C* (*At2g40340*), *HSP17.6* (*At5g12030*), *HSP18* (*At5g59720*), *HSP25.3* (*At4g27670*), *HSP70B*

(*At1g16030*), *HSP90.1* (*At5g52640*), *HSP101* (*At1g74310*), *CBK3* (*At2g41140*), *CaM3* (*At3g56800*), and *HSBP* (*At4g15802*).

Acknowledgements

I am grateful to Changlong Wen, Haitao Zeng, and Jianhua Zhu for their contribution to this project. This work was supported by National Science Foundation Grants IOS0919745 and MCB0950242 to J.Z.

Chapter 3: Heat Stress Induction of *miR398* Triggers a Regulatory Loop That Is Critical for Thermotolerance in *Arabidopsis*

Abstract

microRNAs (miRNAs) play important roles in plant growth and development. Previous studies have shown that down-regulation of *miR398* in response to oxidative stress permits up-regulation of one of its target genes, *CSD2* (copper/zinc superoxide dismutase), and thereby helps plants to cope with oxidative stress. We report here that heat stress rapidly induces *miR398* and reduces transcripts of its target genes *CSD1*, *CSD2,* and *CCS* (a gene encoding a copper chaperone for both CSD1 and CSD2). Transgenic plants expressing the *miR398*-resistant forms of *CSD1*, *CSD2*, and *CCS* under their native promoters are more sensitive to heat stress (as indicated by increased damage at the whole plant level and to flowers) than transgenic plants expressing normal coding sequences of *CSD1*, *CSD2*, or *CCS* under their native promoters. In contrast, *csd1*, *csd2*, and *ccs* mutant plants are more heat-tolerant (as indicated by less damage to flowers) than the wild type. Expression of heat stress transcription factors (*HSFs*) and heat shock proteins (*HSPs*) is reduced in the heat-sensitive transgenic plants expressing *miR398*-resistant forms of *CSD1*, *CSD2*, or *CCS* but is enhanced in the heat-tolerant *csd1*, *csd2*, and *ccs* plants. Chromatin immunoprecipitation (ChIP) assays revealed that HSFA1b and HSFA7b are the two HSFs responsible for the heat-induction of *miR398*. Together, our results suggest that plants use a previously unrecognized strategy to achieve thermotolerance, especially

for the protection of reproductive tissues. This strategy involves the down-regulation of *CSDs* and their copper chaperone *CCS* through the heat-inducible *miR398*.

Keywords: *miR398*, heat stress, CSDs, CCS, HSF, *Arabidopsis*.

Introduction

microRNAs (miRNAs) are non-coding RNAs approximately 20 to 24 nucleotides (nt) long that were first identified in *Caenorhabditis elegans* and then found in other animals and plants (Lee et al., 1993; Llave et al., 2002; Reinhart et al., 2002; Rhoades et al., 2002; Lim et al., 2003; Palatnik et al., 2003). miRNAs are processed from their precursors, which have imperfect stem-loop or hairpin structures, by RNase III-like Dicer enzymes in animals or Dicer-like (DCL) proteins in plants. miRNAs play important regulatory roles in plants by targeting messenger RNAs (mRNAs) for cleavage or translational repression (Bartel, 2004; Beauclair et al., 2010; Yu and Wang, 2010; Yang et al., 2012). Many miRNAs are important for plant growth and development (Jones-Rhoades and Bartel, 2004; Baker et al., 2005; Lauter et al., 2005; Jones-Rhoades et al., 2006; Reyes et al., 2007; Zhou et al., 2007). An increasing number of reports demonstrate that miRNAs are also key regulators in plant responses to nutrient homeostasis and to biotic and abiotic stresses (Sunkar and Zhu, 2004; Jones-Rhoades et al., 2004; Fujii et al., 2005; Khraiwesh et al., 2012).

Superoxide dismutase (SOD) is an important reactive oxygen species (ROS) scavenging enzyme that catalyzes the conversion of superoxide radicals to H_2O_2 and O_2, a reaction that constitutes the first cellular defense against oxidative stress (Fridovich, 1995). Plants have evolved three types of SODs differing in metal

ligands: iron SOD (Fe-SOD), manganese SOD (Mn-SOD), and copper-zinc SOD (Cu/Zn-SOD, also known as CSD) (Bowler et al., 1992). Cu/Zn-SOD is a major copper enzyme in plants. *Arabidopsis* genome encodes three CSD isozymes: CSD1 in the cytoplasm, CSD2 in chloroplasts, and CSD3 in peroxisomes (Kliebenstein et al., 1998). In *Arabidopsis*, *miR398* has four target genes: *CSD1*, *CSD2*, *CCS* (*CCS* is encoded by *At1g12520*, is a copper chaperone of CSD1 and CSD2, and delivers copper to these two SODs), and *COX5b-1* (a zinc-binding subunit of cytochrome c oxidase encoded by *At3g15640*) (Jones-Rhoades and Bartel, 2004; Sunkar and Zhu, 2004; Cohu et al., 2009; Beauclair et al., 2010). When plants are exposed to high light, heavy metals (Cu^{2+}, Fe^{3+}), or methyl viologen (MV), expression of the *miR398* is down-regulated, which permits the up-regulation of one of its target genes, *CSD2* (Sunkar et al., 2006). Overexpression of a *miR398*-resistant version of *CSD2* leads to improved plant performance under oxidative stress caused by high light, heavy metals, and MV (Sunkar et al., 2006).

Heat stress adversely affects the distribution and productivity of horticultural and agricultural important plants worldwide. When the temperature rises $\geq$ 5°C above the optimum, it is experienced as heat stress by all living organisms including plants. Heat stress disrupts normal functions of cellular processes, can severely delay plant growth and development, and can even result in death. A central component of responses to heat stress in all living organisms is the induction of heat shock proteins (HSPs) through the action of heat stress transcription factors (HSFs). HSPs are grouped into five classes based on their approximate molecular weights in kDa: HSP100, HSP90, HSP70, HSP60, and small heat shock proteins (sHSPs, 15–30 kDa)

(Iba, 2002). HSPs function as molecular chaperones essential for maintenance and/or restoration of protein homeostasis. HSFs recognize heat stress elements (HSE: 5'-GAAnnTTC-3') conserved in promoters of heat stress-responsive genes including *HSPs* (Busch et al., 2005). Plant genomes encode a family of HSFs with more than 20 members, and plant HSFs are grouped into three classes (A, B, and C) according to their oligomerization domains (Nover et al., 2001; Baniwal et al., 2004). The interplay and complexity among HSFs in plants are being actively studied, and research has established that HSFA1 members act as master regulators of heat stress responses and of the remaining HSFs in tomato and *Arabidopsis* (Mishra et al., 2002; Liu et al., 2011; Nishizawa-Yokoi et al., 2011; Yoshida et al., 2011). However, the more upstream regulators of HSFs remain to be identified.

We are interested in determining whether any miRNAs might have a role in heat stress responses in plants. We found that, in *Arabidopsis* subjected to heat stress, one miRNA, *miR398*, is rapidly induced and all three of its target genes (*CSD1*, *CSD2*, and *CCS*) are down-regulated. Transgenic plants expressing a *miR398*-resistant version of *CSD1*, *CSD2*, or *CCS* are hypersensitive to heat stress, and expression of many heat stress-responsive genes (*HSF*s and *HSP*s) under heat is reduced in these plants. In contrast, expression levels of *HSF*s and *HSP*s in *csd1*, *csd2*, and *ccs* mutant plants are increased, and *csd1*, *csd2*, and *ccs* plants are more tolerant of heat stress than wild-type plants. We also identified two HSFs (HSFA1b and HSFA7b) that are responsible for the heat-induction of *miR398*. Together, our results reveal an essential regulatory loop for plant thermotolerance that involves *HSFs*, *miR398* and its target genes C*SD1*, *CSD2*, and *CCS*.

Results

miR398 Is Induced by Heat Stress

To study the physiological and molecular function of miRNAs in plant heat stress response, we examined the expression profiles of known miRNAs under heat stress with *Arabidopsis* seedlings grown on MS medium by small RNA Northern hybridization analysis. *miR393* is moderately down-regulated by heat stress while *miR169* is slightly induced by heat stress (Figure 3-2A). We also observed that *miR398* is quickly induced by heat stress at 37ºC and reaches its peak level 2 h after heat stress is initiated (Figure 3-1A). In *Arabidopsis*, the *miR398* family is encoded by three loci (*miR398a*, *miR398b*, and *miR398c*) (Bonnet et al., 2004; Jones-Rhoades and Bartel, 2004; Sunkar and Zhu, 2004). Mature *miR398* sequences produced by the three *miR398* genes are nearly identical (Figure 3-1B). Real-time RT-PCR (qRT-PCR) analysis revealed that expression of *miR398* precursors is also elevated under heat stress and that heat stress induces the expression of *miR398b* to a much higher level than that of the other two *miR398* precursors (Figure 3-1C). We produced transgenic *Arabidopsis* plants expressing a *GUS* reporter gene under the control of the *miR398b* promoter (*miR398b:GUS*) or the *miR398c* promoter (*miR398c:GUS*). The *miR398b:GUS* is heat-inducible (Figure 3-1D). These results suggest that potential *cis* elements present in the promoter regions of *miR398b* may be recognized by certain HSFs under heat stress. Consistent with the subtle level of heat-induction of *miR398c*, *miR398c:GUS* is constitutively expressed (Figure 3-1D). Yamasaki et al. (2009) reported that *SPL7* (SQUAMOSA promoter binding protein–like7) can activate *miR398* transcription under low-copper conditions through directly binding of the

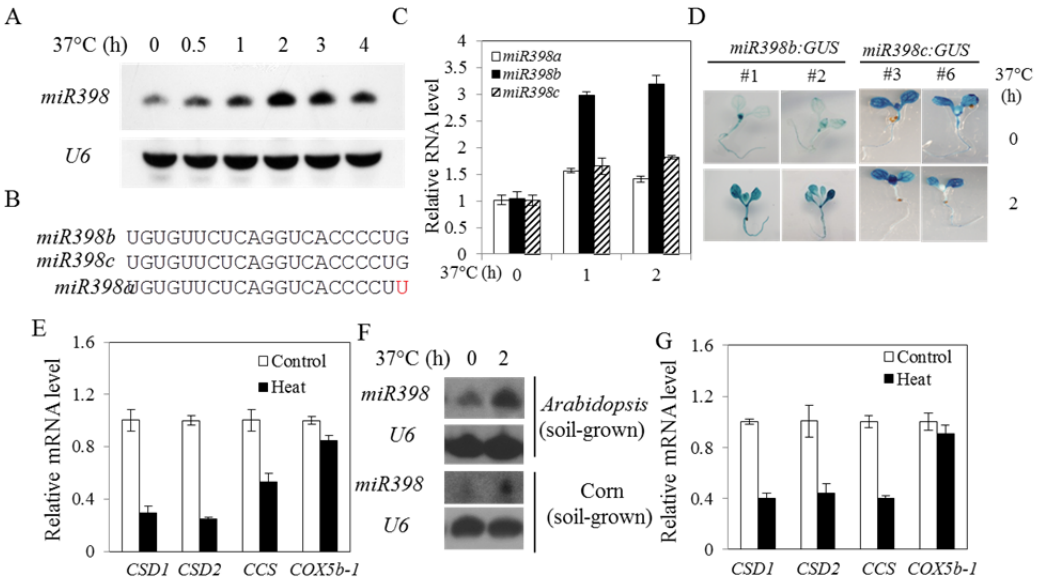

Figure 3-1. Expression of *miR398* Under Heat Stress.

(A) *miR398* expression in response to heat stress as determined by small RNA Northern hybridizations. Small RNA U6 was used as the loading control. (B) Alignment of three mature *miR398* isoforms in *Arabidopsis*. (C) Expression of precursors of *miR398* in response to heat stress. (D) Expression patterns of *miR398b:GUS* or *miR398c:GUS* in two independent lines of transgenic *Arabidopsis* plants subjected to 0 or 2 h of heat stress at 37°C. (E) Expression levels of four *miR398* target genes in wild-type plants subjected to 0 (Control) or 2 h (Heat) of heat stress at 37°C. (F) Expression of *miR398* in soil-grown wild type plants of *Arabidopsis* (one-month-old) and corn (15-d-old) at 37°C for 0 or 2 h. (G) Expression of *miR398* targets genes in one-month-old soil-grown wild type plants subjected to 0 (Control) or 2 h (Heat) of heat stress at 37°C. Error bars in (C), (E) and (G) represent the standard deviation (n = 6).

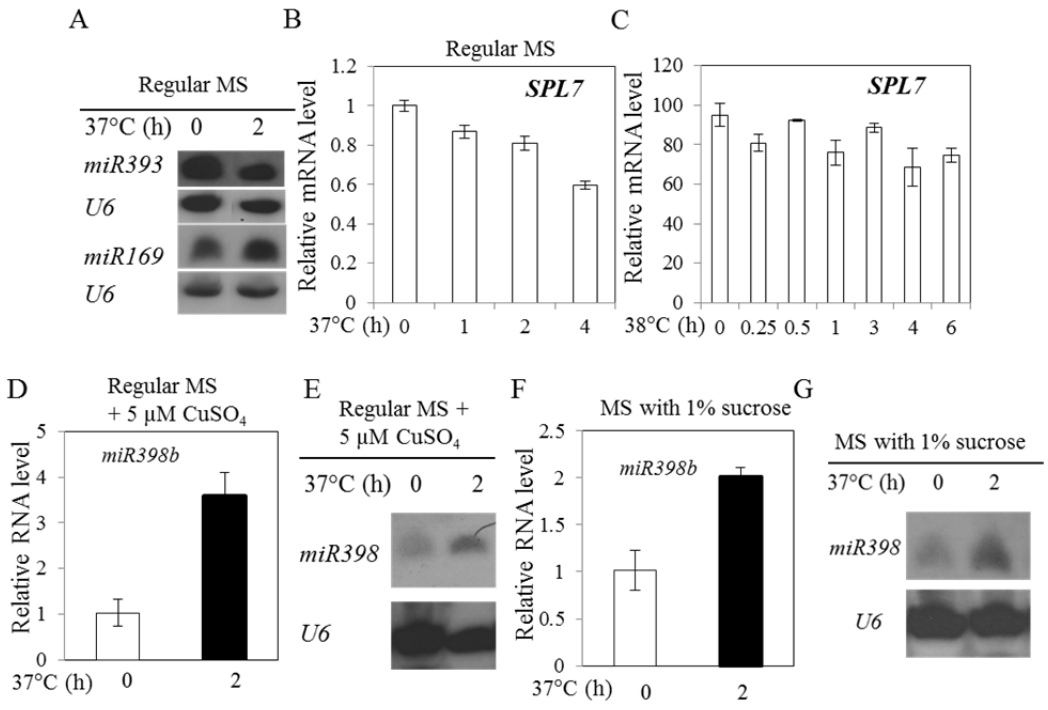

Figure 3-2. Expression of *miR169*, *miR393*, and *SPL7* under Heat Stress, and Heat-Induction of *miR398* under Low Sucrose and High Copper Conditions. Total RNA (for [B], [D] and [F]) and low molecular weight RNAs (for [A], [E] and [G]) were extracted from 15-d-old seedlings grown on various growth media subjected to heat stress for 0 or 2 h at 37°C. (A) Small RNA Northern hybridizations for *miR169*, *miR393*, and *U6*. (B) *SPL7* expression under heat stress. (C) *SPL7* expression in aerial tissues of wild type *Arabidopsis* seedlings under heat stress. Data are collected from publically available gene expression profiles as described (Kilian et al. 2007). (D) Expression of *miR398* precursor b (*miR398b*) determined by qRT-PCR. (E) Small RNA Northern hybridizations for *miR398* and *U6*. (F) Expression of *miR398* precursor b (*miR398b*) determined by qRT-PCR. (G) Small RNA Northern hybridizations for *miR398* and *U6*. Error bars represent the standard deviation (n = 5 in [B], [D] and [F]; n = 2 in [C]).

miR398c promoter. The low-copper conditions ([Cu] = 0.1 μM in growth medium) described by Yamasaki et al. (2009) are the same as the regular MS medium used in this study (see Experimental procedures for details). We examined *SPL7* expression under heat stress with wild type seedlings grown on MS medium to determine whether *SPL7* is responsive to heat stress. qRT-PCR analysis showed that *SPL7* is down-regulated under heat stress (Figure 3-2B). These results are consistent with *SPL7* expression patterns in aerial tissues of *Arabidopsis* wild type seedlings under heat stress summarized from publically available gene expression data (Figure 3-2C; Kilian et al., 2007). We also investigated *miR398b* expression by qRT-PCR and *miR398* expression by small RNA Northern hybridization analysis with wild-type plants grown on MS medium supplemented with 5 μM $CuSO_4$ under heat stress. The 5 μM $CuSO_4$ present in the growth medium is sufficient to dramatically repress *miR398* expression (Yamasaki et al., 2007; Yamasaki et al., 2009). We found that *miR398b* and *miR398* are up-regulated by heat stress in plants grown on MS medium supplemented with 5 μM $CuSO_4$ (Figure 3-2D, E). These results suggest that elevated mature *miR398* expression under heat stress in the current study is not due to increased expression of *miR398c* and its activator *SPL7*. These results further suggest that the increased expression of *miR398* under heat stress in the current study is a response to heat stress and not to low copper level in growth medium.

Another potential concern is that the 2% sucrose used in our growth medium (see Experimental procedures for details) may increase *miR398* expression; *miR398* expression increases when sucrose levels increase from 0 to 3% in plant growth medium (Dugas and Bartel, 2008). Because heat induces the *miR398* precursor

miR398b and mature *miR398* in plants grown on a medium containing only 1% sucrose (Figure 3-2F, G), we conclude that the increased expression of *miR398* under heat stress in the current study is a response to heat stress and not to high sucrose levels.

qRT-PCR analysis indicated that expression of three of four *miR398* target genes (*CSD1*, *CSD2*, and *CCS*) is down-regulated by heat stress (Figure 3-1E). Dugas and Bartel (2008) observed that transcript levels of *COX5b-1* did not decrease in transgenic plants overexpressing *miR398c* suggesting that *COX5b-1* is a poor target of *miR398*. In this study, we found that *COX5b-1* is not responsive to heat stress, suggesting that it may not be targeted by *miR398* under heat stress (Figure 3-1E). These results are further confirmed by the publically available expression data on these genes using aerial tissues of wild type *Arabidopsis* seedlings under heat stress (Kilian et al., 2007).

We also examined expression of *miR398* and its four target genes in one-month-old soil-grown *Arabidopsis* plants under heat stress. Mature *miR398* expression is strikingly induced by heat stress (Figure 3-1F) and expression of three of four *miR398* target genes (*CSD1*, *CSD2*, and *CCS*) is dramatically decreased under heat stress (Figure 3-1G). The expression of *COX5b-1* in soil-grown *Arabidopsis* plants is similar to the case of MS medium-grown *Arabidopsis* seedlings (Figure 3-1G). These results further confirmed *miR398* is induced by heat stress. Furthermore, we examined whether *miR398* is up-regulated under heat stress in 15-d-old soil-grown corn plants. As shown in Figure 3-1E, *miR398* is moderately induced by heat stress in corn plants.

Transgenic plants expressing the *miR398*-resistant forms of *CSD1*, *CSD2* or *CCS* are defective in heat-responsive gene regulation and are more sensitive to heat stress

To study the significance of heat-induction of *miR398*, we generated transgenic plants expressing the *miR398*-resistant forms of *CSD1*, *CSD2*, or *CCS* under the control of their native promoters (Figure 3-3A-C). Transgenic plants expressing the normal forms of *CSD1*, *CSD2*, or *CCS* under the control of their native promoters were used as controls (Figure 3-3A-C). We first determined the thermotolerance of these transgenic plants. All transgenic plants expressing the *miR398*-resistant forms of *CSD1*, *CSD2*, or *CCS* became more sensitive to heat stress at 37°C (as indicated by increased damage at the whole plant level and to flowers) than wild-type or control plants that express the normal forms of *CSD1*, *CSD2*, or *CCS* (Figure 3-4). These results suggest that heat tolerance requires the down-regulation of CSD1, CSD2, and their copper chaperone CCS. We then examined the expression of heat stress-responsive genes in these transgenic plants. Compared to their expression in wild-type or control plants, expression of four *HSF* genes (*HSFA1e*, *HSFA2*, *HSFA3*, and *HSFA7b*) was reduced substantially in all transgenic plants expressing the *miR398*-resistant forms of *CSD1*, *CSD2*, or *CCS* (Figure 3-5A-D). Expression levels of three *HSP* genes (*HSP17.6*, *HSP70B*, and *HSP90.1*) were strongly decreased (relative to their expression in wild-type or control plants) in all transgenic plants expressing the *miR398*-resistant forms of *CSD1*, *CSD2*, or *CCS* (Figure 3-5E-G).

Loss-of-Function Mutants *csd1*, *csd2*, and *ccs* Show Enhanced Heat-Responsive Gene Expression and Are More Heat-Tolerant

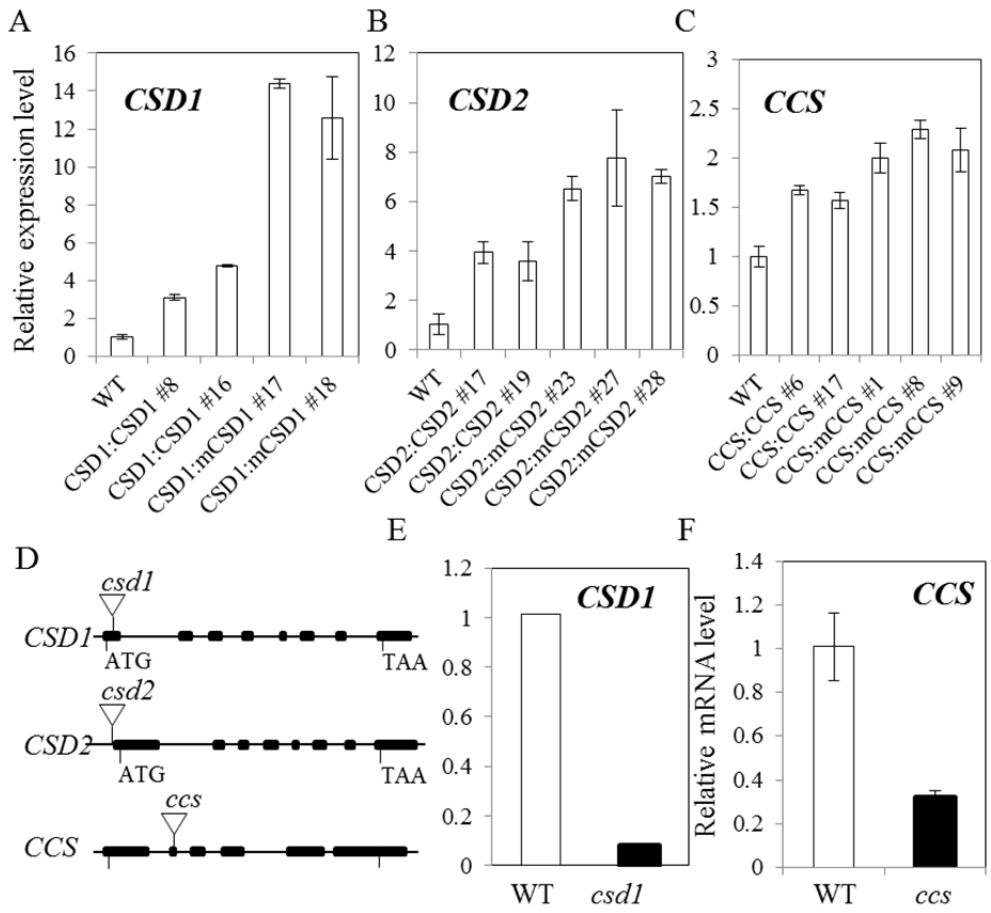

Figure 3-3. Expression Levels of *CSD1, CSD2,* and *CCS* in Ccorresponding Transgenic Plants and Expression of *CSD1* and *CCS* in *csd1* and *ccs* Mutant Plants. (A) Expression levels of *CSD1* in transgenic plants expressing regular and *miR398*-resistant forms of *CSD1* driven by *CSD1* native promoter. (B) Expression levels of *CSD2* in transgenic plants expressing regular and *miR398*-resistant forms of *CSD2* driven by *CSD2* native promoter. (C) Expression levels of *CCS* in transgenic plants expressing regular and *miR398*-resistant forms of *CCS* driven by *CCS* native promoter. (D) Positions of T-DNA insertions in genomes of *csd1*, *csd2*, and *ccs* mutant plants. Black boxes indicate exons and lines between black boxes indicate introns. (E) Expression of *CSD1* in *csd1* mutant. (F) Expression of *CCS* in *ccs* mutant. Error bars represent the standard deviation (n = 5).

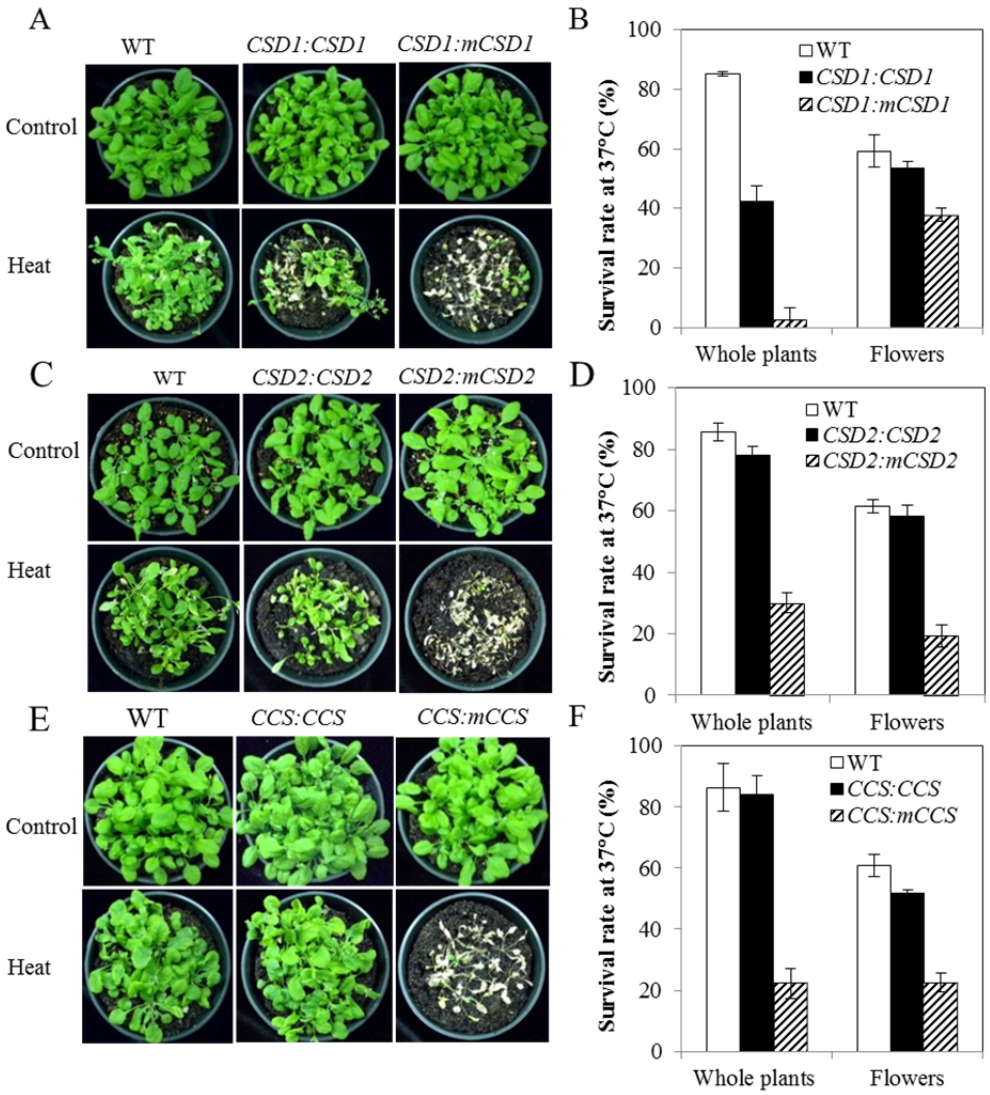

Figure 3-4. Thermotolerance of *CSD1*, *CSD2*, and *CCS* Transgenic Plants.

(A) Thermotolerance of wild-type (WT), and transgenic plants expressing regular form or the *miR398*-resistant form of *CSD1* (*mCSD1*) under the control of its native promoter (referred to as *CSD1* transgenic plants thereafter). Three-week-old soil-grown plants were subjected to 0 (Control) or 7 d (Heat) at 37°C, and damage was recorded 4 d later. (B) Survival rates of *CSD1* transgenic plants as shown in (A) and flowers of separate batches of 1-month-old *CSD1* transgenic plants under heat stress (37°C for 4 d). Flowers which fail to produce viable siliques are considered as dead (Same definition applies hereinafter). (C) Thermotolerance of wild-type (WT), and transgenic plants expressing regular form or the *miR398*-resistant form of *CSD2* (*mCSD2*) under the control of its native promoter (referred

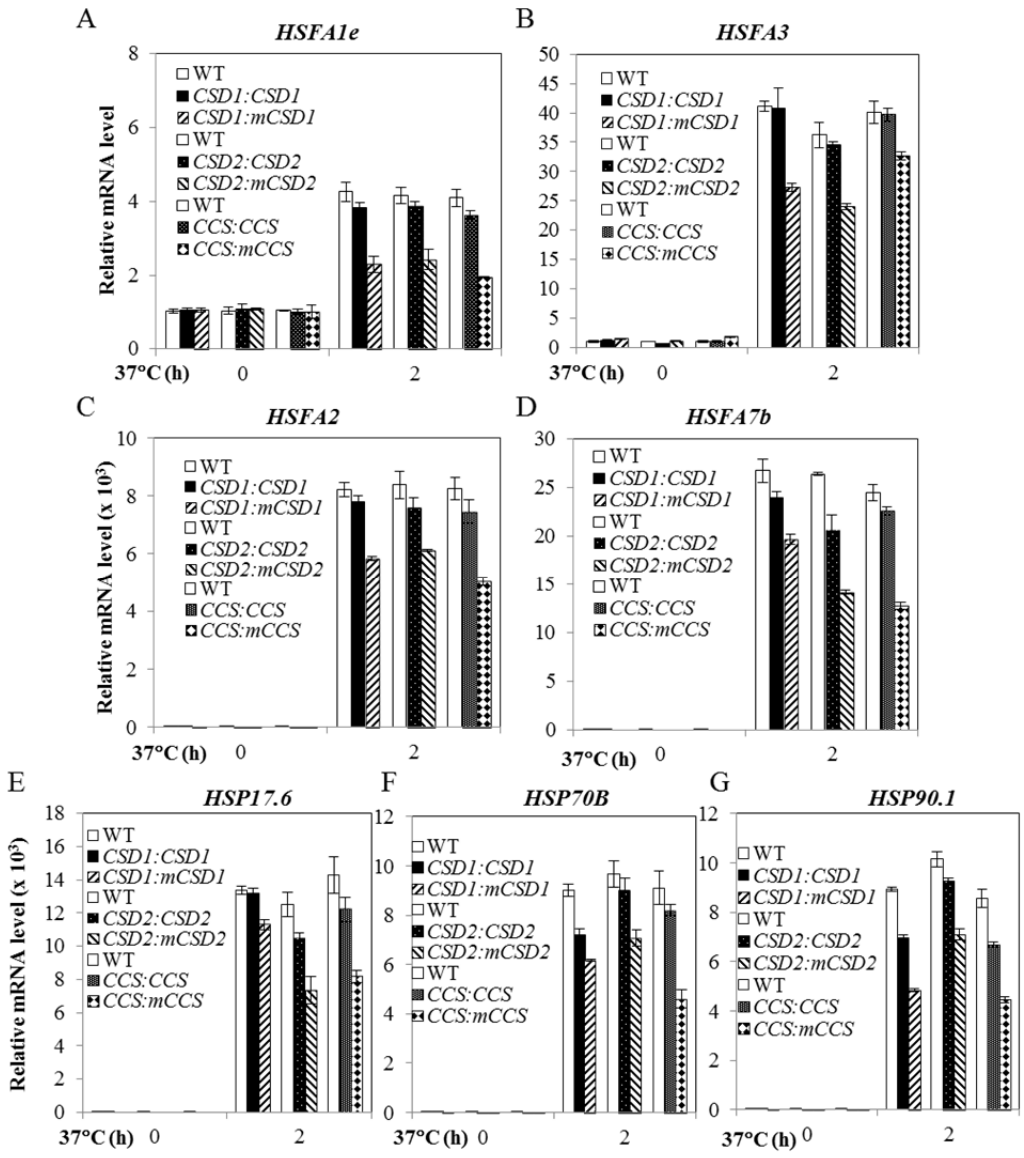

Figure 3-5. Expression Patterns of Heat Stress-Responsive Genes in *CSD1*, *CSD2*, and *CCS* Transgenic Plants. (A–G) Expression of *HSFs* and *HSPs* in *CSD1*, *CSD2*, and *CCS* transgenic plants subjected to 0 or 2 h at 37°C. Error bars represent the standard deviation (n = 5). Data in Figure 3-5 are from one representative individual transgenic plant of each transgene. There are two to three independent transgenic plants per transgene (Figure 3-3A-C).

to as *CSD2* transgenic plants thereafter) under conditions described in (A). (D) Survival rates of *CSD2* transgenic plants as shown in (C) and flowers of separate batches of 1-month-old *CSD2* transgenic plants under heat stress (37°C for 4 d). (E) Thermotolerance of wild-type (WT), and transgenic plants expressing regular form or the *miR398*-resistant form of *CCS* (*mCCS*) under the control of its native promoter (referred to as *CCS* transgenic plants thereafter) under conditions described in (A). (F) Survival rates of *CCS* transgenic plants as shown in (E) and flowers of separate batches of 1-month-old of *CCS* transgenic plants under heat stress (37°C for 4 d). Error bars represent the standard deviation (n = 50–100). Data in Figure 3-4 are from one representative individual transgenic plant of each transgene. There are two to three independent transgenic plants per transgene (Figure 3-3A-C).

To better understand the role of *miR398*, *CSD1*, *CSD2*, and *CCS* under heat stress, we isolated loss-of-function mutants of *CSD1* and *CCS* genes (Figure 3-3D-F) and obtained the knock-down mutant of *CSD2* (Figure 3-3D; Rizhsky et al., 2003). Compared to the wild-type plants, the *csd1*, *csd2*, and *ccs* mutant plants are more tolerant of heat stress at 37°C, as indicated by reduced damage to flowers (Figure 3-6A). The improved thermotolerance in *csd1*, *csd2*, and *ccs* mutant plants is correlated with enhanced expression of *HSFs* and *HSPs* (Figure 3-6B-H). These results further confirm that *CSD1*, *CSD2*, and *CCS* are negative regulators of heat stress-responsive genes and thermotolerance.

ROS Accumulation in *CSD1*, *CSD2*, and *CCS* Transgenic Plants and Loss-of-Function *csd1*, *csd2*, and *ccs* Mutant Plants

To investigate whether changed heat stress-responsive gene expression and thermotolerance are due to changed redox status under heat stress, we measured ROS levels in transgenic plants expressing the *miR398*-normal or -resistant forms of *CSD1*, *CSD2* or *CCS*, and in loss-of-function *csd1*, *csd2*, and *ccs* mutant plants.

We first measured the ROS levels in *CSD1, CSD2,* and *CCS* transgenic plants. Without heat stress, all the transgenic plants expressing the *miR398*-resistant or normal forms of *CSD1*, *CSD2*, or *CCS* accumulate slightly lower levels of superoxide radicals (as indicated by NBT staining) than wild-type plants (Figure 3-7A). Under heat stress, transgenic plants expressing the *miR398*-resistant forms of *CSD1*, *CSD2*, or *CCS* accumulate much lower levels of superoxide radicals than wild type and control plants that express normal forms of *CSD1*, *CSD2*, or *CCS* (Figure 3-7A). As for hydrogen peroxide (H_2O_2) accumulation (as indicated by DAB staining), all

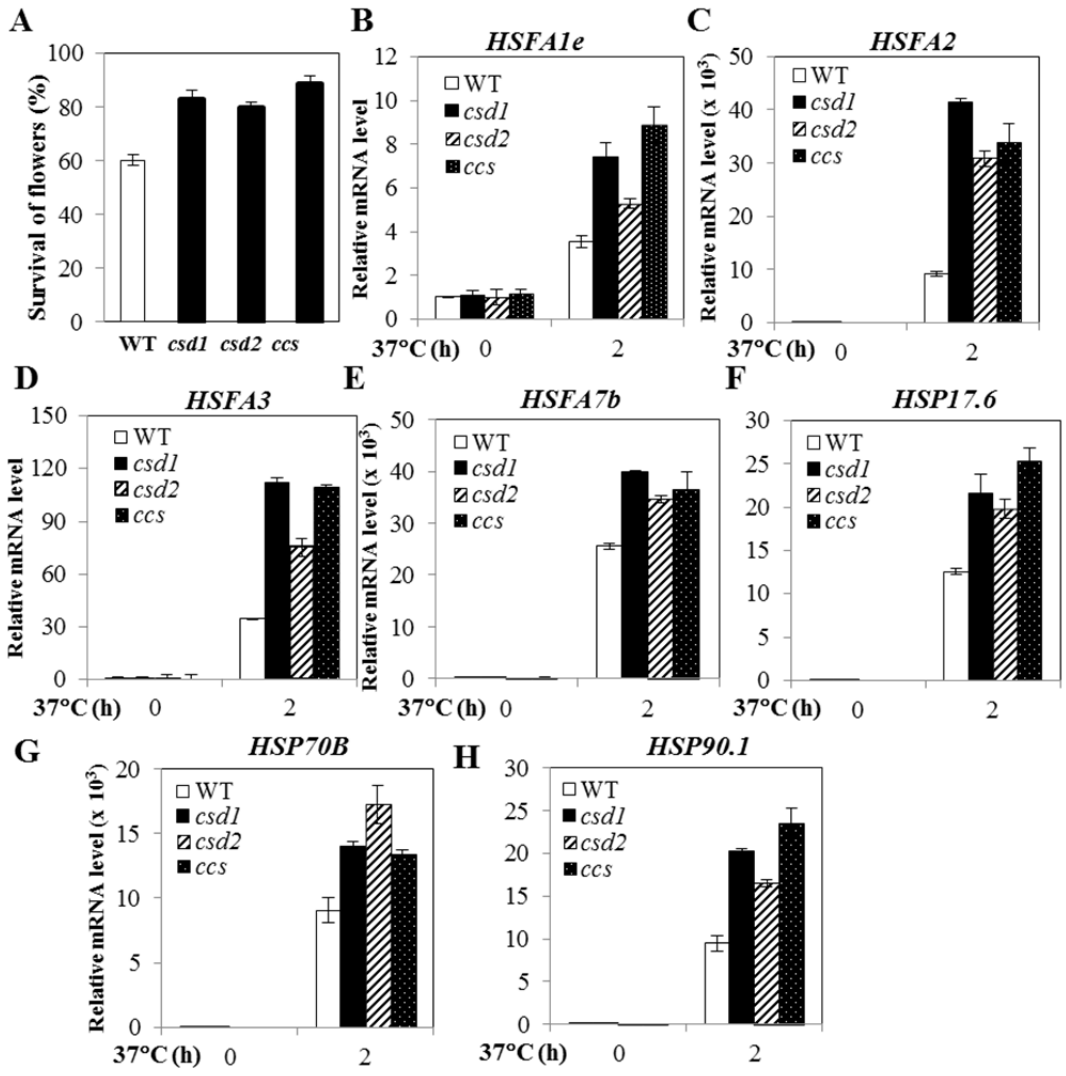

Figure 3-6. Survival Rate of Flowers and Expression Levels of *HSFs* and *HSPs* in *csd1*, *csd2*, and *ccs* Mutant Plants. (A) Survival rate of flowers of wild type (WT), *csd1*, *csd2*, and *ccs* plants under heat stress. One-month-old soil-grown plants were subjected to 10 d at 37°C, and damage to flowers was recorded 4 d later. Error bars represent the standard deviation (n = 50–100). (B–H) Expression of *HSFs* and *HSPs* in WT, *csd1*, *csd2*, and *ccs* seedlings subjected to 0 or 2 h at 37°C. Error bars represent the standard deviation (n = 5).

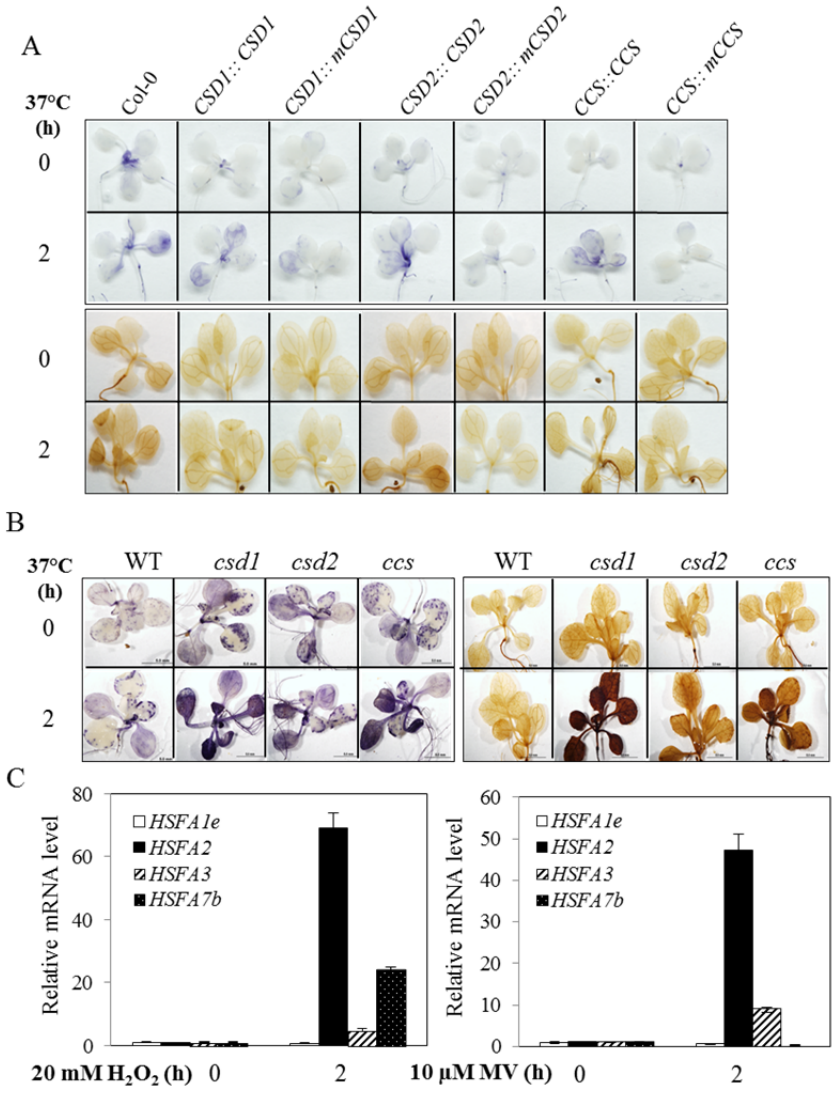

Figure 3-7. ROS Accumulation in *CSD1*, *CSD2*, and *CCS* Transgenic Plants, and *csd* , *ccs* Mutants Under Heat Stress and Heat-Induction of *HSFs* Under Oxidative Stress. (A) NBT staining for superoxide free radicles (left panel) and DAB staining for H_2O_2 (right panel). (B) NBT staining for superoxide free radicles (top panel) and DAB staining for H_2O_2 (bottom panel) (C) Expression of *HSFs* in plants treated with H_2O_2 and methyl viologen (MV). Error bars in (B) represent the standard deviation (n = 5).

transgenic plants expressing the *miR398*-resistant or normal forms of *CSD1*, *CSD2*, or *CCS* accumulate similar amounts of H_2O_2 as wild type plants under control conditions (Figure 3-7A). Under heat stress, transgenic plants expressing the *miR398*-resistant forms of *CSD1*, *CSD2*, or *CCS* accumulate slightly lower levels of H_2O_2 than wild-type plants (Figure 3-7A). We also determined ROS levels in *csd1*, *csd2*, and *ccs* mutant plants under heat stress. Without heat stress, *csd1*, *csd2*, and *ccs* mutant plants accumulate slightly higher levels of superoxide radicals (as indicated by NBT staining) than wild-type plants (Figure 3-7B). With heat stress, the *csd1*, *csd2*, and *ccs* mutant plants accumulate much higher levels of superoxide radicals than wild-type plants (Figure 3-7B). The pattern is similar for H_2O_2. Without heat stress, H_2O_2 accumulation is similar in *csd1*, *csd2*, and *ccs* and their wild-type controls (Figure 3-7B). With heat stress, however, H_2O_2 levels are much higher in *csd1*, *csd2*, and *ccs* mutant plants than in wild-type plants (Figure 3-7B). These results indicate that altered expression of *CSD1*, *CSD2*, and *CCS* genes changes the redox status of cells.

HSFs Are Responsive to Oxidative Stress

It is known that altered redox status can affect expression of heat-responsive genes including *HSFs* and *HSPs* (Desikan et al., 2001; Vandenabeele et al., 2003; Volkov et al., 2006). The altered ROS accumulation results suggested that the effects of CSD1, CSD2 or CCS on heat-responsive gene expression may be due to their impact on ROS. We performed qRT-PCR analysis to determine whether oxidative stress affects expression of *HSFA1e*, *HSFA2*, *HSFA3*, and *HSFA7b* that displayed altered expression patterns in *CSD1*, *CSD2* or *CCS* transgenic plants and their loss-of-function mutant plants. H_2O_2 induces the expression of *HSFA2*, *HSFA3,* and

HSFA7b, but not of *HSFA1e* (Figure 3-7C). Methyl viologen (MV) also induces the expression of *HSFA2* and *HSFA3* but not of *HSFA1e* or *HSFA7b* (Figure 3-7C). These results support the hypothesis that the expression of *HSFs* is responsive to redox status, which is in turn regulated by CSD1, CSD2, and CCS.

HSFA1b and HSFA7b Bind Directly to the Promoter Regions of *miR398b*

Heat stress elements (HSE: 5'-GAAnnTTC-3') were found in the promoter regions of all three *miR398* genes. Because only *miR398b* is strongly responsive to heat stress (Figure 3-1C,D), we therefore generated transgenic plants expressing FLAG-tagged HSFs under the control of their native promoters in *Arabidopsis* to search for HSFs that can bind to promoter of *miR398b* under heat stress (Figure 3-8A-E). We then performed chromatin immunoprecipitation (ChIP) assays followed by real-time PCR (qPCR) analysis (ChIP-qPCR). We found that HSFA1b and HSFA7b, but not HSFA1a, HSFA7a or HSFB2a are able to bind directly to the promoter regions of *miR398b* where core HSEs are located (Figure 3-9A, B; Figure 3-8F-H). Thus, we have identified two HSFs that are responsible for the heat-induction of *miR398*.

Discussion

We have shown that the heat-inducible *miR398* is required for thermotolerance through the down-regulation of its target genes (*CSD1*, *CSD2*, and *CCS*). *miR398* is up-regulated by heat stress, and this up-regulation is not due to high sucrose in the growth medium (Figure 3-1A,C,D,F; Figure 3-2F,G). Previous report showed that endogenous sucrose levels increased at warmer temperatures (31°C [light]/29°C[dark]) at the end of light period in mature leaves of potato plants while sucrose levels remained essentially the same at the end of dark period (Lafta and

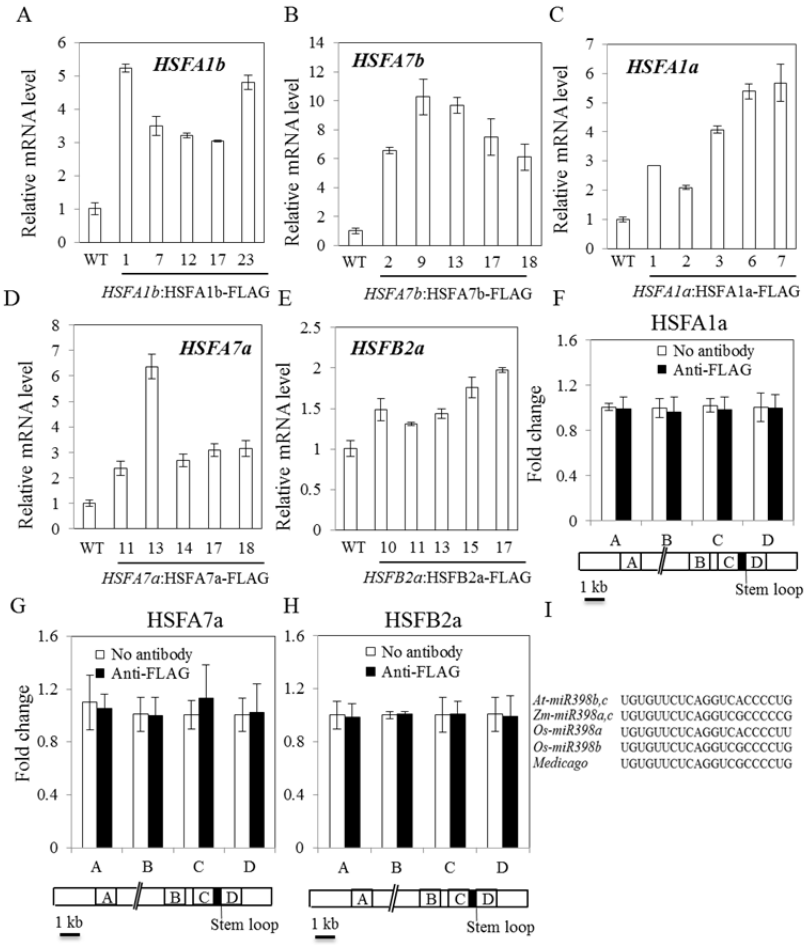

Figure 3-8. Expression Levels of *HSFA1b, HSFA7b, HSFA1a, HSFA7a,* and *HSFB2a* in Their Corresponding Transgenic Plants and Binding Capacity of HSFA1a, HSFA7a and HSFB2a to the Promoter Regions of *miR398b*. (A) to (E) Expression of HSFA1b, HSFA7b, HSFA1a, HSFA7a, and HSFB2a in relevant transgenic plants. (F) to (H) Binding ability of HSFA1a, HSFA7a, and HSFB2a to promoter regions of miR398b under heat stress as determined by ChIP-qPCR analysis. Regions of amplification: A (containing one copy of HSE GAAGGTTC) = -2189 to -2073; B (containing one HSE GAATTTTC) = -679 to -458; C (containing one HSE GAAAGTTC) = -343 to -190; D (containing no HSE; serving as negative control) = +337 to +479 base pairs relative to the stem loop start site. Values in (F) - (H) are results collected from pooled samples of five independent transgenic plants. (I) Comparison of mature miR398 sequences among different plant species. At, Arabidopsis thaliana; Zm, zea mays (corn); Os, Oryza sativa (rice); Medicago, Medicago truncatula. Error bars represent the standard deviation (n = 5).

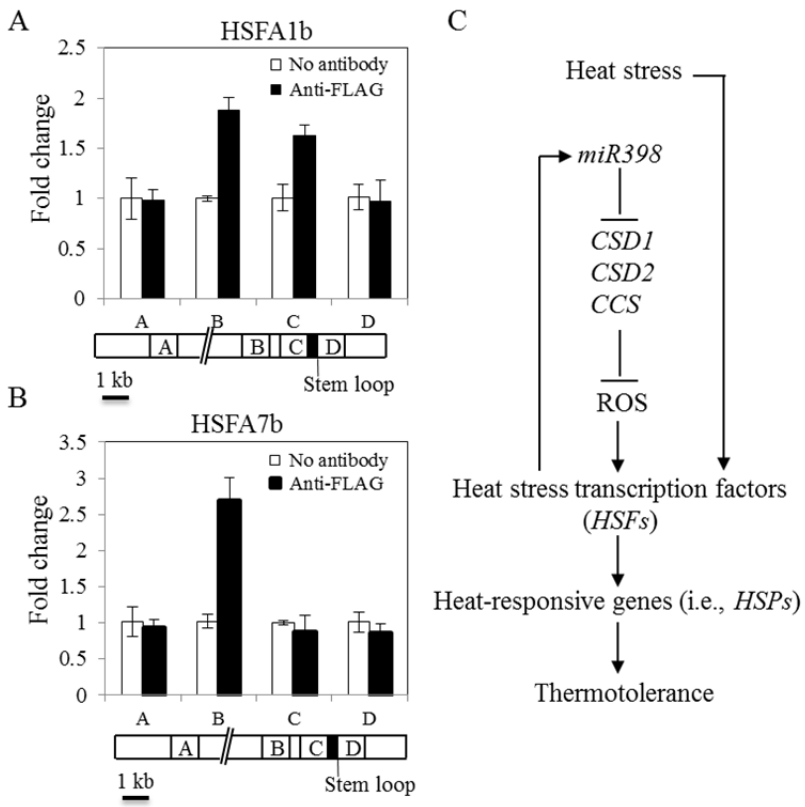

Figure 3-9. Binding of HSFA1 and HSFA7b to *miR398b* Promoter Regions under Heat stress, and a Working Model for *miR398* Function under Heat Stress.

(A) Binding capacity of HSFA1b to three areas of the *miR398b* gene under heat stress as determined by ChIP-qPCR analysis. (B) Binding capacity of HSFA7b to three areas of the *miR398b* gene under heat stress as determined by ChIP-qPCR analysis. Regions of amplification: A (containing one copy of HSE GAAGGTTC) = -2189 to -2073; B (containing one HSE GAATTTTC) = -679 to -458; C (containing one HSE GAAAGTTC) = -343 to -190; D (containing no HSE; serving as negative control) = +337 to +479 base pairs relative to the stem loop start site. (C) A working model for *miR398* function under heat stress. Heat stress induces *HSFs*, which up-regulate expression of *miR398*. Heat-induced *miR398* negatively targets three genes (*CSD1*, *CSD2*, and *CCS*) that control ROS accumulation under heat stress. The changed redox status in the cells contributes to the accumulation of *HSFs* and other heat stress-responsive genes that are critical for thermotolerance in plants. Values in (A) and (B) are results collected from pooled samples of five independent transgenic plants (Figure 3-8A, B). Error bars in (A) and (B) represent the standard deviation (n = 6).

Lorenzen, 1995). Net photosynthesis rates decrease at temperatures above 30°C in most plant species including corn and wheat as a result of inactivation of Rubisco (Ribulose-1,5-bisphosphate carboxylase oxygenase) (Law and Crafts-Brandner, 1999; Crafts-Brandner and Salvucci, 2002). In this study, we always start heat stress treatments at 37°C in the early morning (approximately 9 am when plants have been exposed to light for three hours). Endogenous sucrose levels may not increase significantly under our experimental conditions due to shorter exposure time to light (about 5 h from the beginning of light period) and inactivation of Rubisco at 37°C. Therefore, heat-induction of *miR398* is likely not caused by increase in plant endogenous sucrose levels.

Except for one gene encoding a subunit of cytochrome c oxidase (COX5b-1), all the targets of *miR398*, including *CSD1*, *CSD2*, and *CCS*, are down-regulated by heat stress (Figure 3-1E,G). These results are further confirmed by the publically available expression data on these genes using aerial tissues of wild type *Arabidopsis* seedlings under heat stress (Kilian et al., 2007). Two lines of evidence support our conclusion that down-regulation of *CSD1*, *CSD2*, and *CCS* by heat-induced *miR398* is required for thermotolerance. First, plants expressing the *miR398*-resistant forms of *CSD1*, *CSD2*, or *CCS* are more sensitive to heat stress and display reduced expression levels of heat-induced *HSFs* and *HSPs* (Figure 3-4, 3-5). Second, *csd1*, *csd2*, and *ccs* mutant plants are more heat-tolerant and accumulate increased transcripts of heat-inducible *HSFs* and *HSPs* (Figure 3-6). Therefore, thermotolerance can be achieved by down-regulation of *CSD1*, *CSD2*, and *CCS* through the heat-inducible *miR398*.

Two HSFs are responsible for the heat-induction of *miR398*. Sequence searches detected putative HSF binding sites (HSEs) in the promoter regions of *miR398b*, and a subsequent *miR398b:GUS* experiment demonstrated that *miR398b* is heat-inducible (Figure 3-1D). We identified the two HSFs that bind directly to the promoter regions of *miR398b* by chromatin immunoprecipitation (ChIP) assays followed by qPCR analysis. ChIP-qPCR analysis revealed that HSFA1b and HSFA7b can bind to *miR398b* promoter under heat stress (Figure 3-9A,B). Previous research has demonstrated that members of the HSFA1 subfamily are master regulators of heat stress responses (Mishra et al., 2002; Liu et al., 2011; Nishizawa-Yokoi et al., 2011; Yoshida et al., 2011). In *Arabidopsis*, there are four members of HSFA1: HSFA1a, HSFA1b, HSFA1d, and HSFA1e. Thus, *miR398* is regulated by at least one of the master regulators for heat stress responses. Apparently, there is a feedback loop for HSFA7b. Heat-induction of *miR398* requires HSFA7b, and *miR398* in turn positively impacts the heat-induced accumulation of *HSFA7b* and other *HSFs* (Figure 3-9C).

The altered expression of heat stress-responsive genes observed in plants expressing the *miR398*-resistant forms of *CSD1*, *CSD2*, or *CCS* as well as *csd* and *ccs* mutant plants may be explained by changed activity of HSFA1e. We have two lines of evidence to support this notion. First, decreased heat-induction of other *HSFs* and *HSPs* is correlated with reduced *HSFA1e* transcript level in plants expressing the *miR398*-resistant forms of *CSD1*, *CSD2*, or *CCS* (Figure 3-5). Second, the increased transcript level of *HSFA1e* is correlated with more abundant accumulation of *HSF* and *HSP* genes in *csd1*, *csd2*, and *ccs* mutant plants (Figure 3-6). Furthermore, we suspect that regulation of *HSFs*, *HSPs*, and heat stress responses by *miR398* involves

oxidative stress, in part because signal transduction pathways of heat stress and oxidative stress are inter-connected (Kotak et al., 2007). Production of H_2O_2 transiently increases after very short periods of exposure to high temperature as a result of NADPH oxidase (Vacca et al., 2004). The heat stress-induced H_2O_2 is able to induce heat stress-responsive genes in *Arabidopsis* (Volkov et al., 2006), and this process may be controlled by the sensing of H_2O_2 by HSFs (Miller and Mittler, 2006). In addition, plants become heat-tolerant when pre-treated with H_2O_2 while mutants defective in NADPH oxidases display compromised thermotolerance (Larkindale and Huang, 2004; Larkindale et al., 2005). As shown here, the redox status is altered in the transgenic plants expressing *miR398*-resistant forms of *CSD1*, *CSD2*, or *CCS*, and *csd1*, *csd2*, and *ccs* mutant plants (Figure 3-7A,B). As expected, when expression of CSD1, CSD2, or CCS is at a higher level in the transgenic plants expressing *miR398*-resistant forms of *CSD1*, *CSD2*, or *CCS*, superoxide radicals accumulate to a much lower level. In contrast, when CSD1, CSD2 or CCS is not functional, superoxide radicals are over-accumulated in the corresponding mutant plants. Because of an unknown mechanism presumably involving altered NADPH oxidase activity, the H_2O_2 levels are higher in the *csd1*, *csd2*, and *ccs* mutant background, but are lower in the transgenic plants expressing *miR398*-resistant forms of *CSD1*, *CSD2*, or *CCS* under heat stress than in wild-type plants. We have also shown that oxidative stress can induce expression of *HSFs* (Figure 3-7C). Our results suggest that down-regulation of *CSD1*, *CSD2*, and *CCS* by heat-induced *miR398* alters cellular redox status and creates a situation similar to the redox status in *csd1*, *csd2*, and *ccs* mutant

plants. The changed redox status could be sensed directly or indirectly by certain plant HSFs for regulating the expression of *HSFs* and *HSPs*.

Although multiple abiotic stresses (including low availability of copper; high levels of sucrose, ABA, and salt; or drought stress) can lead to up-regulation of *miR398* in *Arabidopsis*, *Populus tremula*, and *Medicago truncatula* plants (Yamasaki et al., 2007; Yamasaki et al., 2009; Dugas and Bartel, 2008; Jia et al., 2009; Trindade et al., 2010), except for low copper response mediated by SPL7, no biological function of such up-regulation had been determined before the current study. Under field conditions, multiple stresses may occur simultaneously, for example, the combination of drought and heat stress. The combination of drought and heat stress lead to greater damage to plants compared with the effect caused by each individual stress (Craufurd and Peacock, 1993; Savin and Nicolas, 1996; Jiang and Huang, 2001; Wang and Huang, 2004). As mentioned above, *miR398* is up-regulated by drought stress in *Medicago truncatula* (Trindade et al., 2010). It is very possible that *miR398* will be up-regulated in the combination of drought and heat stress to degrade transcripts of its target genes. Yu et al. (2012) reported that the *miR398* level is reduced in Chinese cabbage under extreme high temperature (46°C) for 1 h, although the study did not address the functional significance of such a regulation. In this study, we have provided multiple lines of evidence that *miR398* is up-regulated by heat stress (37°C) in *Arabidopsis*. The up-regulation of *miR398* by heat stress revealed in this study is probably independent of copper and sucrose levels in plant growth medium. We have shown that heat-induction of *miR398* in *Arabidopsis* results in down-regulation of *CSDs* and their copper chaperone *CSS* and the consequent

accumulation of *HSFs* and *HSPs* required for thermotolerance (Figure 3-9C). Because the *miR398* family members and their target genes are greatly conserved across plant species (Figure 3-8i; Sunkar and Zhu, 2004; Dugas and Bartel, 2008; Beauclair et al., 2010), down-regulation of *CSDs* and their copper chaperone *CCS* by heat-inducible *miR398* might be a common mechanism by which plants cope with the deleterious effects of heat stress. We determined *miR398* levels in soil-grown corn plants subjected to heat stress at 37°C for 0 or 2 h. Indeed, we found that *miR398* is induced by heat stress in corn plants (Figure 3-1F). Heat waves experienced in the summer in the corn belt of US and other regions of the world greatly reduce corn yield by damaging the reproductive tissues of corn, so manipulation of *miR398* and/or its target genes might be viable strategies for improving the thermotolerance and yield stability of corn.

Methods

Plant Materials and Growth Conditions

Arabidopsis thaliana (ecotype Columbia) was used as the wild type in this study. Seeds of the *csd2* knockdown were kindly provided by Dr. Ron Mittler (Rizhsky et al., 2003). Seeds of *csd1* (SALK_024857) and *ccs* (SALK_025986) were obtained from the *Arabidopsis* Biological Resource Center (ABRC). Homozygous plants were identified by diagnostic PCR analysis with primers listed in Appendix C1. *Arabidopsis* seedlings on Murashige and Skoog (MS) medium agar plates (1x MS salts [product ID M519 where the sole source of copper from $CuSO_4$ is 0.1 μM, Phyto

Technology Laboratories, Shawnee Mission, KS; Murashige and Skoog, 1962], 2% sucrose, 0.6% agar, pH 5.7) were routinely grown under cool, white light (~120 μmol m^{-2} s^{-1}) at 21℃ with a 16-h-light/8-h-dark photoperiod (light is on at 6 am). Soil-grown *Arabidopsis* plants were kept under cool, white light (~100 μmol m^{-2} s^{-1}) with a 16-h-light/8-h-dark photoperiod at 21℃ and with a 1:1 ratio of potting soil Metro Mix 360 and LC1 (Sun Gro Horticulture, Bellevue, WA). Corn (*Zea mays* L., inbred line B73) seedlings were grown in a 1:1 ratio of potting soil Metro Mix 360 and LC1 with a 14-h-light/10-h-dark photoperiod at 26℃ under cool, white light (~450 μmol m^{-2} s^{-1}). The corn plants were supplied with Hoagland solution twice weekly.

Generation of *miR398b:GUS* and *miR398c:GUS* Constructs

The DNA fragments containing the *miR398b* and miR398c promoters were amplified by PCR with the primers listed in Appendix C1. The PCR products were cloned into the binary vector pMDC164 through Gateway technology (Invitrogen). The resulting constructs (*miR398b:GUS* and *miR398c:GUS*) were transferred to *Arabidopsis* wild-type plants (ecotype Columbia) via floral dip transformation mediated by *Agrobacterium tumefaciens* (strain GV3101) (Clough and Bent, 1998). Seedlings or tissues from the T_2 populations were first immersed in a 5-bromo-4-chloro-3-indoyl glucuronide (X-Gluc) solution (2 mM X-Gluc, 100 mM sodium phosphate buffer [pH 7.5], 0.5% Triton X-100, 2 mm $K_3[Fe(CN)_6]$, 2 mM $K_4[Fe(CN)_6]$, 0.02% NaN_3) and vacuum infiltrated for 10 min and then incubated at 37°C for at least 12 h in the dark, followed by incubation in 70% ethanol to remove chlorophyll (Jefferson et al., 1987).

Generation of *CSD1:CSD1*, *CSD1:mCSD1*, *CSD2:CSD2*, *CSD2:mCSD2*, *CCS:CCS*, and *CCS:mCCS* Constructs

CSD1:CSD1, *CSD2:CSD2*, and *CCS:CCS* plasmids in pDONR-zeo were constructed with genomic DNA fragments (including native promoters, coding sequences, and 3'-UTRs) that were amplified by PCR reactions with BAC clones F22O13, F24D13, and F5O11 as templates using the primers listed in Appendix C1. The *miR398*-resistant versions of constructs of *CSD1:mCSD1*, *CSD2:mCSD2*, and *CCS:mCCS* as described previously (Sunkar et al., 2006; Dugas and Bartel, 2008; Beauclair et al., 2010) were generated by site-directed mutagenesis with the primers in the Appendix C1 with *CSD1:CSD1*, *CSD2:CSD2*, and *CCS:CCS* plasmids in pDONR-zeo as templates. *CSD1:CSD1*, *CSD1:mCSD1*, *CSD2:CSD2*, *CSD2:mCSD2*, *CCS:CCS*, and *CCS:mCCS* in pDONR-zeo were transferred to the binary vector pMDC99. The resulting constructs were transformed to wild-type (Columbia) plants via floral dip transformation mediated by *Agrobacterium tumefaciens* (strain GV3101).

Real-Time RT-PCR Analysis

Fifteen-d-old seedlings grown on MS medium were used for total RNA extraction with Trizol reagent (Invitrogen). Total RNA was treated with DNase I (New England Biolabs) for potential genomic DNA contaminations. For real-time RT-PCR (qRT-PCR) analysis, 5 µg of total RNA was used for synthesis of the first-strand cDNA with the Maxima First-Strand cDNA Synthesis Kit (Fermentas) in a 20-µL reaction volume according to the manufacturer's instructions. The cDNA reaction mixture was diluted two times, and 5 µL was used as a template in a 20-µL PCR reaction. PCR reactions included a pre-incubation at 95°C for 2 min followed by 45 cycles of denaturation at 95°C for 15 s, annealing at 56°C for 40 s, and extension at 72°C for 45 s. All the reactions were performed in the CFX96 Real-Time PCR Detection System

using iQ SYBR Green Supermix (Bio-Rad). Each experiment had five to six biological replicates (three technical replicates for each biological replicate). Each experiment was repeated at least four times. The comparative Ct method was applied. *TUB8* was used as a reference gene. The primers used in this study are listed in Appendix C1.

Determination of Reactive Oxygen Species (ROS) Levels

Superoxide free radicals were detected as described (Lee et al., 2002) with minor modifications. Fifteen-d-old seedlings grown on MS medium were treated at 21°C or 37°C for 2 h. These seedlings were vacuum-infiltrated with 0.1 mg/ml nitroblue tetrazolium (NBT) (Sigma) in 25 mM Hepes buffer (pH 7.6). In a control treatment, 10 mM $MnCl_2$ and 10 units/ml of superoxide dismutase were added to the 0.1 mg/ml nitroblue tetrazolium solution. Samples were subsequently incubated at room temperature in darkness for 2 h. Chlorophyll was removed with 70% ethanol.

Hydrogen peroxide (H_2O_2) was detected with 3,3'-diaminobenzidine (DAB) staining as described (Lee et al., 2002) with minor modifications. To detect H_2O_2, seedlings of the same batch of plants used for superoxide detection were vacuum-infiltrated with 0.1 mg/mL of DAB (Sigma) in 50 mM Tris-acetate buffer (pH 5.0). As a control, ascorbic acid at a final concentration of 10 mM was added to the staining solution. Samples were incubated for 24 h at room temperature in darkness. Chlorophyll was removed with 70% ethanol.

Chromatin Immunoprecipitation (ChIP) Assays

Genomic DNA fragments of *HSFA1a*, *HSFA1b*, *HSFB2a*, *HSFA7a*, and *HSFA7b* (including their native promoters) genes were amplified by PCR and cloned into

pEarlyGate302. The resulting constructs were then transformed into *Arabidopsis* wild-type plants via floral dip transformation mediated by *Agrobacterium tumefaciens* (strain GV3101). ChIP assays were carried out with pooled 15-d-old seedlings of five independent transgenic plants in the T_3 generation grown on MS medium as described (Gendrel et al., 2002). Briefly, heat-treated (37°C, 2 h) seedlings were crosslinked with 1% formaldehyde, and chromatin was isolated, sonicated (Fisher, Biodismembrator model 120), and pre-cleared with salmon sperm DNA/protein-G agarose beads for 1 h. Samples were then immunoprecipitated with anti-FLAG antibody (Sigma, F1804) at 4°C overnight. The chromatin antibody complex was precipitated with salmon sperm DNA/protein-G agarose beads, washed for 5 min with each of four buffers, and reverse-crosslinked in elution buffer (1% SDS, 0.1 M $NaHCO_3$) for 6 h at 65°C. Proteins in the complex were removed by proteinase K at 45°C for 1 h. DNA was precipitated in the presence of two volumes of ethanol, 1/10 volume of 3 M sodium acetate (pH 5.2), and 2 µg of glycogen. Real-time PCR analysis was performed with immunoprecipitated DNA using a Bio-Rad CFX96 Real-Time PCR Detection System.

Small RNA Northern Hybridization Analysis

Total RNA was extracted from 15-d-old seedlings with Trizol reagent (Invitrogen). High molecular weight RNAs and low molecular weight RNAs were separated by adding an equal volume of 20% PEG (average molecular weight 8000) in 1 M NaCl on ice for 2–4 h. The supernatant containing low molecular weight RNAs was further purified by phenol/chloroform extraction and precipitated with isopropyl alcohol.

For small RNA Northern hybridization analysis, 30 μg of small RNAs was resolved on a 17% polyacrylamide–7 M urea gel and transferred to Hybond-N^+ membranes (Amersham Biosciences). The membranes were UV-crosslinked and baked in an oven at 80°C for 1 h. DNA oligos complementary to *miR398b* and U6 were labeled with γ-ATP-^{32}P by using T_4 Polynucleotide Kinase. Hybridization was performed overnight at 38°C with the Perfect Hyb Plus Buffer (Sigma-Aldrich). Blots were washed twice for 15 min each time in 2 X SSC and 0.1% SDS at 38°C.

ACCESSION NUMBERS

Sequence data from this article can be found in the Arabidopsis Genome Initiative or GenBank/EMBL databases under the following accession numbers: *miR398a* (*At2g03445*), *miR398b* (*At5g14545*), *miR398c* (*At5g14565*), *CSD1* (*At1g08830*), *CSD2* (At2g28190), *CCS* (*At1g12520*), *COX5b-1* (*At3g15640*), *HSFA1b* (*At5g16820*), *HSFA1e* (*At3g02990*), *HSFA2* (*At2g26150*), *HSFA3* (*At5g03720*), *HSFA7b* (*At3g63350*), *HSP17.6* (*At1g59860*), *HSP70B* (*At1g16030*), and *HSP90.1* (*At5g52640*).

Acknowledgements

I thank Xiaoyan Lu, Yanyan Zhang, Haitao Zeng and Jianhua Zhu for their contribution to this work. This work was supported by US National Science Foundation grants IOS0919745 and MCB0950242 to J.Z, and by US National Science Foundation grant DBI0922650.

Chapter 4: A Bi-Functional Xyloglucan Galactosyltransferase Is an Indispensable Salt Stress Tolerance Determinant in *Arabidopsis*

Abstract

Salinity is an abiotic stress that substantially limits crop production worldwide. To identify salt stress tolerance determinants, we screened for *Arabidopsis* mutants that are hypersensitive to salt stress and designated these mutants as *short root in salt medium* (*rsa*). One of these mutants, *rsa3-1*, is hypersensitive to NaCl and LiCl but not to CsCl or to general osmotic stress. Reactive oxygen species (ROS) over-accumulate in *rsa3-1* plants under salt stress. Gene expression profiling with Affymetrix microarray analysis revealed that RSA3 controls expression of many genes including genes encoding proteins for ROS detoxification under salt stress. Map-based cloning showed that *RSA3* encodes a xyloglucan galactosyltransferase, which is allelic to a gene previously named *MUR3*/*KAM1*. The *RSA3/MUR3/KAM1*-encoded xylogluscan galactosyltransferase regulates actin microfilament organization (and thereby contributes to endomembrane distribution) and is also involved in cell wall biosynthesis. In *rsa3-1*, actin cannot assemble and form bundles as it does in the wild type but instead aggregates in the cytoplasm. Furthermore, addition of phalloidin, which prevents actin depolymerization, can rescue salt hypersensitivity of *rsa3-1*. Together, these results suggest that RSA3/MUR3/KAM1 along with other cell wall-associated proteins plays a critical role in salt stress tolerance by maintaining the

proper organization of actin microfilaments in order to minimize damage caused by excessive ROS.

Key words: salt stress tolerance, xyloglucan galactosyltransferase, endomembranes, actin microfilaments, RSA3.

Introduction

Salt stress is one of the main abiotic stresses that limit crop production worldwide. High levels of soluble salts including chlorides of sodium, calcium, and magnesium often result in soil sodicity, alkalinity, and other soil problems. NaCl represents most of the soluble salt in saline soils, whose saturated-paste extracts have, by definition, an electrical conductivity (EC_e) of 4 dSm^{-1} (1 dS m^{-1} is equivalent to 10 mM NaCl) (Chinnusamy et al., 2006). Progress in the development of salt-tolerant crops through conventional breeding and genetic engineering has been slow mainly because of the incomplete understanding of the molecular mechanisms of salt tolerance. In addition to benefitting the development of salt-tolerant plants, a comprehensive understanding of the molecular basis of plant salt tolerance will also benefit the design of drought-, cold-, and heat-tolerant crops because osmotic and oxidative stresses are common to these abiotic stresses.

Salt stress imposes ion toxicity, nutrient deficiency, osmotic stress, and oxidative stress on plants during any phase of their life cycle. Ion toxicity results from the replacement of cytoplasmic K^+ by Na^+ in biochemical reactions, and by Na^+- and Cl^-[1]-induced conformational alterations in protein structures (Zhu, 2003). High levels of

salts in soil can also cause osmotic stress, which limits water uptake by roots. Plants have evolved mechanisms to cope with salt stress. To reduce cytoplasmic Na^+ concentration or adjust osmotic pressure, Salt Overly Sensitive (SOS) pathway proteins (SOS1, SOS2, and SOS3) transport Na^+ out of the cytoplasm and coordinate activities of other tonoplast-localized ion transporters to sequester Na^+ in the vacuole (Cheng et al. 2004; Qiu et al. 2004; Chinnusamy et al., 2006). ABA and Ca^{2+} signaling are also involved in salt tolerance and have some crosslink with the SOS pathway (Tuteja N. 2007; Mahajan et al., 2008; Chinnusamy et al., 2006).

Salt stress and many other abiotic and biotic stresses in plants can lead to the generation of reactive oxygen species (ROS) including superoxide ($O_2^{\cdot-}$) and hydroxyl ($OH^{\cdot}$) free radicals, hydrogen peroxide (H_2O_2), and free singlet oxygen during aerobic cellular processes such as mitochondrial and chloroplast electron transport and oxidation of glycolate (photorespiration), xanthine, and glucose (Apel and Hirt, 2004; Gill and Tuteja, 2010; Nanda et al., 2010). In plants, ROS are mainly generated in chloroplasts, peroxisomes, mitochondria, and the apoplast. Over-accumulated ROS can cause oxidative damage to membrane lipids, proteins, and nucleic acids (Møller et al., 2007). When present at a lower level that is not harmful to plant cells, however, H_2O_2 is able to function as a messenger molecule to initiate signal transduction cascades involving MAP kinase in response to various environmental cues (Kovtun et al., 2000; Jonak et al., 2002). Plants utilize enzymatic and non-enzymatic strategies to efficiently detoxify excessive ROS (Apel and Hirt, 2004; Gill and Tuteja, 2010; Nanda et al., 2010). Non-enzymatic ROS scavenging involves antioxidants including the major cellular redox buffers ascorbate, glutathione,

and tocopherol, and some secondary metabolites (flavonoids, alkaloids, and carotenoids) whereas enzymatic ROS detoxification in plants involves superoxide dismutase, peroxidase, and catalase, and enzymes of the ascarbate-glutothione cycle (Chinnusamy et al., 2006).

Abiotic stresses including salt stress can cause dynamic cytoskeletal changes in plants. In plant cell microtubules, actin microfilaments, microtubule-related proteins, actin-related proteins, and others are integrated into the cytoskeletal network. The plant cytoskeleton coordinates many fundamental processes such as cell division, growth and development, cell support, cell inner and outer motility, vesicle transport, polymer cross-linking, and membrane anchorage (Foster et al., 2003; Wasteneys and Yang, 2004). Because the plant cell cytoskeleton is highly dynamic, it can be adaptively rearranged in response to many environmental stimuli (Baluška et al., 2003; Wasteneys and Yang, 2004). Örvar et al. (2000) reported that reorganization of actin microfilaments is required for cold stress tolerance in alfalfa. Salt stress can affect cortical microtubule organization and subsequent re-organization (Shoji et al., 2006; Wang et al., 2007), although the underlying mechanisms remain unknown.

Here, we identify and characterize an *Arabidopsis* mutant, *rsa3-1*. *rsa3-1* is hypersensitive to NaCl and LiCl but not to CsCl or to the general osmotic stress conferred by mannitol. Map-based cloning revealed that *RSA3* is allelic to a previously identified gene *MURUS3* (*MUR3*)/ *KATAMARI1* (*KAM1*), which encodes a bi-functional protein involved in cell wall biosynthesis and in the maintenance of endomembrane organization by interacting with actin microfilaments. RSA3/MUR3/KAM1 functions to limit ROS levels in cells under salt stress because

ROS over-accumulate in *rsa3-1* plants under salt stress. We further show that RSA3/MUR3/KAM1 is essential for the assembly of actin that is required for salt tolerance. Our results suggest that, by interacting with actin microfilaments so as to maintain endomembrane organization, RSA3/MUR3/KAM1 together with other cell wall proteins minimizes cellular damage caused by excessive ROS and thereby plays an important role in salt tolerance.

Results

Isolation of the *rsa3-1* Mutant

Because we are interested in identifying proteins that are essential for salt tolerance, we carried out a forward genetic screen for mutants with increased sensitivity to 100 mM NaCl as indicated by a modified root-bending assay (Wu et al., 1996; Zhu et al., 2002). We used an ethyl methanesulfonate (EMS)-mutagenized M_2 population in *Arabidopsis* and designated these mutants as *short root in salt medium* (*rsa*). One mutant, *rsa3-1*, was chosen for further characterization. Under control conditions, *rsa3-1* mutant seedlings grown on MS medium were indistinguishable from wild-type seedlings (Figure 4-1A [a]). Root growth was more inhibited for *rsa3-1* than for wild-type seedlings on MS medium containing various levels of NaCl (Figure 4-1A [a] and C). The *rsa3-1* mutant plants were shorter than wild-type plants when grown in soil (Figure 4-1A [b]). Unlike soil-grown wild-type plants, few soil-grown *rsa3-1* plants survived when irrigated with 200 mM NaCl, and those that survived were stunted (Figure 4-1A [b] and B). We then determined whether the increased sensitivity of *rsa3-1* to NaCl represents a general sensitivity to all salts. We found that *rsa3-1* is also hypersensitive to LiCl but not to CsCl or to the general osmotic stress conferred

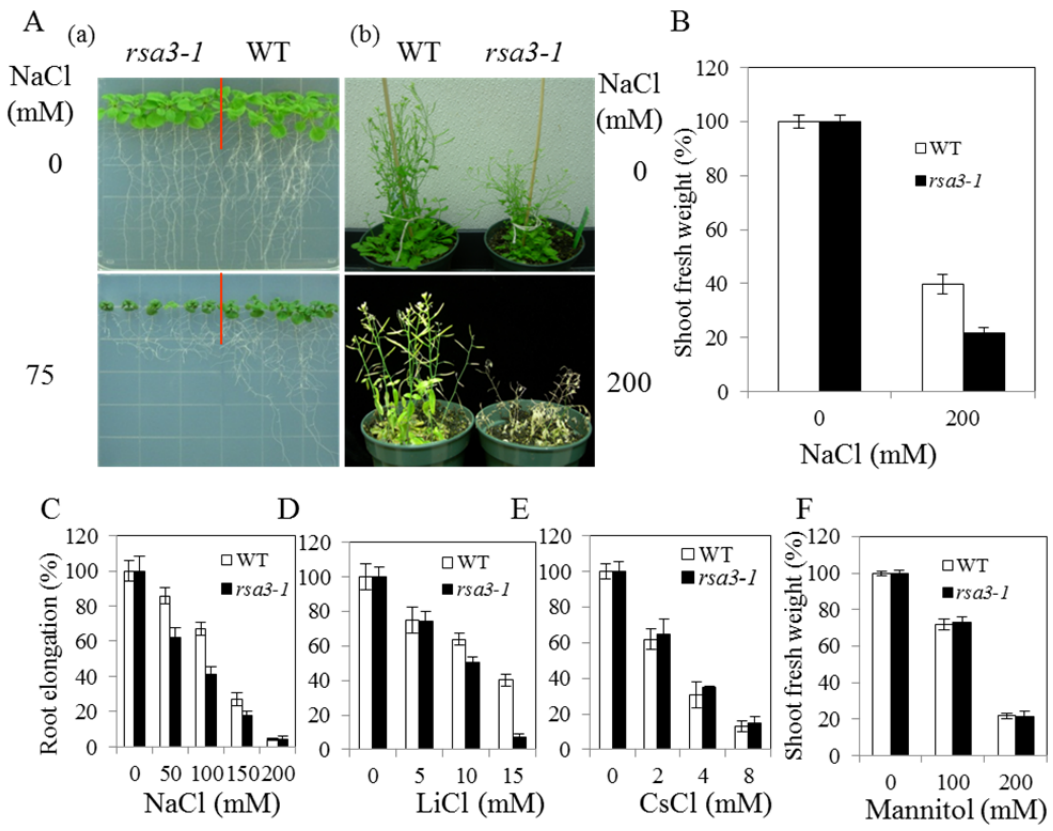

Figure 4-1. Sensitivity of *rsa3-1* to Various Salts. Five-d-old seedlings grown on MS medium (except for plants shown in A [b]) were transferred to MS medium containing different concentrations of various salts as indicated and allowed to grow for an additional 7 d (A[a], [C]-[E]) and 14 d (F). WT, wild type. (A) Sensitivity of *rsa3-1* to NaCl. (a) *rsa3-1* and WT grown on MS medium supplemented with 0 or 75 mM NaCl. (b) Three-week-old soil-grown wild-type and *rsa3-1* plants were treated with 0 or 200 mM NaCl for an additional 14 d. (B) Shoot fresh weights of plants in (A [b]). (C) – (F) Sensitivity of wild type and *rsa3-1* to different salts. Root elongation or shoot fresh weight was measured and is shown as a percentage relative to values obtained with normal MS medium. Error bars represent the standard deviation (n = 40-60).

by mannitol (Figure 4-1D-F). Thus, responses of *rsa3-1* mutant plants to salts are similar to those exhibited by *sos1*, *sos2*, and *sos3* mutants (Chinnusamy et al., 2006).

We backcrossed *rsa3-1* plants with wild-type plants. All F_1 plants showed a wild-type phenotype, and the F_2 progeny from the self-pollinated F_1 plants displayed a segregation ratio of ~3:1 wild-type phenotypes: *rsa3-1* mutant phenotypes. These results suggest that *rsa3-1* is a recessive mutation in a single nuclear gene.

Accumulation of ROS in *rsa3-1*

Salt stress and other biotic and abiotic stresses can increase production of ROS (Apel and Hirt, 2004; Gill and Tuteja, 2010; Nanda et al., 2010). We determined ROS levels in *rsa3-1*. Under control condition, *rsa3-1* plants accumulate slightly more total ROS than the wild type (Figure 4-2A and B). Relative to wild-type plants, *rsa3-1* plants over-accumulate ROS under salt stress (Figure 4-2A and B). We subsequently quantified the H_2O_2 levels in *rsa3-1*. H_2O_2 content under control conditions is slightly higher in *rsa3-1* than in the wild type but is significantly higher in *rsa3-1* than in the wild type under salt stress (Figure 4-2C). These data are consistent with the observation that total ROS are more abundant in *rsa3-1* than in the wild type. Together, these results suggest that RSA3 is required for maintaining proper ROS levels in order to minimize the deleterious effects of ROS on the plant cells.

Molecular Cloning of *RSA3*

To understand the mechanism of *RSA3* function in salt tolerance, we identified the *RSA3* gene with a map-based cloning approach. A total of 964 homozygous *rsa3-1* mutant plants were selected from the segregating F_2 population generated from a cross between *rsa3-1* (in Columbia) and *Landsberg erecta*. *RSA3* was mapped

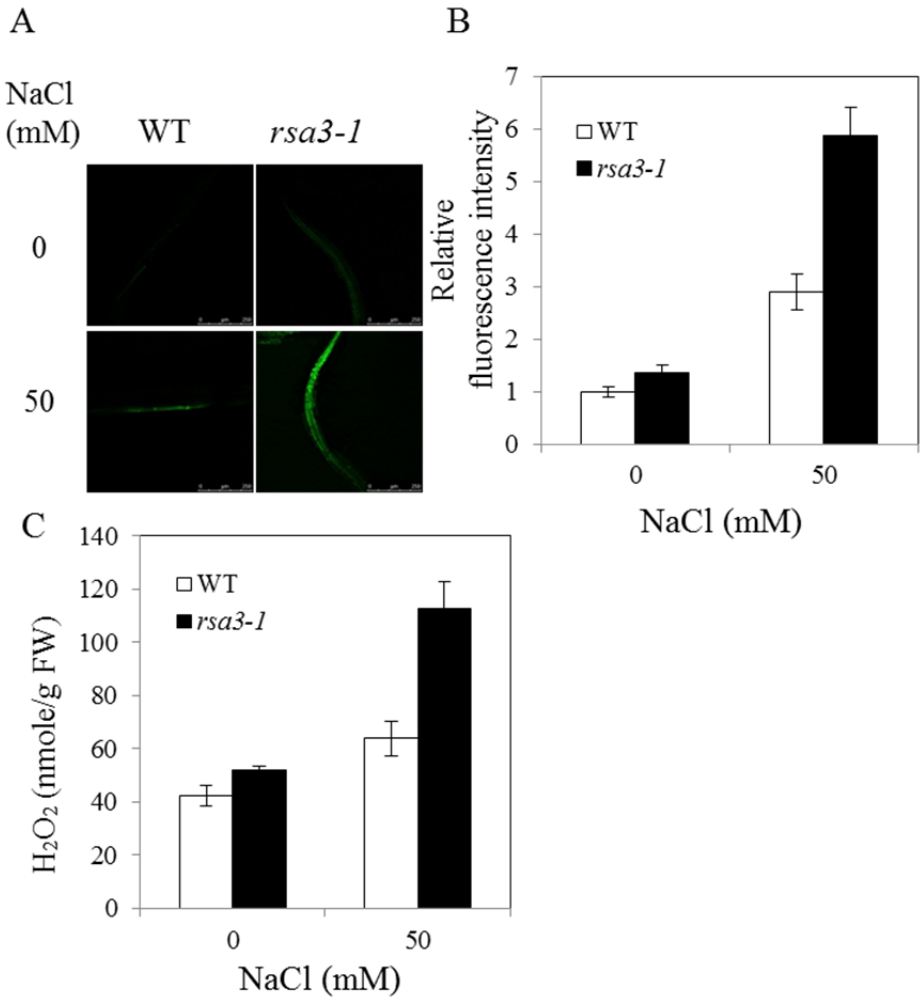

Figure 4-2. ROS Accumulation in Wild-Type and *rsa3-1* Plants. (A) Total ROS accumulation in wild-type and *rsa3-1* seedlings. Five-d-old seedlings grown on MS medium were transferred to MS medium containing 0 or 50 mM NaCl and allowed to grow for an additional 9 h. Total ROS was detected in roots stained with CM-H2DCFDA using a laser scanning confocal microscope. Bars = 200 µm. (B) Relative fluorescence intensity in plants shown in (A). (C) H_2O_2 content of five-d-old wild-type and *rsa3-1* seedlings subjected to 50 mM NaCl for 0 or 9 h. Error bars in (B) and (C) indicate the standard deviation (n = 24). WT, wild-type.

initially to chromosome 2 between the simple sequence length polymorphism (SSLP) markers F6F22-94K and F5H14-24K. Fine mapping with additional SSLP markers within this chromosomal section narrowed the *RSA3* locus to an ~120-kb region covered by the bacterial artificial chromosome (BAC) clones T2G17 and F11A3 (Figure 4-3A). Within this region, 28 putative genes were predicted from the TAIR (www.arabidopsis.org) database. Candidate genes were sequenced to reveal the *rsa3-1* mutation. In the *rsa3-1* mutant, a single base-pair mutation from G to A was found in the gene *F11A3.8* (*At2g20370*); this results in a nonsense mutation from TGG (Trp-254) to TAG (stop codon) (Figure 4-3A).

We confirmed the identity of *RSA3* by a gene complementation analysis. The wild-type *RSA3* gene is able to restore the *rsa3-1* phenotype (Figure 4-3B and 4-3C). Furthermore, soil-grown *rsa3-1* complementation lines resemble wild type in morphology and they showed the wild-type phenotype when treated with 200 mM NaCl (Figure 4-3F and 4-3G). These results confirm that *At2g20370* is the *RSA3* gene. *RSA3* is allelic to previously identified *MURUS3* (*MUR3*)/KATAMARI1 (KAM1) (Madson et al., 2003; Tamura et al., 2005). RSA3/MUR3/KAM1 is a bi-functional protein involved in cell wall biosynthesis and in maintaining endomembrane organization through interaction with actin microfilaments. We then determined salt sensitivity of other alleles of *RSA3*/*MUR3*/*KAM1*: *mur3-1*, *mur3-2, kam1-1*, and *kam1-3* (Figure 4-3A [b]). The *mur3-1*, *mur3-2*, *kam1-1*, and *kam1-3* mutant plants are hypersensitive to salt stress (Figure 4-3D and 4-3E). Two additional mutants defective in cell wall biosynthesis (*mur1-3*, and *mur2-1*; O'Neill et al., 2001; Madson *et al*., 2003; Peña, *et al*., 2004) and another mutant defective in endomembrane

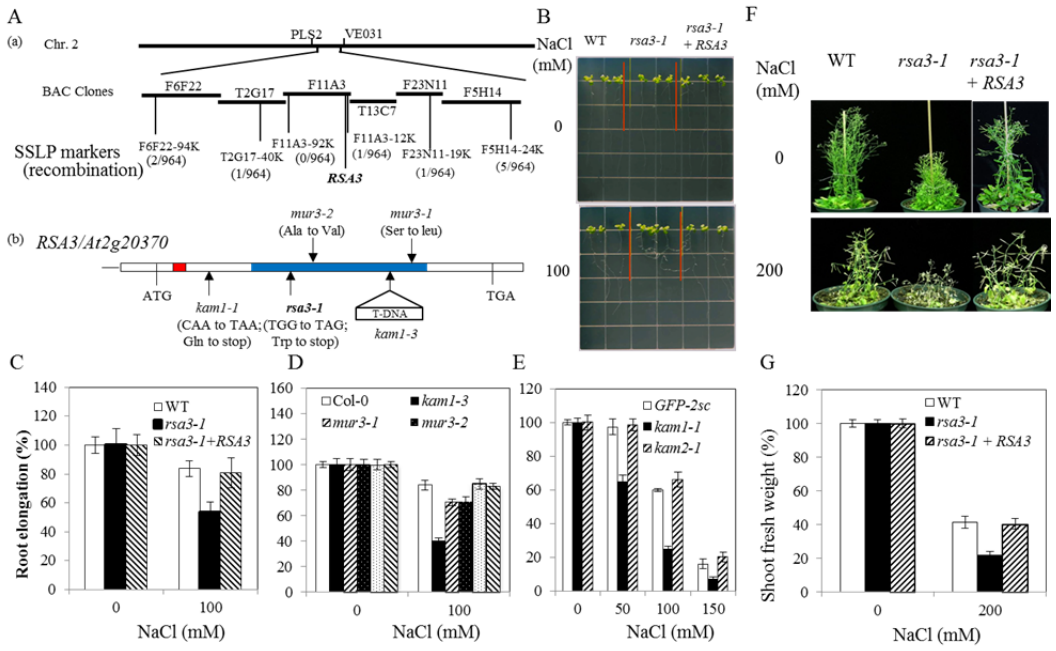

Figure 4-3. Molecular cloning of *RSA3*. (A) Positional cloning of *RSA3*. (a) Map-based cloning of *RSA3*. The SSLP markers and the number of recombinants are indicated. (b) Gene structure of *RSA3*. The positions of *rsa3-1* mutation and other known alleles of *RSA3* are indicated. The red box indicates the coding region for a putative transmembrane domain, and the blue box indicates the coding region for an exostosin-like domain. (B) Gene complementation of *rsa3-1* with the wild type *RSA3*. Over 20 independent *rsa3-1* complementation lines (*rsa3-1* plants transformed with wild type *RSA3* gene) displayed wild-type phenotype in response to salt stress and data from one representative line were shown. (C) Root elongation of seedlings in (B). (D) Root elongation of Col-0, *kam1-3*, *mur3-1*, *mur3-2*, *mur1-3*, and *mur2-1* seedlings in response to salt stress. (E) Root elongation of *kam1-1* and *kam2-1* in response to different levels of NaCl. Five-d-old seedlings grown on MS medium were transferred to MS medium supplemented with different concentrations of NaCl and allowed to grow for an additional 7 d (for data presented in [B]-[E]). Error bars in represent the standard deviation (n = 30-45 in [C]- [E], 40-60 in [G]).

organization (*kam2-1*; Tamura et al., 2007) are not more sensitive to salt stress than their control plants (Figure 4-3D and 4-3E). These results further confirm that *At2g20370* encodes *RSA3* and that RSA3 is specifically required for salt stress tolerance.

RSA3 is induced by salt stress (Figure 4-4A). We also produced transgenic *Arabidopsis* plants expressing a GUS reporter gene under the control of the *RSA3* promoter (*RSA3::GUS*). *RSA3::GUS* is induced by salt stress treatment (Figure 4-4B and C).

RSA3 Controls Gene Expression under Salt Stress

We determined the effect of the *rsa3-1* mutation on expression of genes under salt stress with whole-genome microarray analysis using Affymetrix *Arabidopsis* ATH1 GeneChips. Statistical analysis of the microarray data revealed that, compared to their expression in wild-type plants, expression of 62 genes was increased in *rsa3-1* by at least 2-fold while expression of 59 genes was reduced in *rsa3-1* by at least 2-fold (Appendix D1 and D2). The differentially expressed genes in *rsa3-1* under salt stress encode proteins involved in diverse biological processes, and substantial percentages of these genes (41.9% of the up-regulated genes and 27.1% of the down-regulated genes in *rsa3-1* under salt stress) are involved in responses to biotic or abiotic stress (Appendix D1 and D2). We selected 10 genes that are involved in gene regulation, ROS scavenging, and stress responses to validate the microarray data by qRT-PCR analysis: *At5g10760*, *At1g21250*, *At5g06720*, *At5g01670*, *At1g32560*, *At1g48130*, *At2g35300*, *At5g66400*, *At3g11050*, and *At5g67060*. *At5g10760* encodes a eukaryotic aspartyl protease family protein. *At1g21250* encodes a cell wall-associated kinase

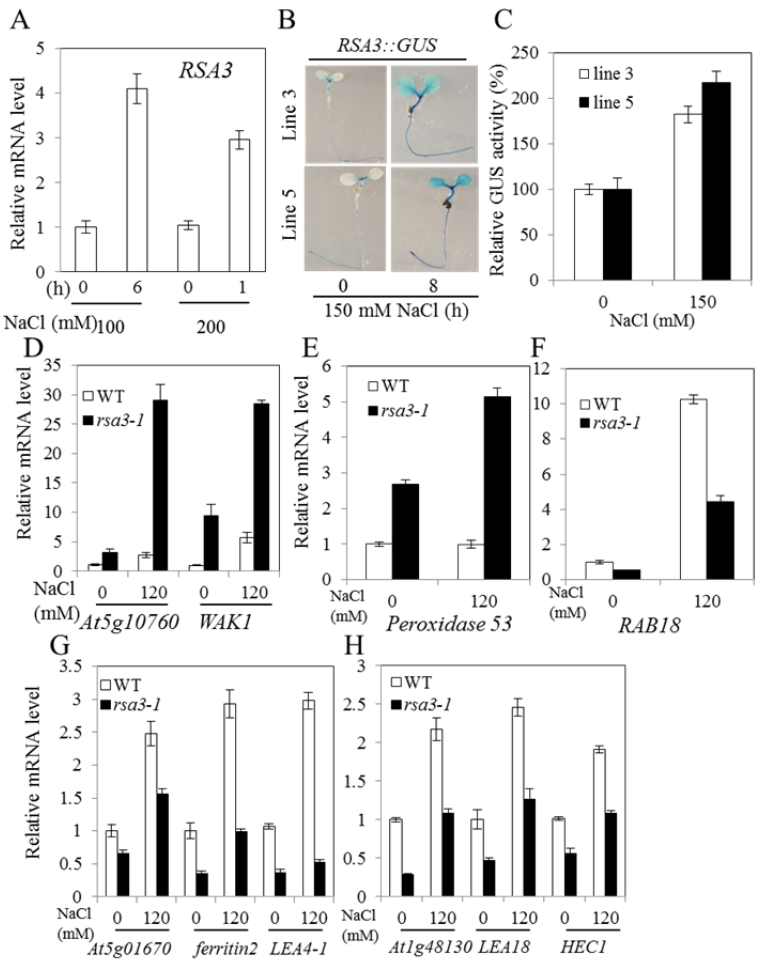

Figure 4-4. Expression Profiles of *RSA3* under Salt Stress and Validation of the Microarray Results. (A) Transcript levels of *RSA3* in wild-type seedlings under salt stress as determined by qRT-PCR analysis. Fourteen-d-old seedlings grown on MS medium were treated with 100 mM NaCl for 0 or 6 h or with 200 mM NaCl for 0 or 1 h. (B) *RSA3::GUS* expression patterns under salt stress. (C) Quantification of GUS activities of plants in (B). (D) – (H) qRT-PCR analysis of ten genes in six-d-old *rsa3-1* and wild –type plants subjected to 0 or 120 mM NaCl for 24 h. These genes are up-regulated ([D]-[E]) or down-regulated ([F] – [H]) in *rsa3-1* under salt stress as determined in the microarray analysis. Error bars indicate the standard deviation (n = 5 in [A] and [D]–[H], and 4 in [C]).

(WAK1). *At5g06720* encodes PEROXIDASE 53. *At5g01670* encodes an NAD(P)-linked oxidoreductase superfamily protein. *At1g32560* encodes a late embryogenesis abundant protein (LEA4-1). *At1g48130* encodes a protein similar to an antioxidant (1-CYSTEINE PEROXIREDOXIN 1). *At2g35300* encodes a late embryogenesis abundant protein (LEA18). *At5g66400* encodes an ABA- and drought-induced glycine-rice dehydrin protein (RAB18). *At3g11050* encodes ferritin 2 (FER2) with oxidoreductase activity. *At5g67060* encodes a sequence-specific DNA-binding transcription factor (HECATE 1 [HEC1]). qRT-PCR analysis confirmed the microarray results (Figure 4-4D-H). Under control condition, all the genes tested showed similar expression patterns as those determined under salt stress (Figure 4-4D-H). According to publically available gene expression data, about half of the up-regulated genes in *rsa3-1* are responsive to salt stress in root tissues but not in green tissues of wild-type plants (Appendix D3), and about one-third of the down-regulated genes in *rsa3-1* are responsive to salt stress in wild-type plants (Appendix D4).

Actin Microfilaments Organization Is Disrupted in *rsa3-1* under Salt Stress

The dynamic organization of actin is very important for salt tolerance in plants (Wang et al., 2010). Previous study showed that RSA3/MUR3 maintains endomembrane organization through interaction with actin microfilaments (Madson et al., 2003). We examined actin organization of *rsa3-1* and the wild type. Under normal growth conditions, the organization of actin microfilaments was similar for *rsa3-1* and the wild type (Figure 4-5A). After 18 h of salt treatment, wild-type plants show salt-induced actin microfilament assembly and bundle formation (Figure 4-5A). In contrast, actin microfilaments of *rsa3-1* plants under salt stress were aggregated in the

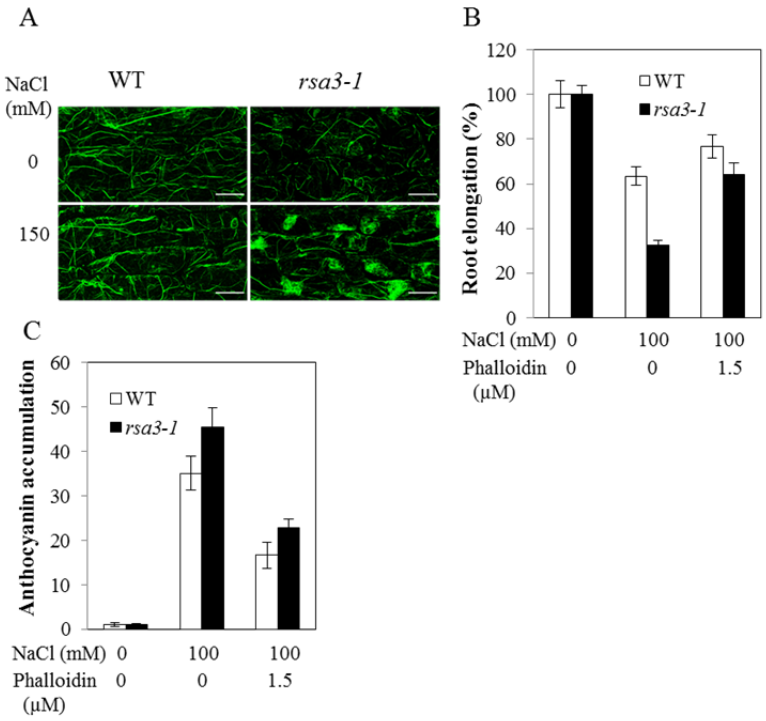

Figure 4-5. Microfilament Organization of Wild-Type and *rsa3-1* Seedlings with or without Salt Stress, and Rescue of Salt Hypersensitivity of *rsa3-1* by Phalloidin. (A) Microfilament organization of wild type and *rsa3-1* seedlings with or without salt stress. Five-d-old seedlings grown on MS medium were transferred to MS medium containing 0 or 150 mM NaCl and allowed to grow for an additional 18 h. Microfilaments were visualized with seedlings stained with 0.66 μM Alexa Fluor 488 phalloidin. Bars = 20 μm. (B) and (C) Sensitivity of wild type and *rsa3-1* seedlings to NaCl with or without phalloidin. Five-d-old seedlings grown on MS medium were transferred to MS medium supplemented with 0 or 100 mM NaCl or with 100 mM NaCl plus 1.5 μM phallodin and allowed to grow for an additional 7 d. Data for root elongation (B) and anthocyanin accumulation (relative to the wild type or *rsa3-1* without salt stress) (C) were shown. Error bars in (B) and (C) represent the standard deviation (n = 30).

cytoplasm, and only a few cortical networks were evident (Figure 4-5A). These results indicated that assembly of actin microfilaments in *rsa3-1* is impaired under salt stress and that the disruption of actin microfilament organization may contribute to increased salt sensitivity in *rsa3-1*. To test this inference, we added phalloidin, which can prevent depolymerization of actin microfilaments, to the NaCl-containing medium; if disruption of actin microfilament organization contributes to increased salt sensitivity in *rsa3-1*, addition of phalloidin should counter that effect. As shown in Figure 4-5B and C, phalloidin rescued the salt-hypersensitive phenotype of *rsa3-1*. These results indicate that the disruption of actin microfilament organization in *rsa3-1* is at least partially responsible for the increased sensitivity to salt stress.

Discussion

Salt stress limits agricultural sustainability. In an effort to identify essential genes for salt stress tolerance in plants, we isolated the salt hypersensitive mutant *rsa3-1*, which has a mutation in a xyloglucan galactosyltransferase. We confirmed the identity of *RSA3* with two lines of evidence. First, the wild-type *RSA3* gene is able to fully restore the *rsa3-1* phenotype in a gene complementation analysis (Figure 4-3B, C, F and G). Second, four other alleles of the *RSA3/MUR3/KAM1* gene (*mur3-1*, *mur3-2*, *kam1-1*, and *kam1-3*) are hypersensitive to salt stress. RSA3/MUR3/KAM1 is a bi-functional xyloglucan galactosyltransferase involved in cell wall biosynthesis and in maintaining endomembrane organization through interaction with actin microfilaments (Madson et al., 2003; Tamura et al., 2005). *kam2-1*, which shows abnormal endomembrane organization (Tamura et al., 2007), is not more sensitive to salt stress than the wild type (Figure 4-3E). These results indicate that altered

endomembrane organization is not the sole cause of increased salt sensitivity seen in *rsa3-1*. Although *Arabidopsis* mutants *mur1-3* and *mur2-1* are the two *Arabidopsis* mutants which have similar defects in fucose biosynthesis as the *mur3-1* and *mur3-2* mutants (Bonin, *et al*., 1997; Peña, *et al*., 2004; Madson *et al*., 2003), neither *mur1-3* nor *mur2-1* shows increased salt sensitivity (Figure 4-3D), indicating that cell wall biosynthesis deficiency is not always associated with increased salt sensitivity. Together, these data suggest that RSA3/MUR3/KAM1 is specifically important in salt stress tolerance pathway.

Actin microfilaments formed from physiological polymerization of actin molecules are a main component of the cytoskeleton. Actin microfilaments are essential for almost every intracellular activity that regulates plant growth and development, including organelle movement, cytoplasmic streaming, and cell morphogenesis (Hussey et al., 2006; Higaki et al., 2007). The construction and reorganization of actin microfilament structure are regulated by actin-binding proteins (Dos Remedios et al., 2003; Winder et al., 2005). Several families of actin-binding proteins have been studied in plants, including villins, fimbrins, and myosins (Higaki et al., 2007). Although a number of reports have shown that actin microfilaments play an important role in plant responses to abiotic stresses including salt stress (Wasteneys and Yang, 2004; Huang et al., 2007; Wang et al., 2010), little is known about the role of actin-binding proteins in salt stress. Disruption of the actin microfilament organization reduces salt tolerance in *Arabidopsis* seedlings while stabilization of actin microfilaments increases salt tolerance (Wang *et al*., 2010). RSA3/MUR3/KAM1 interacts with actin microfilaments to maintain endomembrane

organization (Tamura et al., 2005). Mutations in *RSA3/MUR3/KAM1* (*rsa3-1*, *mur3-1*, *mur3-2*, *kam1-1*, and *kam1-3*) lead to hypersensitivity to salt stress (Figure 4-1 and 4-3). We observed that assembly of actin microfilaments in *rsa3-1* is impaired under salt stress and that the disrupted organization of actin microfilaments may contribute to the overall increased salt sensitivity in *rsa3-1* (Figure 4-5A). Indeed, addition of phalloidin, which prevents actin depolymerization, to a medium that causes salt stress in *rsa3-1* mutant plants improved mutant performance. These results also suggest that proteins like RSA3 that interact with actin microfilaments are important in salt stress-tolerance pathways in plants. In a separate study, a plant C2 phospholipase D (PLD) that interacts with actin which hydrolyzes the phosphatidylcholine in cell membranes to generate phosphatidic acid (PA), a second messenger in response to salt, drought, or cold stress (Wang, 2002; Wang et al., 2006). Furthermore, NtPLDβ1, which is a C2 PLD in tobacco, is involved in the regulation of actin microfilament organization (Pleskot, et al., 2010). However, whether PLDβ1 plays a role in salt stress remains unknown.

Studies in yeast and microglia have suggested that actin might be a regulator of ROS production (Gourlay et al. 2004; Rasmussen et al. 2010). Liu et al. (2012) reported that disruption of actin dynamics triggers the generation of ROS in *Arabidopsis* roots under salt stress. We found that ROS over-accumulate in *rsa3-1* under salt stress, and this might result from the disruption of actin microfilaments in *rsa3-1* (Figure 4-2 and 4-5). Under salt stress, the efficiency of ROS scavenging in *rsa3-1* may have been compromised. The deleterious effects of excessive ROS levels in *rsa3-1* may at least partially contribute to the overall increased sensitivity to salt

stress. Consistent with this observation, our whole-genome microarray analysis detected the altered expression of many genes involved in ROS detoxification, stress responses, and gene regulation in *rsa3-1* under salt stress (Figure 4-4 and Appendix D1 and D2). Which other factors are required for the control of ROS accumulation by RSA3/MUR3/KAM1 under salt stress is unclear. The *SOS6* gene, which encodes a cellulose synthase like D 6 (CSLD6), is required for limiting ROS levels under salt stress (Zhu et al., 2010). RSA3/MUR3/KAM1 is part of the cell wall biosynthesis complex (Madson et al., 2003) and therefore may function together with other cell wall-related proteins (i.e., SOS6) to limit ROS accumulation under salt stress.

Finally, the altered expression of many genes in *rsa3-1* under salt stress, as revealed in the microarray analysis, may contribute to the overall increased salt sensitivity. About half of genes in *rsa3-1* that were determined to be up-regulated in the microarray experiments are not responsive to salt stress in the wild-type (Appendix D3). Similarly, most of the down-regulated genes in *rsa3-1* are not responsive to salt stress in wild-type plants according to publically available gene expression data (Appendix D4). Substantial percentages of the differentially expressed genes in *rsa3-1* under salt stress (41.9% of the up-regulated genes and 27.1% of the down-regulated genes) encode proteins involved in responses to biotic or abiotic stress (Appendix D1 and D2). Although we do not know how RSA3 controls gene expression, mis-regulation of these genes in *rsa3-1* mutant plants may at least partially contribute to the overall increased salt sensitivity.

Methods

Plant Material and Growth Conditions

Arabidopsis thaliana plants (ecotype Columbia) with the *glabrous1* mutation were transformed with the *RD29A::LUC* transgene (Ishitani et al., 1997). Plants expressing one copy of the homozygous *RD29A::LUC* gene were mutagenized with EMS, and the M_2 population was screened for *rsa* mutants by a modified root-bending assay with 100 mM NaCl (Zhu et al., 2002). Seeds of *GFP-2SC* transgenic plants, *kam1-1*, and *kam2-1* mutant plants were kindly provided by Dr. Ikuko Hara-Nishimura (Kyoto University, Kyoto, Japan). These mutants and transgenic plants were in Col-0 background. Seeds for *mur3-1*, *mur3-2*, and *kam1-3* (seed stock number CS8566, CS8567, and SALK_141953) were obtained from the Arabidopsis Biological Resource Center (ABRC, Columbus, OH).

Arabidopsis thaliana seeds were surface sterilized and stratified at 4°C for 4–7 d in 0.01% low-melting agarose to break dormancy. Seeds were then sown on Murashige and Skoog (MS) medium agar plates (1x MS salts, 2% sucrose, 1.2% agar, pH 5.7) and were routinely grown under cool, white light (~120 μmol m^{-2} s^{-1}) at 21℃ with a 16-h-light/8-h-dark photoperiod and in a vertical orientation. Soil-grown plants were kept under cool, white light (~100 μmol m^{-2} s^{-1}) with a 16-h-light/8-h-dark photoperiod at 21℃ with 1:1 ratio of Metro Mix 360 and LC1 potting soil (Sun Gro Horticulture, Bellevue, WA).

For salt stress treatment, 5-d-old seedlings grown on germination medium were transferred to a medium containing various levels of salts and allowed to grow for an additional 7 d. Seedlings at the end of stress treatments were photographed with a digital camera (Coolpix 7900, Nikon, Japan), and elongation of roots was measured using Image J 1.46 software (NIH, http://rsb.info.nih.gov/ij).

Quantification of ROS

Five-d-old seedlings grown on vertically oriented MS medium (1X MS salts, 2% sucrose, 1.2% agar, pH 5.7) were transferred to MS medium supplemented with 0 or 50 mM NaCl and allowed to grow for an additional 9 h. Seedlings were incubated with 5-(and 6)-chloromethyl-2'7'-dichlorodihydrofluorescein diacetate acetyl ester (CM-H2DCFDA) for 30 min and then washed with distilled H_2O to remove excess CM-H2DCFDA. Fluorescence images were obtained with a Leica SPX5 confocal microscope (Leica Microsystems), and ROS levels were quantified based on the intensity of fluorescence with ImageJ software (NIH, http://rsb.info.nih.gov/ij/).

For quantification of H_2O_2, 5-d-old wild-type and *rsa3-1* seedlings were transferred to MS medium containing 0 or 50 mM NaCl and allowed to grow for an additional 9 h. Seedlings were then harvested, and H_2O_2 content was determined with an Amplex red hydrogen/peroxidase assay kit (Invitrogen) according to the manufacturer's instructions.

Positional Cloning of *RSA3* and Gene Complementation of *rsa3-1*

The *rsa3-1* (ecotype Columbia) was crossed with Landsberg *erecta* wild-type plants to generate a mapping population. Homozygous *rsa3-1* mutant plants were selected from the segregating F_2 population with 100 mM NaCl and recovered on MS germination medium for 1 week. Genomic DNA was isolated, and simple sequence length polymorphism (SSLP) markers were used for initial and fine mapping (Konieczny and Ausubel, 1993; Bell and Ecker, 1994).

The 4.3-kb genomic DNA fragment of *RSA3*, which included approximately 2 kb of the putative promoter sequence upstream of the start codon, the coding region, and

472 bp downstream of the stop codon, was amplified by PCR with the F11A3 BAC clone as a template. The PCR product was introduced into pCAMBIA1303 between SacI and KpnI sites and sequenced. The resulting binary vector (pCMBIA1303-RSA3) was transferred to *rsa3-1* by a floral dip method with *Agrobacterium tumefaciens* (strain GV3101)-mediated transformation (Clough and Bent, 1998). T_2 transgenic plants were examined for sensitivity to 100 mM NaCl.

***RSA3::GUS* Construct and GUS Assay**

An approximately 2.0-kb promoter region of the *RSA3* gene was amplified by PCR with F11A3 BAC DNA as a template. The PCR product was cloned into the binary vector pCAMBIA1381Z between EcoRI and SalI sites and sequenced. The binary vector was transferred to wild-type (Columbia) plants as described above. Seven-d-old hygromycin-resistant T_2 transgenic seedlings grown vertically on MS agar plates were transferred to MS plates containing 0 or 150 mM NaCl and allowed to grow for an additional 8 h. The plants were submerged in X-Gluc (5-bromo-4-chloro-3-indoyl glucronide) solution (2 mM X-Gluc, 100 mM sodium phosphate buffer (pH 7.5), 0.5% Triton X-100, 2mM K_3 [Fe $(CN)_6$], 2 mM K_4[Fe$(CN)_6$], 0.02% NaN_3) and incubated at 37°C overnight in the dark as described (Jefferson, 1987). Chlorophyll was removed with 70% ethanol. In parallel experiments with the same growth and stress treatment conditions described above, the β-Glucuronidase activity was measured and quantified as described (Jefferson, 1987).

Microarray Analysis and Real-Time RT-PCR Analysis

Six-d-old wild-type and *rsa3-1* mutant seedlings grown on MS medium (1x MS salts, 2% sucrose, 1.2% agar, pH 5.7) were transferred to MS medium supplemented with 0

or 120 mM NaCl and allowed to grow for an additional 24 h. Seedlings were then harvested, and total RNA was extracted with Trizol reagent (Invitrogen) and treated with DNase I to remove potential genomic DNA contaminations.

Microarray analysis was carried out using *Arabidopsis* Affymetrix ATH1 GeneChips in the School of Medicine, University of Maryland, Baltimore. Total RNA was used to prepare biotin-labeled complementary RNA targets, and microarray analysis was performed as described (Breitling et al., 2004). Three biological replicates were used for each treatment. The array data sets were subjected to the Robust Multiarray Averaging (RMA) normalization method. The RMA method for computing an expression measure begins by computing background-corrected perfect match intensities for each perfect match cell on every GeneChip. The normalized data were further analyzed, and p-values were generated by the affylmGUI component of Bioconductor in statistics environment R with the default parameters (Irizarry et al., 2003; Gentleman et al., 2004). Genes with statistically significant changes between the *rsa3-1* mutant and the wild type were selected by the RankProd method, which is a non-paramteric method for identifying differentially up- or down-regulated genes based on the estimated percentage of false discoveries (p value < 0.05) (Hong et al., 2006). RankProd results were summarized with script written in PERL. The microarray data discussed in this study have been deposited in the Gene Expression Omnibus at NCBI (Edgar et al., 2002) and are accessible through GEO Series accession number GSE41626.

For real-time RT-PCR (qRT-PCR) analysis, 5 μg of total RNA was used for synthesis of the first-strand cDNA with the Maxima First-Strand cDNA Synthesis Kit

(Fermentas) in a 20-µL reaction volume according to the manufacturer's instructions. The cDNA reaction mixture was diluted two times, and 5 µL was used as a template in a 20-µL PCR reaction. PCR reactions included a pre-incubation at 95°C for 2 min followed by 45 cycles of denaturation at 95°C for 15 s, annealing at 56°C for 40 s, and extension at 72°C for 45 s. All reactions were performed in the CFX96 Real-Time System using iQ SYBR Green Supermix (Bio-Rad). Each experiment had five biological replicates (three technical replicates for each biological replicate). The comparative Ct method was applied. Primers are listed in Appendix D5.

Visualization of Actin Microfilaments

Arabidopsis seedlings were fixed and permeabilized with fixation buffer (100 mM PIPES, 5 mM $MgSO_4$, 0.5 mM $CaCl_2$, 0.05% triton X-100, 3% paraformaldehyde, 0.5% glutaraldehyde, pH 9.0) for 45 minutes. MBS (3-mleimidobenzoic acid N-hydroxysuccinimide ester, Sigma) was added to fixation buffer to a final concentration of 300 µM and additional 1 h incubation was allowed. The fixed seedlings were washed three times with washing buffer (100 mM PIPES, 5 mM $MgSO_4$, 0.5 mM $CaCl_2$, 10 mM EGTA, pH 7.0). The fixed seedlings were then incubated with 20 units/mL (equivalent to approximately 0.66 µM) of Alexa Fluor 488 phalloidin (catalog no. A12379, Invitrogen) in full-strength MS solution (1x MS salts, 2% sucrose, pH 5.7) for 1 h in the dark. Images were captured with a Zeiss LSM 700 confocal microscope (Carl Zeiss Microscopy, LLC, Thornwood, NY).

Acknowledgements

I am grateful to Wenbo Li, Zhen-Yu Wang, Yingdian Wang and Jianhua Zhu for their contribution to this work. This work was supported by US National Science Foundation grants IOS0919745 and MCB0950242 to J.Z, and by US National Science Foundation grant DBI0922650.

Chapter 5: Conclusions and Perspectives

The objective of this dissertation is to identify critical signaling components involved in plant abiotic stress tolerance pathways. The long-term goal is to enhance our understanding of the molecular mechanisms of plant abiotic stress responses and provide a basis for genetic engineering of stress-tolerant crops.

We first identified RCF1, an important component for cold stress signaling through a forward genetic analysis. As a cold inducible DEAD box RNA helicase, RCF1 is a positive regulator for chilling and freezing tolerance and negative regulator for expression of cold-responsive genes including *CBF* genes. RCF1 functions to maintain proper splicing of pre-mRNAs because many cold-responsive genes are mis-spliced in *rcf1-1* mutant plants under cold stress. Functional characterization of four genes *PRR5*, *AtSK12*, *CIR1*, and *SPFH* that are mis-spliced in *rcf1-1* revealed that these genes are cold-inducible, positive (*CIR1* and *SPFH*) and negative (*PRR5* and *AtSK12*) regulators of cold-responsive genes and cold tolerance.

RCF3 was identified in the same mutant screen process for RCF1. RCF3 is another component involved in cold and heat stress. RCF3 encodes a KH-domain containing RNA-binding protein. Although we do not know how RCF3 mediates cold-responsive gene expression, RCF3 appears to be a negative regulator of most *HSFs*. Consistent with the overall increased accumulation of heat-responsive genes, the *rcf3* mutant plants are more tolerant than the wild type to heat stress.

We also identified RSA3, a xyloglucan galactosyltransferase essential for salt stress. *rsa3-1* is hypersensitive to NaCl and LiCl but not to CsCl or to general osmotic stress. Reactive oxygen species (ROS) over-accumulate in *rsa3-1* plants under salt

stress. Microarray analysis revealed that RSA3 controls expression of many genes including genes encoding proteins for ROS detoxification under salt stress. Our study revealed that RSA3 functions to maintaining the proper organization of actin microfilaments in order to minimize damage caused by excessive ROS.

In addition, we determined role of the heat-inducible *miR398* in plant thermotolerance. Our results suggest that plants use a previously unrecognized strategy to achieve thermotolerance, especially for the protection of reproductive tissues. This strategy involves the down-regulation of two copper/zinc superoxide dismutases (*CSDs*) and their copper chaperone *CCS* through the heat-inducible *miR398*.

Although some progresses were achieved to advance our understanding of the molecular mechanisms of RCF1, and RCF3 under abiotic stresses, there are still some questions to be addressed. RCF1 plays a positive role for cold tolerance even without cold acclimation, thus important CBF-independent regulons targeted by RCF1 under normal conditions should not be ruled out. We have identified six RCF1 targets whose transcripts display intron-retention in *rcf1-1* under normal conditions. Their roles under cold stress, however, need to be clarified. Another splicing factor, STA1, which controls *CBF2* expression in the same pathway as RCF1, plays a role in miRNA processing (Ben Chaabane et al., 2013). Is RCF1 also involved in miRNA processing? If so, what is the molecular mechanism? To address these two questions, more experiments need to be carried out. A large-scale miRNA array might shed light upon the role of RCF1 in miRNA processing with or without cold stress. In addition, overexpression of RCF1 leads to increased cold stress tolerance in *Arabidopsis.* Will

overexpression of RCF1 or its close homologs in crops improve cold stress tolerance of cold-sensitive crops?

We isolated *RCF3* gene through a genetic screen under cold stress, but the role of RCF3 under cold stress remains unclear. RCF3 does not control the expression of *CBF* genes under cold stress, but it is still possible that RCF3 controls expression of other cold-responsive genes that are CBF-independent. A large-scale array analysis such as microarray or RNA-seq experiment may help unravel this question. Another question to be examined is the role of RCF3 in cold stress tolerance. The sensitivity of *rcf3-1* and wild type plants to chilling stress and freezing stress can be evaluated easily through hypocotyl growth and whole-plant freezing tolerance analysis.

Appendix A1. Genes with Increased (1A) and Reduced (1B) Expression in *rcf1-1* without Cold Treatment as Determined by Microarray Analysis.

Appendix A1A. Genes with Increased Expression in *rcf1-1* without Cold Treatment as Determined by Microarray Analysis.

AGI ID	Fold Change	P Value	Gene Description
AT5G04150	9.44	0.00	basic helix-loop-helix (bHLH) DNA-binding protein
AT3G56980	10.41	0.03	basic helix-loop-helix (bHLH) DNA-binding protein
AT3G04320	3.10	0.00	Kunitz family trypsin and protease inhibitor protein
AT3G55970	3.44	0.01	jasmonate-regulated gene 21
AT2G29460	3.70	0.00	glutathione S-transferase tau 4
AT1G54020	8.15	0.01	GDSL-like Lipase/Acylhydrolase superfamily protein
AT2G39030	21.05	0.00	Acyl-CoA N-acyltransferases (NAT) superfamily protein
AT5G39850	3.34	0.01	Ribosomal protein S4
AT5G47220	3.17	0.00	ethylene responsive element binding factor 2
AT5G51440	3.25	0.00	HSP20-like chaperones superfamily protein
AT1G27730	3.26	0.00	salt tolerance zinc finger
AT1G74930	3.36	0.00	Integrase-type DNA-binding superfamily protein
AT1G52400	3.56	0.00	beta glucosidase 18
AT1G80840	3.81	0.00	WRKY DNA-binding protein 40
AT5G24770	4.11	0.03	vegetative storage protein 2
AT4G15210	4.20	0.01	beta-amylase 5
AT1G52410	4.24	0.01	TSK-associating protein 1
AT1G61120	4.54	0.01	terpene synthase 04
AT5G05600	4.61	0.00	2-oxoglutarate (2OG) and Fe(II)-dependent oxygenase superfamily protein
AT3G48360	4.95	0.01	BTB and TAZ domain protein 2
AT3G49620	5.42	0.01	2-oxoglutarate (2OG) and Fe(II)-dependent oxygenase superfamily protein
AT5G44420	20.75	0.00	plant defensin 1.2
AT1G72450	3.11	0.00	jasmonate-zim-domain protein 6
AT5G51440	3.25	0.00	HSP20-like chaperones superfamily protein
AT1G72920	3.46	0.00	Toll-Interleukin-Resistance (TIR) domain family protein
AT2G43530	4.05	0.00	Scorpion toxin-like knottin superfamily protein
AT1G52040	8.15	0.01	myrosinase-binding protein 1
AT2G21640	13.92	0.00	oxidative stress responsive protein
AT2G26020	23.77	0.00	plant defensin 1.2b
AT1G72260	3.10	0.02	thionin 2.1
AT3G23550	4.98	0.01	MATE efflux family protein
AT5G35940	3.60	0.00	Mannose-binding lectin superfamily protein
AT5G09570	5.29	0.00	Cox19-like CHCH family protein
AT2G39330	17.43	0.00	jacalin-related lectin 23
AT4G33720	30.39	0.00	Pathogenesis-related 1 protein

Appendix A1B. Genes with Reduced Expression in rcf1-1 without Cold Treatment as Determined by Microarray Analysis.

AGI ID	Fold Change	P Value	Gene Description
AT4G28250	3.13	0.01	expansin B3
AT5G22460	3.08	0.00	alpha/beta-Hydrolases superfamily protein
AT5G59130	4.26	0.00	subtilase family protein
AT1G17870	3.85	0.00	ethylene-dependent gravitropism-deficient and yellow-green-like 3
AT5G52300	3.63	0.01	LTI65 (LOW-TEMPERATURE-INDUCED 65)

Appendix A2. Genes with Increased (1A) and Reduced (1B) Expression in *rcf1-1* after 12 h Cold Treatment as Determined by Microarray Analysis.

Appendix A2A. Genes with Increased Expression in *rcf1-1* after 12 h Cold Treatment as Determined by Microarray Analysis.

AGI ID	Fold Change	P Value	Gene Description
At3g61630	5.68	0.01	cytokinin response factor (CRF6)
At3g16530	7.75	0.00	putative lectin
At2g42270	3.65	0.00	U5 small nuclear ribonucleoprotein helicase (Brr2b)
At3g50930	15.70	0.01	cytochrome BC1 synthesis (BCS1)
At4g16680	15.46	0.00	putative DEAD/DEATH box RNA helicase
At5g59450	3.47	0.02	scarecrow-like 11
At1g43800	3.39	0.04	stearoyl acyl carrier protein desaturase, putative
At1g78340	3.60	0.00	glutathione transferase, putative
At2g32020	28.90	0.00	putative alanine acetyl transferase
At4g21830	4.86	0.05	putative protein CGI-131 protein
At5g15950	4.91	0.00	S-adenosylmethionine decarboxylase (adoMetDC2)
At5g40010	3.65	0.04	a mitochondrial ATPase involved in seed and silique development
At5g43450	3.04	0.02	1-aminocyclopropane-1-carboxylate oxidase
At5g62480	11.73	0.00	glutathione S-transferase-like protein
At1g69880	4.02	0.01	putative thioredoxin
At1g05680	3.99	0.04	putative indole-3-acetate beta-glucosyltransferase
At1g32870	4.17	0.02	NAC domain protein 13 (NAC13)
At1g42990	2.84	0.01	BASIC REGION/LEUCINE ZIPPER MOTIF 60 (bZIP60)
At1g52400	4.60	0.01	beta-glucosidase, putative
At1g73260	3.72	0.02	trypsin inhibitor involved in modulating programmed cell death in plant-pathogen interactions
At1g80840	4.90	0.00	Pathogen-induced transcription factor (WRKY40)
At2g03760	9.52	0.00	putative steroid sulfotransferase
At2g38470	3.67	0.02	putative WRKY-type DNA binding protein
At2g43510	4.50	0.01	putative trypsin inhibitor
At3g04720	4.24	0.02	hevein-like protein precursor (PR-4)
At3g09940	3.85	0.02	putative monodehydroascorbate reductase (NADH)
At3g22830	4.52	0.00	heat stress transcription factor family (HSFA6b)
At3g45140	3.11	0.01	lipoxygenase AtLOX2
At4g12490	6.58	0.01	pEARLI 1-like protein
At4g16260	4.23	0.01	beta-1,3-glucanase class I precursor
At4g37370	11.35	0.00	Member of CYTOCHROME P450 (CYP81D8)
At5g44420	36.57	0.00	an ethylene- and jasmonate-responsive plant defensin (PDF1.2A)
At5g51440	5.93	0.04	mitochondrial heat shock 22 kd protein-like
At5g57220	4.11	0.01	Member of CYTOCHROME P450 (CYP81F2), involved in glucosinolate metabolism
At1g49570	3.50	0.05	peroxidase, putative
At1g52040	10.80	0.01	myrosinase-binding protein homolog, putative
At1g72260	4.60	0.05	thionin
At2g26020	34.07	0.01	putative antifungal protein
At2g43530	3.05	0.01	putative trypsin inhibitor
At2g47520	7.44	0.01	HYPOXIA RESPONSIVE ERF2
At3g25250	3.60	0.05	protein kinase, putative
At4g21830	4.86	0.05	putative protein CGI-131 protein
At4g25470	2.55	0.02	DRE CRT-binding protein DREB1C/CBF2 involved in low-temperature-responsive gene expression
At5g59820	2.77	0.01	zinc finger protein ZAT12 involved in high light and cold acclimation
At3g25610	3.45	0.01	ATPase II, putative
At4g22470	3.08	0.00	extensin - like protein
At2g39330	21.06	0.00	putative myrosinase-binding protein

At4g33720	38.69	0.00	Pathogenesis-related 1 protein
At5g40690	7.31	0.01	putative calcium binding protein

Appendix A2B. Genes with Reduced Expression in rcf1-1 after 12 h Cold Treatment as Determined by Microarray Analysis.

AGI ID	Fold Change	P Value	Gene Description
At4g33240	3.57	0.01	a protein that is predicted to act as a 1-phosphatidylinositol-3-phosphate (PtdIns3P) 5-kinase
At5g08430	3.47	0.02	SWIB complex BAF60b domain-containing protein
At1g43620	4.87	0.00	sterol glucosyltransferase, putative
At5g35170	3.04	0.04	adenylate kinase -like protein
At2g21210	5.08	0.01	putative auxin-regulated protein
At5g06690	4.00	0.02	thioredoxin-like
At5g58900	3.39	0.03	Homeodomain-like transcriptional regulator
At1g10060	4.03	0.01	a mitochondrial branched-chain amino acid aminotransferase
At1g18870	3.00	0.02	isochorismate synthase, putative
At1g60890	4.79	0.01	phosphatidylinositol-4-phosphate 5-kinase family protein
At2g23840	3.92	0.02	HNH endonuclease domain-containing protein
At4g01130	7.97	0.00	acetylesterase, putative
At4g25280	3.07	0.03	DNAJ heat shock N-terminal domain-containing protein
At5g23240	3.09	0.02	K Efflux antiporter KEA1
At1g01790	3.10	0.01	a member of the WNK family (9 members in all) of protein kinases
At1g51805	3.66	0.01	leucine-rich repeat protein kinase, putative
At1g53430	7.84	0.00	protein kinase family protein
At1g56300	3.24	0.02	DnaJ protein, putative
At5g20220	3.54	0.01	zinc knuckle (CCHC-type) family protein
At5g28080	3.12	0.01	a member of the WNK family (9 members in all) of protein kinases
At5g59130	3.78	0.03	subtilisin-like serine protease
At5g09410	2.64	0.00	CALMODULIN-BINDING TRANSCRIPTION ACTIVATOR 1 (CAMTA1)
At1g17870	3.03	0.01	S2P-like putative metalloprotease
At1g18710	3.36	0.03	Member of the R2R3 MYB transcription factor family (ATMYB47)
At2g02950	3.05	0.02	PHYTOCHROME KINASE SUBSTRATE 1 (PKS1)
At2g23030	3.21	0.00	SNF1-RELATED PROTEIN KINASE 2-9 (SNRK2.9)
At4g23270	3.41	0.00	CYSTEINE-RICH RLK (RECEPTOR-LIKE PROTEIN KINASE) 19
At5g63320	4.01	0.01	NPX1 (Nuclear Protein X1), a nuclear factor regulating abscisic acid responses
At5g58720	3.26	0.01	PRLI-interacting factor, putative
At1g07650	5.39	0.00	leucine-rich repeat transmembrane protein kinase, putative
At3g50660	3.01	0.01	steroid 22-alpha-hydroxylase (DWF4)
At5g07580	3.79	0.00	a member of the AP2 transcription factor family
At5g57630	4.66	0.00	SNF1-RELATED PROTEIN KINASE 3.4 (SNRK3.4)

Appendix A3. Genes with Increased (2A) and Reduced (2B) Expression in *rcf1-1* after 24 h Cold Treatment as Determined by Microarray Analysis.

Appendix A3A. Genes with Increased Expression in *rcf1-1* after 24 h Cold Treatment as Determined by Microarray Analysis.

AGI ID	Fold Change	P Value	Gene Description
At5g55200	4.31	0.00	chaperone GrpE-like protein
At2g22540	3.05	0.00	putative MADS-box protein
At3g61630	17.22	0.00	cytokinin response factor (CRF6)
At4g01550	3.05	0.01	a plasma-membrane bound NAC transcription factor whose controlled proteolytic activation allows it to enter the nucleus
At5g18270	6.10	0.00	NAM (no apical meristem)-like protein
At5g43330	6.02	0.00	cytosolic malate dehydrogenase
At5g56350	3.76	0.00	pyruvate kinase
At1g28330	6.81	0.00	dormancy-associated protein, putative
At3g28210	4.79	0.00	zinc finger protein (PMZ), putative
At1g07520	4.55	0.01	transcription factor scarecrow-like 14
At1g28050	3.08	0.01	CONSTANS family zinc finger protein, putative
At2g39920	3.04	0.01	HAD superfamily, subfamily IIIB acid phosphatase
At2g42270	9.81	0.00	U5 small nuclear ribonucleoprotein helicase (Brr2b)
At3g04030	3.28	0.00	Homeodomain-like superfamily protein
At4g16680	36.20	0.00	putative DEAD/DEATH box RNA helicase
At5g24110	3.05	0.00	member of WRKY Transcription Factor (WRKY30)
At1g70810	3.20	0.01	Calcium-dependent lipid-binding (CaLB domain) family protein
At2g36320	3.08	0.04	A20/AN1-like zinc finger family protein
At3g26740	3.12	0.01	light regulated protein, putative
At3g55580	5.25	0.00	regulator of chromosome condensation-like protein
At3g56710	10.19	0.00	SigA binding protein
At5g13200	3.63	0.03	GRAM domain family protein
At1g36370	3.74	0.04	putative hydroxymethyltransferase
At1g64900	10.87	0.00	cytochrome P450 (CYP89A2)
At1g69880	3.08	0.01	putative thioredoxin
At2g20800	29.44	0.00	putative NADH-ubiquinone oxireductase
At2g29490	4.42	0.03	putative glutathione S-transferase
At2g32020	33.98	0.00	putative alanine acetyl transferase
At2g36790	33.75	0.00	putative glucosyl transferase
At3g26280	3.06	0.00	cytochrome P450 monooxygenase (CYP71B4)
At3g29250	6.15	0.02	short-chain alcohol dehydrogenase, putative
At3g50930	30.98	0.00	cytochrome BC1 synthesis (BCS1)
At4g12430	3.44	0.02	putative trehalose-6-phosphate phosphatase (AtTPPA)
At4g15490	4.00	0.01	indole-3-acetate beta-glucosyltransferase like protein
At4g15680	3.44	0.00	glutaredoxin
At4g33070	4.27	0.03	pyruvate decarboxylase-1 (Pdc1)
At5g62480	66.43	0.00	glutathione S-transferase-like protein
At1g16670	3.03	0.03	receptor-like serine/threonine kinase, putative
At1g69790	5.36	0.00	putative protein kinase
At1g70530	3.06	0.01	putative protein kinase
At1g71530	3.70	0.00	serine/threonine protein kinase, putative
At3g53810	3.10	0.01	serine/threonine-specific protein kinase
At3g57760	6.29	0.00	putative wall-associated kinase 1,
At4g36410	3.14	0.00	E2, ubiquitin-conjugating enzyme 17 (UBC17)
At5g25930	3.19	0.01	receptor-like protein kinase
At5g63370	3.06	0.02	protein kinase
At1g08920	4.69	0.02	putative sugar transport protein, ERD6
At1g20030	3.26	0.00	calreticulin, putative
At1g27730	3.61	0.00	salt-tolerance zinc finger protein
At1g42990	9.10	0.00	bZIP transcription factor, putative
At1g52340	5.17	0.00	short chain alcohol dehydrogenase, putative
At1g52560	13.08	0.01	chloroplast-localized small heat shock protein, putative

At1g54040	3.35	0.01	jasmonate inducible protein, putative
At1g71030	3.68	0.01	putative myb family transcription factor
At1g80840	8.61	0.00	putative WRKY transcription factor
At2g03760	51.93	0.00	putative steroid sulfotransferase
At2g17840	4.48	0.00	putative senescence-associated protein 12
At2g22540	3.05	0.00	putative MADS-box protein
At2g26150	4.36	0.03	Heat Stress Transcription Factor (HSFA2)
At2g30250	12.38	0.00	putative WRKY-type DNA binding protein
At2g38340	3.64	0.03	DRE BINDING PROTEIN 19 (DREB19)
At2g38470	4.47	0.00	putative WRKY-type DNA binding protein
At2g40880	3.67	0.00	putative cysteine proteinase inhibitor B (cystatin B)
At2g47000	7.83	0.00	putative ABC transporter
At3g15500	4.45	0.00	putative jasmonic acid regulatory protein
At3g19580	9.94	0.00	zinc finger protein, putative
At4g17260	5.45	0.01	lactate dehydrogenase (LDH1)
At4g37370	32.84	0.00	Member of CYTOCHROME P450 (CYP81D8)
At5g12030	10.86	0.02	heat shock protein 17.6A
At5g18470	3.10	0.00	putative protein S-receptor kinase PK3 precursor
At5g25110	4.56	0.01	serine/threonine protein kinase, putative
At5g44420	22.64	0.00	an ethylene- and jasmonate-responsive plant defensin (PDF1.2A)
At5g48410	3.54	0.00	ligand-gated ion channel protein-like; glutamate receptor-like
At5g51440	22.07	0.00	mitochondrial heat shock 22 kd protein-like
At1g67970	5.23	0.00	Heat Stress Transcription Factor (HSFA8)
At2g21640	95.84	0.00	oxidative stress responsive protein
At2g47520	15.16	0.00	HYPOXIA RESPONSIVE ERF (ETHYLENE RESPONSE FACTOR) 2
At3g11020	13.73	0.00	DRE binding transcription factor DREB2B
At3g25250	9.53	0.00	protein kinase, putative
At3g50950	3.03	0.00	putative disease resistance protein
At4g03430	5.18	0.01	putative pre-mRNA splicing factor (STABILIZED 1)
At4g18880	8.02	0.00	Heat Stress Transcription Factor (HSFA4a)
At4g23450	3.71	0.00	putative protein zinc finger protein
At4g24960	3.02	0.04	Homologous to a eukaryote specific ABA- and stress-inducible gene first isolated from barley
At4g25470	3.93	0.00	DRE/CRT-binding protein DREB1C/CBF2 involved in low-temperature-responsive gene expression
At4g25480	4.11	0.02	DRE/CRT-binding protein DREB1A/CBF3 involved in low-temperature-responsive gene expression
At4g25490	3.00	0.01	DRE/CRT-binding protein DREB1B/CBF1 involved in low-temperature-responsive gene expression
At5g59820	5.39	0.00	zinc finger protein ZAT12 involved in high light and cold acclimation
At4g33720	12.67	0.00	Pathogenesis-related 1 protein
At2g02710	3.30	0.00	putative receptor-like protein kinase
At3g25600	3.20	0.00	calmodulin, putative
At5g40690	22.93	0.00	putative calcium binding protein
At1g20350	5.00	0.00	mitochondrial inner membrane translocase component, putative
At2g04050	162.31	0.00	MATE efflux family
At5g61810	4.65	0.01	peroxisomal Ca-dependent solute carrier - like protein

Appendix A3B. Genes with Reduced Expression in *rcf1-1* after 24 h Cold Treatment as Determined by Microarray Analysis.

AGI ID	Fold Change	P Value	Gene Description
At3g58070	3.89	0.00	zinc finger-like protein
At3g55480	3.66	0.00	AP3-complex beta-3A adaptin subunit-like protein
At4g33240	3.26	0.00	FAB1 protein
At4g16280	3.03	0.01	FCA gamma protein
At1g43710	4.67	0.00	histidine decarboxylase, putative
At1g34210	3.31	0.00	somatic embryogenesis receptor-like kinase
At2g03150	3.52	0.00	putative calmodulin

At3g14940	3.28	0.00	phosphoenolpyruvate carboxylase (PPC)
At1g74670	5.42	0.00	GAST1-like protein
At5g25520	3.27	0.00	PHD finger protein
At5g59950	5.80	0.02	RNA-binding (RRM/RBD/RNP motifs) family protein
At4g00050	3.18	0.01	putative transcriptional regulator
At3g18600	3.04	0.00	DEAD box helicase protein, putative
At1g79950	3.18	0.01	RAD3-like DNA-binding helicase protein
At2g36010	3.43	0.00	putative E2F5 family transcription factor
At2g30800	3.49	0.00	putative RNA helicase A
At4g14130	4.54	0.00	xyloglucan endotransglycosylase-related protein XTR-7
At5g62670	4.53	0.01	plasma membrane proton ATPase-like
At5g48880	5.39	0.00	3-keto-acyl-CoA thiolase 2
At3g52940	3.61	0.01	nuclear envelope membrane protein
At4g37560	4.25	0.00	formamidase - like protein
At3g30180	3.50	0.01	cytochrome P450 homolog, putative
At3g14650	5.81	0.00	putative cytochrome P450
At3g17970	3.53	0.01	phosphoprotein phosphatase, putative
At3g17970	3.53	0.01	phosphoprotein phosphatase, putative
At1g60890	3.06	0.01	putative phosphatidylinositol-4-phosphate 5-kinase
At1g64390	4.97	0.03	endo-beta-1,4-glucanase, putative
At2g47240	5.94	0.00	putative acyl-CoA synthetase
At1g62960	3.31	0.00	1-aminocyclopropane-1-carboxylate synthase, putative
At1g11545	6.12	0.00	endo-xyloglucan transferase, putative
At1g60590	4.25	0.00	polygalacturonase, putative
At2g27360	3.44	0.00	putative lipase
At5g59010	3.24	0.00	putative protein kinase
At5g59130	4.23	0.01	subtilisin-like serine protease
At5g53540	3.44	0.00	26S proteasome regulatory particle chain RPT6-like protein
At5g45650	3.30	0.01	subtilisin-like protease
At5g23210	3.97	0.00	serine carboxypeptidase II-like protein
At5g02760	3.48	0.03	protein phosphatase - like protein
At4g23290	3.67	0.00	serine/threonine kinase - like protein
At3g14840	3.24	0.01	receptor-like serine/threonine kinase, putative
At3g23340	3.08	0.01	putative casein kinase I
At3g11910	3.85	0.02	putative ubiquitin carboxyl-terminal hydrolase
At1g53430	3.14	0.01	receptor-like serine/threonine kinase, putative
At1g11350	3.45	0.00	serine/threonine kinase, putative
At1g60800	3.08	0.00	receptor-like kinase, putative
At2g27420	4.82	0.00	cysteine proteinase
At2g41560	4.26	0.00	putative Ca2+-ATPase
At5g15840	3.40	0.00	CONSTANS
At5g60890	5.12	0.00	Myb transcription factor homolog (ATR1)
At5g07990	4.80	0.03	flavonoid 3-hydroxylase - like protein
At4g35770	3.07	0.03	senescence-associated protein sen1
At3g22420	5.37	0.00	putative protein kinase
At1g06180	4.31	0.00	MYB-related protein
At1g18710	7.60	0.00	Myb-related transcription factor mixta, putative
At1g22430	3.32	0.01	alcohol dehydrogenase ADH
At1g12110	3.94	0.01	putative NPK1-related protein kinase 2
At2g26330	3.61	0.00	putative receptor-like protein kinase, ERECTA
At5g65730	4.20	0.00	xyloglucan endo-transglycosylase-like protein
At5g61420	3.66	0.00	putative transcription factor MYB28
At4g33420	3.17	0.00	peroxidase ATP17a -like protein
At2g35380	3.00	0.01	putative peroxidase
At4g30610	4.23	0.00	SERINE CARBOXYPEPTIDASE II-like protein
At1g31420	3.05	0.01	protein kinase, putative
At3g14350	3.22	0.00	putative leucine-rich repeat transmembrane protein kinase
At1g07650	4.62	0.00	receptor-like serine/threonine kinase, putative
At5g62670	4.53	0.01	plasma membrane proton ATPase-like

Appendix A4. Common Genes with Altered Expression Levels in *rcf1-1* after 0 h, 12 h and 24 h Cold Treatment (3A and 3B) and Common Genes with Altered Expression Levels in *rcf1-1* after 12 h and 24 h Cold Treatment (3C and 3D) as Determined by Microarray Analysis.

Appendix A4A. Genes with Increased Expression in *rcf1-1* after 0 h, 12 h and 24 h Cold Treatment as Determined by Microarray Analysis.

AGI ID	4°C, 0 h		4°C, 12 h		4°C, 24 h		Gene Description
	Fold Change	P Value	Fold Change	P Value	Fold Change	P Value	
AT1G80840	3.81	0.0022	4.90	0.002	8.61	8.4E-05	WRKY DNA-binding protein 40
AT5G44420	20.75	0.0027	36.57	0.003	22.64	1.0E-03	plant defensin 1.2
AT5G51440	3.25	0.0035	5.93	0.036	22.07	1.0E-03	HSP20-like chaperones superfamily protein
AT5G51440	3.25	0.0035	5.93	0.036	22.07	1.0E-03	HSP20-like chaperones superfamily protein
AT4G33720	30.39	0.0005	38.69	0.004	12.67	4.2E-03	Pathogenesis-related 1 protein

Appendix A4B. Genes with decreased Expression in *rcf1-1* after 0 h, 12 h and 24 h Cold Treatment as Determined by Microarray Analysis.

AGI ID	4°C, 0 h		4°C, 12 h		4°C, 24 h		Gene Description
	Fold Change	P Value	Fold Change	P Value	Fold Change	P Value	
AT5G59130	4.26	0.0004	3.78	0.025	4.23	6.5E-03	subtilase family protein

Appendix A4C. Genes with Increased Expression in *rcf1-1* after 12 h and 24 h Cold Treatment as Determined by Microarray Analysis.

AGI ID	4°C, 12 h		4°C, 24 h		Gene Description
	Fold Change	P Value	Fold Change	P Value	
At3g61630	5.68	0.00872	17.22	0.00030	cytokinin response factor (CRF6)
At2g42270	3.65	0.00100	9.81	0.00001	U5 small nuclear ribonucleoprotein helicase (Brr2b)
At3g50930	15.70	0.00545	30.98	0.00051	cytochrome BC1 synthesis (BCS1)
At4g16680	15.46	0.00108	36.20	0.00006	putative DEAD/DEATH box RNA helicase
At2g32020	28.90	0.00031	33.98	0.00006	putative alanine acetyl transferase
At5g62480	11.73	0.00004	66.43	0.00000	glutathione S-transferase-like protein
At1g69880	4.02	0.01052	3.08	0.00932	putative thioredoxin
At1g42990	2.84	0.00603	9.10	0.00004	bZIP transcription factor, putative
At1g80840	4.90	0.00192	8.61	0.00008	putative WRKY transcription factor
At2g03760	9.52	0.00004	51.93	0.00000	putative steroid sulfotransferase
At2g38470	3.67	0.01849	4.47	0.00342	putative WRKY-type DNA binding protein
At4g37370	11.35	0.00108	32.84	0.00004	Member of CYTOCHROME P450 (CYP81D8)
At5g44420	36.57	0.00273	22.64	0.00104	an ethylene- and jasmonate-responsive plant defensin (PDF1.2A)
At5g51440	5.93	0.03600	22.07	0.00103	mitochondrial heat shock 22 kd protein-like
At2g47520	7.44	0.00653	15.16	0.00044	HYPOXIA RESPONSIVE ERF (ETHYLENE RESPONSE FACTOR) 2
At3g25250	3.60	0.04573	9.53	0.00128	protein kinase, putative
At4g25470	2.55	0.01857	3.93	0.00110	DRE/CRT-binding protein DREB1C/CBF2 involved in low-temperature-responsive gene expression
At5g59820	2.77	0.00900	5.39	0.00030	zinc finger protein ZAT12 involved in high light and cold acclimation
At4g33720	38.69	0.00358	12.67	0.00422	Pathogenesis-related 1 protein
At5g40690	7.31	0.00723	22.93	0.00028	putative calcium binding protein

Appendix A4D. Genes with Reduced Expression in *rcf1-1* after 12 h and 24 h Cold Treatment as Determined by Microarray Analysis.

AGI ID	4°C, 12 h		4°C, 24 h		Gene Description
	Fold Change	P Value	Fold Change	P Value	
At1g60890	4.79	0.00603	3.06	0.00783	phosphatidylinositol-4-phosphate 5-kinase family protein
At4g33240	3.57	0.00773	3.26	0.00335	a protein that is predicted to act as a 1-phosphatidylinositol-3-phosphate (PtdIns3P) 5-kinase
At5g59130	3.78	0.02504	4.23	0.00646	subtilisin-like serine protease
At1g53430	7.84	0.00298	3.14	0.00981	protein kinase family protein

At1g18710	3.36	0.02731	7.60	0.00091	Member of the R2R3 MYB transcription factor family (ATMYB47)
At1g07650	5.39	0.00433	4.62	0.00141	leucine-rich repeat transmembrane protein kinase, putative

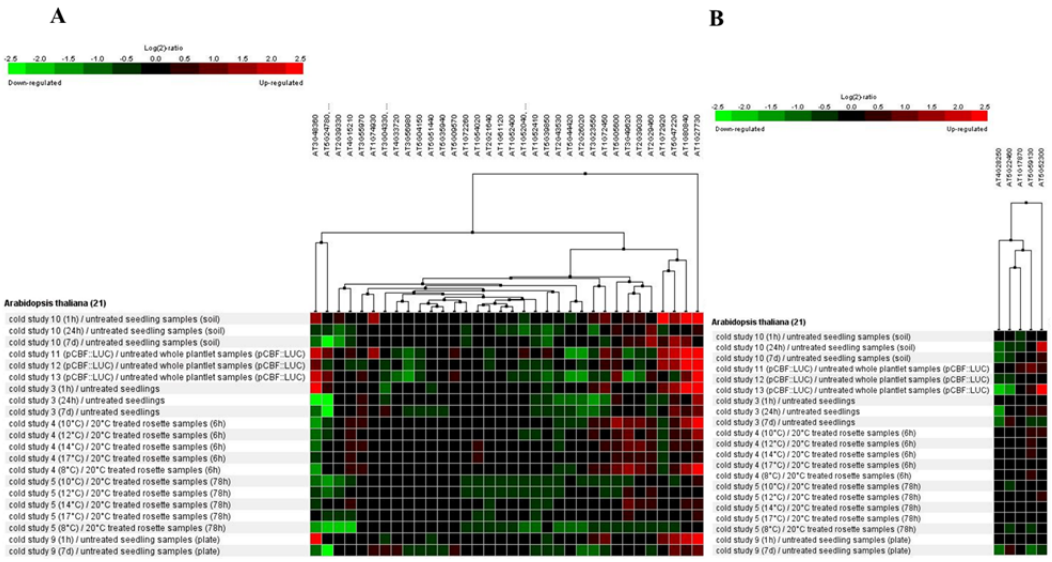

Appendix A5. Hierarchical Clustering Analysis of Genes in Wild-Type Plants in Response to Cold Stress Treatments Based on Publically Available Gene Expression Data; These Genes Showed Increased (A) and Reduced (B) Expression in *rcf1-1* without Cold Treatment as Determined by the ATH1 Microarray Analysis. Hierarchical clustering analysis was performed in Genevestigator with Hierarchical Clustering Tool (https://www.genevestigator.com/gv/user/gvLogin.jsp) (Hruz et al., 2008). Scale bars at the top indicates relative expression level (green, repression; red, induction) of a gene compared to non-stressed condition.

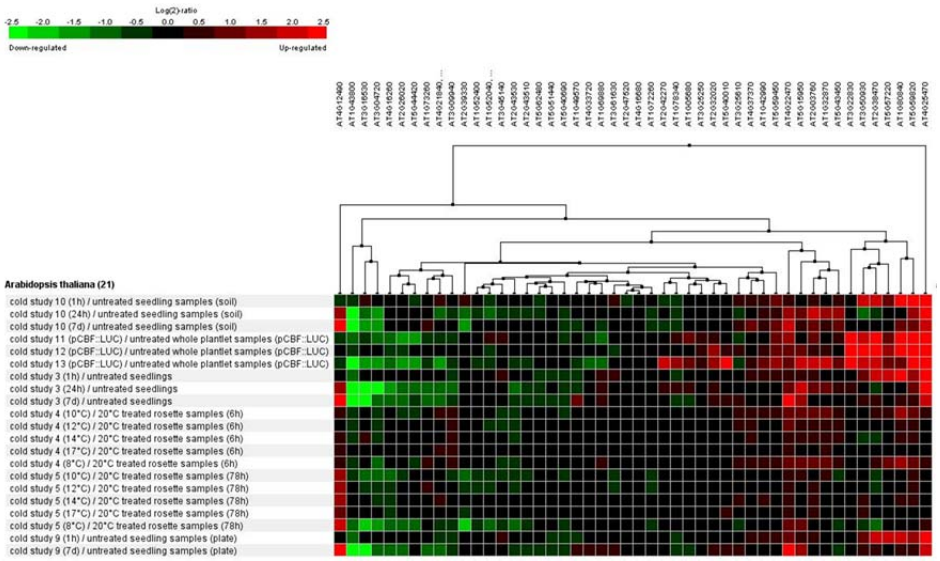

Appendix A6. Hierarchical Clustering Analysis of Genes in Wild-Type Plants in Response to Cold Stress Treatments Based on Publically Available Gene Expression Data; These Genes Showed Increased Expression in *rcf1-1* after 12-h Cold Treatment as Determined by the ATH1 Microarray Analysis. Hierarchical clustering analysis was performed in Genevestigator with Hierarchical Clustering Tool (https://www.genevestigator.com/gv/user/gvLogin.jsp) (Hruz et al., 2008). Scale bar at the top indicates relative expression level (green, repression; red, induction) of a gene compared to non-stressed condition.

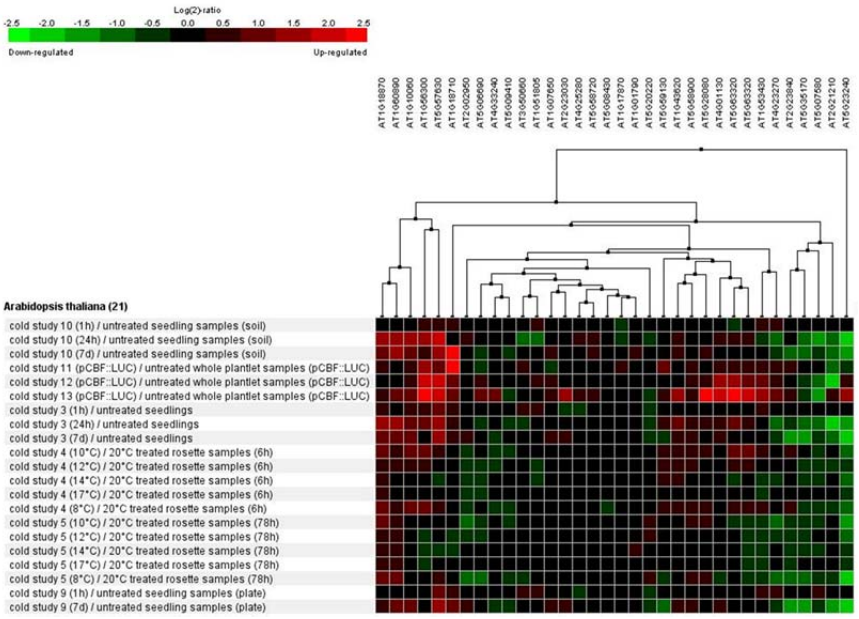

Appendix A7. Hierarchical Clustering Analysis of Genes in Wild-Type Plants in Response to Cold Stress Treatments Based on Publically Available Gene Expression Data; These Genes Showed Reduced Expression in *rcf1-1* after 12-h Cold Treatment as Determined by the ATH1 Microarray Analysis. Hierarchical clustering analysis was performed in Genevestigator with Hierarchical Clustering Tool (https://www.genevestigator.com/gv/user/gvLogin.jsp) (Hruz et al., 2008). Scale bar at the top indicates relative expression level (green, repression; red, induction) of a gene compared to non-stressed condition.

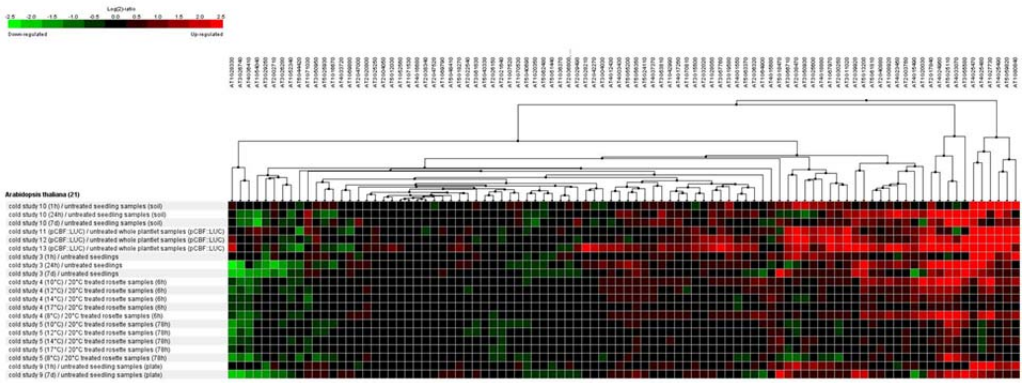

Appendix A8. Hierarchical Clustering Analysis of Genes in Wild-Type Plants in Response to Cold Stress Treatments Based on Publically Available Gene Expression Data; These Genes Showed Increased Expression in *rcf1-1* after 24-h Cold Treatment as Determined by the ATH1 Microarray Analysis. Hierarchical clustering analysis was performed in Genevestigator with Hierarchical Clustering Tool (https://www.genevestigator.com/gv/user/gvLogin.jsp) (Hruz et al., 2008). Scale bar at the top indicates relative expression level (green, repression; red, induction) of a gene compared to non-stressed condition.

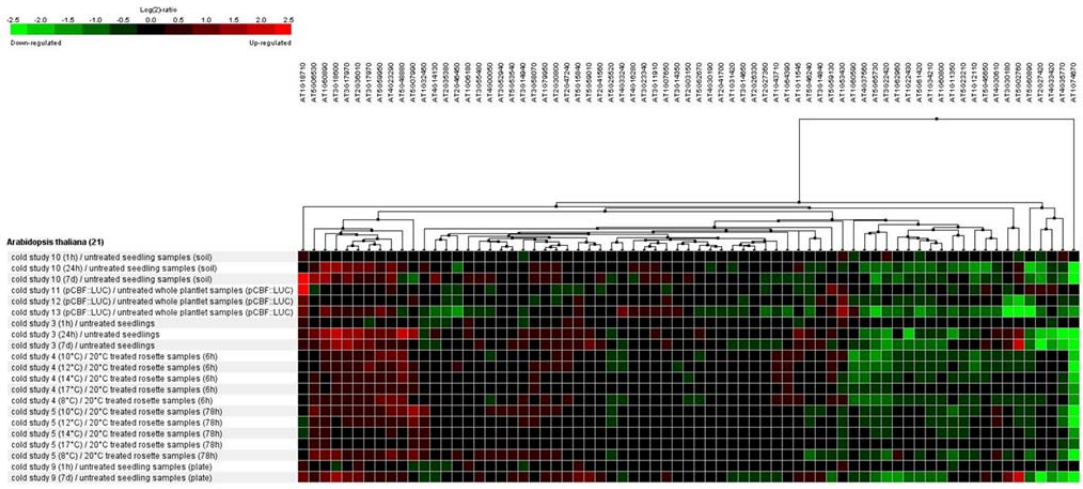

Appendix A9. Hierarchical Clustering Analysis of Genes in Wild-Type Plants in Response to Cold Stress Treatments Based on Publically Available Gene Expression Data; These Genes Showed Reduced Expression in *rcf1-1* after 24-h Cold Treatment as Determined by the ATH1 Microarray Analysis. Hierarchical clustering analysis was performed in Genevestigator with Hierarchical Clustering Tool (https://www.genevestigator.com/gv/user/gvLogin.jsp) (Hruz et al., 2008). Scale bar at the top indicates relative expression level (green, repression; red, induction) of a gene compared to non-stressed condition.

Appendix A10. Mis-Spliced Genes in *rcf1-1* as Determined by Tiling Array Analysis.
Appendix A10A. Mis-Spliced Genes in *rcf1-1* under Cold Treatment as Determined by Tiling Array Analysis.

AGI ID	Position of Retained Intron in a Gene in *rcf1-1*	False Discovery Rate (%)	Fold Change	Gene Description
AT1G26110	1	1.92	4.98	decapping 5
AT2G13370	2	4.41	4.17	chromatin remodeling 5
AT2G35110	3	4.21	3.48	Component of the WAVE protein complex which act as activators of ARP2/3 complex involved in actin nucleation
AT2G38440	8	0.00	4.73	Component of the WAVE protein complex which act as activators of ARP2/3 complex involved in actin nucleation
AT4G00100	4	4.21	3.92	ribosomal protein S13A
AT4G02990	1	4.41	3.32	Mitochondrial transcription termination factor family protein
AT2G16700	1	0.00	5.87	actin depolymerizing factor 5
AT5G18400	1	3.19	4.84	Cytokine-induced anti-apoptosis inhibitor 1, Fe-S biogenesis
AT1G01550	1	4.21	4.07	Protein of unknown function (DUF793)
AT1G34190	3	0.00	7.32	NAC domain containing protein 17
AT1G55900	2	0.70	4.42	Haloacid dehalogenase-like hydrolase
AT1G80410	25	4.41	3.66	tetratricopeptide repeat (TPR)-containing protein
AT3G02310	4	0.70	6.33	K-box region and MADS-box transcription factor family protein
AT3G07780	1	0.00	9.48	Protein of unknown function (DUF1423)
AT3G16830	7	2.26	3.97	TOPLESS-related 2
AT3G55620	5	0.00	7.99	Translation initiation factor IF6
AT3G55620	6	1.18	4.15	Translation initiation factor IF6
AT5G57930	1	4.21	4.54	protein of unknown function (DUF794)
AT5G06370	2	4.41	3.45	NC domain-containing protein-related
AT5G25540	1	0.70	5.07	CTC-interacting domain 6
AT1G06670	1	0.00	5.02	nuclear DEIH-box helicase
AT3G52730	1	1.68	4.25	ubiquinol-cytochrome C reductase UQCRX
AT3G48990	2	0.00	5.68	AMP-dependent synthetase and ligase family protein
AT1G03905	2	1.18	4.79	P-loop containing nucleoside triphosphate hydrolase
AT1G04600	24	1.92	4.16	myosin XI A
AT1G06150	9	4.41	4.04	basic helix-loop-helix (bHLH) DNA-binding superfamily protein
AT1G73870	1	1.92	4.19	B-box type zinc finger protein with CCT domain
AT1G76810	1	4.41	3.37	eukaryotic translation initiation factor 2 (eIF-2) family protein
AT1G78420	7	1.18	4.74	RING/U-box superfamily protein
AT1G78420	1	4.21	3.26	RING/U-box superfamily protein
AT2G31260	3	4.41	3.49	autophagy 9 (APG9)
AT2G31380	1	0.00	6.24	salt tolerance homologue
AT2G41900	1	0.00	6.43	CCCH-type zinc finger protein with ARM repeat domain
AT2G42680	2	4.21	4.13	multiprotein bridging factor 1A
AT2G47220	2	1.68	6.46	DOMAIN OF UNKNOWN FUNCTION 724 5
AT3G05670	3	0.70	5.10	RING/U-box protein
AT3G08530	27	0.00	9.71	Clathrin, heavy chain
AT3G13940	1	1.68	3.87	DNA binding;DNA-directed RNA polymerases
AT3G20970	1	0.70	6.64	NFU domain protein 4
AT3G57090	4	3.19	3.65	Tetratricopeptide repeat (TPR)-like superfamily protein

AT3G57090	3	0.00	9.35	Tetratricopeptide repeat (TPR)-like superfamily protein
AT3G57090	1	0.70	5.26	Tetratricopeptide repeat (TPR)-like superfamily protein
AT3G57090	2	0.00	7.75	Tetratricopeptide repeat (TPR)-like superfamily protein
AT3G57880	1	4.21	3.41	Ca^{2+}-dependent lipid-binding phosphoribosyltransferase
AT3G63120	1	1.68	5.80	cyclin p1;1
AT4G02010	3	0.00	5.33	Protein kinase superfamily protein
AT4G11175	1	3.19	3.98	Nucleic acid-binding, OB-fold-like protein
AT4G31985	1	0.70	5.27	Ribosomal protein L39 family protein
AT4G33650	10	0.00	7.77	dynamin-related protein 3A
AT4G35040	2	1.18	5.31	Basic-leucine zipper (bZIP) transcription factor
AT4G35310	1	4.41	3.57	calmodulin-domain protein kinase 5
AT5G02290	1	4.41	3.88	Protein kinase superfamily protein
AT5G03300	1	4.21	4.11	adenosine kinase 2
AT5G19450	7	4.21	3.62	calcium-dependent protein kinase 19
AT5G27840	2	3.19	5.61	Calcineurin-like metallo-phosphoesterase
AT5G40850	1	1.18	3.86	urophorphyrin methylase 1
AT5G51260	2	1.92	4.33	HAD superfamily, subfamily IIIB acid phosphatase
AT5G54680	1	4.41	3.40	basic helix-loop-helix (bHLH) DNA-binding
AT5G55200	1	4.41	3.38	Co-chaperone GrpE family protein
AT5G56350	1	0.00	6.74	Pyruvate kinase family protein
AT5G58380	1	4.21	4.22	SOS3-interacting protein 1
AT5G65900	4	4.21	4.21	DEA(D/H)-box RNA helicase family protein
AT1G19880	3	1.18	5.05	Regulator of chromosome condensation (RCC1)
AT1G21790	2	0.00	5.91	TRAM, LAG1 and CLN8 (TLC) lipid-sensing domain containing protein
AT1G21790	1	0.70	5.71	TRAM, LAG1 and CLN8 (TLC) lipid-sensing domain containing protein
AT1G60560	4	1.18	3.88	SWIM zinc finger family protein
AT1G66260	1	1.92	4.36	RNA-binding (RRM/RBD/RNP motifs) family protein
AT2G36320	1	1.18	4.60	A20/AN1-like zinc finger family protein
AT3G03790	2	4.21	4.05	regulator of chromosome condensation (RCC1)
AT3G10770	1	4.21	4.19	Single-stranded nucleic acid binding R3H protein
AT3G55580	1	1.18	5.71	Regulator of chromosome condensation (RCC1)
AT3G55580	6	4.21	4.17	Regulator of chromosome condensation (RCC1)
AT4G10610	1	4.41	3.79	CTC-interacting domain 12
AT4G17150	2	1.92	4.96	alpha/beta-Hydrolases superfamily protein
AT4G23630	2	0.00	8.72	VIRB2-interacting protein 1
AT4G32620	1	4.41	3.49	Enhancer of polycomb-like transcription factor protein
AT5G19250	1	0.70	6.14	Glycoprotein membrane precursor GPI-anchored
AT5G37290	1	1.18	4.33	ARM repeat superfamily protein
AT5G41600	1	1.18	4.02	VIRB2-interacting protein 3
AT5G50170	7	2.26	4.25	C2 calcium/lipid-binding and GRAM domain containing protein
AT5G54100	7	0.00	29.20	SPFH/Band 7/PHB domain-containing membrane-associated protein
AT5G54100	8	0.00	25.04	SPFH/Band 7/PHB domain-containing membrane-associated protein
AT5G54100	6	0.00	54.74	SPFH/Band 7/PHB domain-containing membrane-associated protein
AT5G54100	4	0.00	11.00	SPFH/Band 7/PHB domain-containing membrane-associated protein
AT5G58210	2	0.00	7.44	hydroxyproline-rich glycoprotein family protein
AT1G06410	1	0.00	5.68	trehalose-phosphatase/synthase 7
AT1G18500	11	4.21	4.64	methylthioalkylmalate synthase-like 4
AT1G27480	1	3.19	3.52	alpha/beta-Hydrolases superfamily protein

AT1G48100	2	0.00	5.58	Pectin lyase-like superfamily protein
AT1G48100	5	4.21	3.34	Pectin lyase-like superfamily protein
AT1G62570	2	0.70	4.18	flavin-monooxygenase glucosinolate S-oxygenase 4
AT1G67490	16	3.19	4.05	glucosidase 1
AT1G71950	1	2.26	5.68	Proteinase inhibitor, propeptide
AT1G77680	1	4.41	4.20	Ribonuclease II/R family protein
AT2G02390	4	1.68	3.59	glutathione S-transferase zeta 1
AT2G15620	1	0.00	7.03	nitrite reductase 1
AT2G24560	1	2.26	4.32	GDSL-like Lipase/Acylhydrolase family protein
AT2G39480	8	4.21	3.27	P-glycoprotein 6
AT2G45670	1	0.70	6.03	calcineurin B subunit-related
AT3G08590	7	0.00	18.89	Phosphoglycerate mutase, 2,3-bisphosphoglycerate-independent
AT3G08590	4	0.70	4.83	Phosphoglycerate mutase, 2,3-bisphosphoglycerate-independent
AT3G14890	4	0.70	7.57	phosphoesterase
AT3G14890	5	1.92	5.32	phosphoesterase
AT3G24170	9	4.41	3.10	glutathione-disulfide reductase
AT3G24170	5	3.19	3.45	glutathione-disulfide reductase
AT3G24180	17	0.70	5.38	Beta-glucosidase, GBA2 type family protein
AT3G62370	4	1.92	3.75	heme binding
AT4G21990	1	1.18	6.10	APS reductase 3
AT4G24160	2	1.92	4.37	alpha/beta-Hydrolases superfamily protein
AT4G24160	1	1.18	5.04	alpha/beta-Hydrolases superfamily protein
AT4G29010	4	4.41	3.19	Enoyl-CoA hydratase/isomerase family
AT4G36580	7	2.26	3.99	AAA-type ATPase family protein
AT4G38950	11	3.19	5.22	ATP binding microtubule motor family protein
AT5G14310	1	2.26	3.81	carboxyesterase 16
AT5G16010	1	0.00	10.81	3-oxo-5-alpha-steroid 4-dehydrogenase family protein
AT5G19550	1	0.00	7.16	aspartate aminotransferase 2
AT5G19550	6	0.00	5.30	aspartate aminotransferase 2
AT5G19550	7	0.00	8.21	aspartate aminotransferase 2
AT5G19550	11	1.68	5.40	aspartate aminotransferase 2
AT5G27970	15	4.41	3.61	ARM repeat superfamily protein
AT5G36890	12	0.00	5.30	beta glucosidase 42
AT5G43450	1	4.41	3.35	2-oxoglutarate and Fe(II)-dependent oxygenase
AT5G43860	1	4.41	3.12	chlorophyllase 2
AT5G48840	3	3.19	3.81	homolog of bacterial PANC
AT5G55070	1	0.70	4.76	Dihydrolipoamide succinyltransferase
AT1G08460	1	4.21	3.99	histone deacetylase 8
AT1G27910	1	1.18	5.75	plant U-box 45 (PUB45)
AT1G27910	5	0.00	11.17	plant U-box 45 (PUB45)
AT1G47710	1	4.41	3.77	Serine protease inhibitor (SERPIN) family protein
AT1G63690	3	1.68	4.66	SIGNAL PEPTIDE PEPTIDASE-LIKE 2
AT1G76140	1	3.19	4.25	Prolyl oligopeptidase family protein
AT5G02880	3	2.26	5.24	ubiquitin-protein ligase 4
AT5G48760	1	2.26	3.42	Ribosomal protein L13 family protein
AT5G58870	12	2.26	3.73	FTSH protease 9
AT1G04850	11	0.00	5.25	ubiquitin-associated (UBA)/TS-N domain-containing protein
AT1G10760	15	4.41	4.50	Pyruvate phosphate dikinase, PEP/pyruvate binding domain
AT1G10760	11	4.21	3.83	Pyruvate phosphate dikinase, PEP/pyruvate binding domain
AT1G23190	4	4.21	4.77	Phosphoglucomutase/phosphomannomutase family protein
AT1G24180	2	4.41	3.38	Thiamin diphosphate-binding fold superfamily protein
AT1G32230	2	0.00	9.57	WWE domain protein /RCD1 (RADICAL-INDUCED CELL DEATH1)
AT1G32870	1	0.00	7.71	NAC domain protein 13

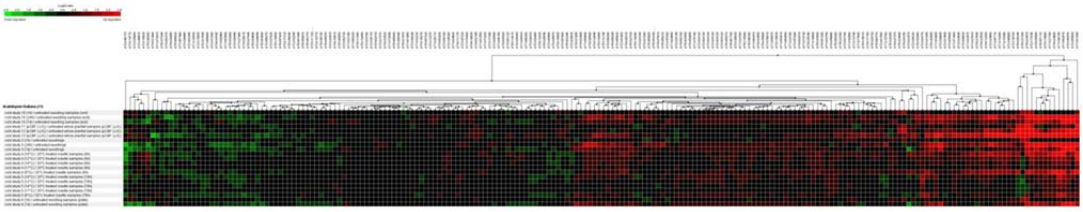

Appendix A11. Mis-Spliced Transcripts of *EBF2* and *PUB45* in *rcf1-1* as Determined by RT-PCR and Hierarchical Clustering Analysis of Genes in Wild-Type Plants in Response to Cold-Stress Treatments Based on Publically Available Gene Expression Data. (A) Mis-spliced transcripts of *EBF2* and *PUB45* in *rcf1-1*, *rcf1-1 sta1-2* and *rcf1-1 brr2b* but not in *sta1-2* or *brr2b* under cold stress (4°C for 12 h) determined by RT-PCR analysis. Arrows indicate mis-spliced transcripts. (B) Visualization of intron retention of *EBF2* and *PUB45* in *rcf1-1* with the integrated genome browser. Vertical bars represent averaged log2 expression values of unique probes in the gene region; introns that were retained in *rcf1-1* under cold treatment were indicated with black boxes; gene structures on the bottom of each panel are based on TAIR10 annotation. (C) Transcripts of genes tested in (A) under unstressed condition. (D) Hierarchical clustering analysis of genes in wild type plants in response to cold stress treatments using publically available gene expression data. These genes showed mis-spliced patterns in *rcf1-1* by our tiling array analysis after 12 h cold treatment. Hierarchical clustering analysis was performed in Genevestigator with Hierarchical Clustering Tool (https://www.genevestigator.com/gv/user/gvLogin.jsp) (Hruz et al., 2008). Scale bar at the top indicates relative expression level (green, repression; red, induction) of a gene compared to non-stressed condition.

Appendix A12. Primers Used in This Study.

Primer Name	Sequence (5' to 3')	Purpose
RCF1 comp-F	AGTCGCGGCCGCACGGGGTTATATGGTGTGACG	Construction of pMDC99-RCF1 for complementation of *rcf1-1*
RCF1 comp-R	ACTGCTCGAGTAACTCTACGTTGTTTACAATGCGAGTCC	
RCF1-DAAD-F	TGGTAATGGATGCAGCTGATCGTATGTTTGAC	Site-directed mutagenesis for pDEST15-RCF1 (DAAD) and pMDC99-RCF1 (DAAD) for *rcf1-1*
RCF1-DAAD-R	AACCCATGTCAAACATACGATCAGCTGCATCC	
RCF1-DEAD-F	GGGGACAAGTTTGTACAAAAAAGCAGGCTTCTCTAGGATGACACAAGAAGAAG	Construction of pDEST15-RCF1, pMDC32-RCF1
RCF1-DEAD-R	GGGGACCACTTTGTACAAGAAAGCTGGGTCCTAAGCAAGTGCTTTCAGATCATC	
RCF1-F	GGGGACAAGTTTGTACAAAAAAGCAGGCTTCTCTAGGATGACACAAGAAGAAG	Construction of pMDC83-RCF1
RCF1-R	GGGGACCACTTTGTACAAGAAAGCTGGGTCAGCAAGTGCTTTCAGATCATC	
At5g24470 attB1 F	GGGGACAAGTTTGTACAAAAAAGCAGGCTATGTGGCAAACGTGGCCACGTCAGCCA	Construction of pMDC32-PRR5
At5g24470 attB1 R	GGGGACCACTTTGTACAAGAAAGCTGGGTCCTATGGAGCTTGTGTGGATTGGACTTG	
At3g05840 attB1 F	GGGGACAAGTTTGTACAAAAAAGCAGGCTTCATGGCCTCGGTGGGCATAGAGCCTAGTGC	Construction of pMDC32-AtSK12
At3g05840 attB1 R	GGGGACCACTTTGTACAAGAAAGCTGGGTCTCACAAACTGAGCCACGGACATTGCTTCCT	
At5g37260 attB1 F	GGGGACAAGTTTGTACAAAAAAGCAGGCTTCATGGCTATGCAGGAACGTTGTGAGAG	Construction of pMDC32-CIR1
At5g37260 attB2 R	GGGGACCACTTTGTACAAGAAAGCTGGGTTCACCACAAAGGATATGATAATTTTACATTG	
At5g54100 attB1 F	GGGGACAAGTTTGTACAAAAAAGCAGGCTATGAATCAGCTCGCGCTTTCAAGATCCGGT	Construction of pMDC32-SPFH
At5g54100 attB2 R	GGGGACCACTTTGTACAAGAAAGCTGGGTCCTACTCCAGAAGTTTCCCTGAAACCAC	
cs856017 LP	GGTGGACCAATGAATCAAGCTGGTTGGCAAG	Genotyping
cs856017 RP	GTCCTTATCCTACATTCACCGATGTATC	
SALK_135000C LP	GTCACGAGTGGGATTTTTATAGGTACTC	Genotyping
SALK_135000C RP	GTAACATTTAGCCGCACGCGAATCAGATTC	
CS812234 LP	CACAAAATTGCTGCAAAAATG	Genotyping
CS812234 RP	TCGGACAATAAGATCGAATCG	
SALK_048780 LP	AGACTCGTATCCTCCTTTGCC	Genotyping
SALK_048780 RP	AGTTAAAACGGATTGAACCGG	
SALK_051843 LP	CACAAACGAACACTTCACCACAAAGGATATG	Genotyping
SALK_051843 RP	CAGAAGCAGAGCATGAGAAGTTTGTAGAAGC	
SALK_090074C LP	GACGGCGAAGGTTTATTGATTTGGTAGCTAC	Genotyping
SALK_090074C RP	CTGAGGAAGTTTGGGCTTTAAAAGTCCATACATC	
At5g24470 3I F	AGGTGCGGCTGATTATCTTGTTAAGCCGT	RT-PCR to detect intron retention in *rcf1-1*
At5g24470 3I R	CTCTCTTTCCGTTCGAGTTGTTTGCAG	

At3g05840 11I F	TTGGTCCACCCATTCTTTGACGAGCTAAG	RT-PCR to detect intron retention in *rcf1-1*
At3g05840 11I R	CATTGCTTCCTCGCATGTTCTGGAACTA	
At5g37260-3I-F	CTGATGAACTTATATCTTCCTCAGATGCCTT	RT-PCR to detect intron retention in *rcf1-1*
At5g37260-3I-R	CTGCGCATGGCTTCGAATCTGAACTGCAGT	
At5g54100 6I F	GATATCATGCCTCCTAATGGAGTGAGAG	RT-PCR to detect intron retention in *rcf1-1*
At5g54100 6I R	CACGATTGACTTGGTCCATCATTGC	
At1g27910 5I F	GTTGAAGCGTTGCTTCAGTTTCTGGGATC	RT-PCR to detect intron retention in *rcf1-1*
At1g27910 5I R	CTTTGCTTCTTCAAGACACGAGAGGTTCAG	
At5g25350 1I F	CTTCGAATTATGTCTGGAATCTTCAGATTTAGTG	RT-PCR to detect intron retention in *rcf1-1*
At5g25350 1I R	GAAGTTTGCTTCTCCTCAAAACCGCTGT	
AtSK12 I11 F	GTACTACCACACCTTCCTTTGTCTTCAAAAAGTAGC	To make a probe in the 11th intron for Northern blot
AtSK12 I11 R	CTGTTAAACACAACAAATTAATACGAGTTTAAGTCAC	
PRR5 I3 F	GTATGTTTCATATCCATCTTTTGTTTTAAGCTTTATGTGTG	To make a probe in the 3rd intron for Northern blot
PRR5 I3 R	CTGTAAAAGATAATCAAAACCAAAAACAAATCTGAGAACTC	
CIR1 I3 F	GTGTGTGTGCTTATCTGACTTTAGAGAGTCTAATGC	To make a probe in the 3rd intron for Northern blot
CIR1 I3 R	CTGTTCCATAGAAGAACCAACAAAAGTCAGATCTCT	
SPFH I6 F	GTAAAATTGCTTGAAAGTATATGTTCTGGGATTG	To make a probe in the 6th intron for Northern blot
SPFH I6 R	CTGTTAAAGTCAGTACAGCAGATTATGAGAATC	
CAMTA1 qPCR F	GAACCGCCTGTATCAGCTATATGTCCTA	qRT-PCR
CAMTA1 qPCR R	CACGGAAGCCCTCAACAACCGTTAGGA	
COR15A qPCR F	AGAGTCGGCCAGAAAACTCAGTTCG	qRT-PCR
COR15A qPCR R	AGCTTTCTCAGCTTCTTTACCCAATG	
AT5G59950 qPCR F	ACGTCGATCGGAGAACCTTTGAAATGTCG	qRT-PCR
AT5G59950 qPCR R	TGTCGTGACCCCAGGTGGACTCC	
RD29A qPCR F	ATCATGAGAATGGTGCGACTAAG	qRT-PCR
RD29A qPCR R	ATGAGCCGGTGCATCGTGTC	
LUC qPCR F	TGAACATCACGTACGCGGAATAC	qRT-PCR
LUC qPCR R	ATCCCTGGTAATCCGTTTTAGAATCC	
CBF1 qPCR F	AGATGAGACGTGTGATACGACGACCACG	qRT-PCR
CBF1 qPCR R	ACGACTATCGAATATTAGTAACTCCAAAGC	
CBF2 qPCR F	TGTCGAGGGAGATGATGACGTGTCC	qRT-PCR
CBF2 qPCR R	TCTGCACTCAAAAACATTTGCATTTGACAAC	
CBF3 qPCR F	ACTAGAACAGAAAGAGAGAGAAACTATTATTTCAG	qRT-PCR
CBF3 qPCR R	TACGACCCGCCGGTTTCTTGGGGCAGCTGCTC	
ZAT12 qPCR F	TGATGCTTTTATCTAGAGTTGGAC	qRT-PCR
ZAT12 qPCR R	TGCTAGATTTCTTCAACGTAGTCACC	

At3g05840 qPCR F	TTCAATACTCTCCCAATCTCCGTTGTGCTGCT	qRT-PCR
At3g05840 qPCR R	CTCGCATGTTCTGGAACTAACTTCGCCAC	
At5g24470 qPCR F	CACAATGTTCAGCCTCCCCAGTGGTTAC	qRT-PCR
At5g24470 qPCR R	GTCCCGGCCAAGAATTCAGCTGATTACT	
RCF1 qPCR-F	TCCTCGATGGGTTTGCTAATGAGCATTACC	qRT-PCR
RCF1 qPCR-R	ACTGAATAAGCTCCAAGTCTTACCCATTGG	
STA1 qPCR F	GCTACAGCGGCTGCTCCAGGAGTAGGTC	qRT-PCR
STA1 qPCR R	CAAATCCGCAAACTGCTCAGTAATC	
Brr2b qPCR F	AGGTGGTCAAGTGTTGGAGGTAATTGTCTCT	qRT-PCR
Brr2b qPCR R	CTTGTTCTTGGCATGCTGTACTATGGCAGTG	
At5g54100 qPCR F	GATATCATGCCTCCTAATGGAGTGAGAG	qRT-PCR
At5g54100 qPCR R	CTTGAGGGATTGAGATACCATGGCCA	
At5g37260 qPCR F	CTGAAGATGGCAAGAAGAAGCTATACTCAG	qRT-PCR
At5g37260 qPCR R	GAACCCTCTCATGTTGTTCATCTCAGTC	
At4g25080 1I F	AGGAAGGAGCAATCGTCTCTGCTTCCGA	RT-PCR to detect intron retention in *rcf1-1*
At4g25080 1I R	CTGCGGGTAATGTATCAACACGTCGAGAC	
At3g52115_1I F	CTCCTGACAGTGTTCTTCACCAAAGCAG	RT-PCR to detect intron retention in *rcf1-1*
At3g52115_1I R	GTTGCCACTCGAGCCAGTACCAATTCTC	
At1g73670_6I F	TCGGCCCTTCGCCTGTTGGAACGCCTG	RT-PCR to detect intron retention in *rcf1-1*
At1g73670_6I R	TCGGCTGTGTCGATGGTTCCCGCAC	
At3g21350_2I F	GAGATGGTCCTGAGAAAGTCACACCGATGC	RT-PCR to detect intron retention in *rcf1-1*
At3g21350_2I R	GTCTAATGGTCTCCAATTTCGATGCAGC	
At1g21590_3I F	GATTGCTGGGTTCTGGCTGTTGACAATG	RT-PCR to detect intron retention in *rcf1-1*
At1g21590_3I R	CATACACTAAAGACCGCCGAAGACTCTG	
At1g65660_3I F	CACTAAGTCGTGGTATGATAGAGGTGC	RT-PCR to detect intron retention in *rcf1-1*
At1g65660_3I F	CATCAGGTGCAATGTTCATGTTTGTGTAC	
TUB8 F	ATAACCGTTTCAAATTCTCTCTCTC	qRT-PCR as a reference gene or RT-PCR as a loading control
TUB8 R	TGCAAATCGTTCTCTCCTTG	
EF1a-F	TGTGGTCATTGGCCACGTC	To make a probe for Northern blot
EF1a-R	TCACAACCATACCAGGCTTG	

Appendix B1. Primers Used in This Study.

Primer Name	Sequence (5' to 3')	Purpose
RCF3 Pro attB1 F	GGGGACAAGTTTGTACAAAAAAGCAGGCTCTTCC AACCCAAATGATCCAACTGAGC	Construction of pMDC99-RCF3
RCF3 Utr attB2 R	GGGGACCACTTTGTACAAGAAAGCTGGGTAAGC GGCAATGCTACGACGGTGGAAATGG	
RCF3 Pro attB1 F	GGGGACAAGTTTGTACAAAAAAGCAGGCTCTT CCAACCCAAATGATCCAACTGAGC	Construction of pMDC107-RCF3
RCF3 PG attB2 R	GGGGACCACTTTGTACAAGAAAGCTGGGTCCGG TCCATCCTCTTGTACTGCACCAAAC	
RCF3 attB1 F	GGGGACAAGTTTGTACAAAAAAGCAGGCTT CATGGAGAGATCTAGATCCAAGAGAAAC	Construction of pEarleyGate202-RCF3
RCF3 attB2 R	GGGGACCACTTTGTACAAGAAAGCTGGG TTCACGGTCCATCCTCTTGTATGCT	
rcf3-2 LP	CTTCAACTATGGTTACACTAGCTC	Genotyping primers for *rcf3-2*
rcf3-2 RP	CTATTGAGGAGTCATATGTTCAAGG	
HSFA1a F	GTGTTACCGGCGGAGGAACGAATATC	qRT-PCR analysis
HSFA1a R	TGTTCGTCGGACTCCATGAGACAATCG	
HSFA1b F	TGAGCAGGAGAATCGTGGTGACAATGTG	qRT-PCR analysis
HSFA1b R	CTCTACTTGAAGGGTTCCCATTGTCTAC	
HSFA1d F	TGACTTGGAATCAAAAATCCGAATGGATGTGAG	qRT-PCR analysis
HSFA1d R	ACTGTTGTTATTAGCACTCCAAGAGACAATCG	
HSFA1e F	ATGGGAACGGTTTGCGAATCTGTAGCGAC	qRT-PCR analysis
HSFA1e R	AGCTGGAGAAATTGTTGTGCTTGAAATACTTTGG	
HSFA2 F	GAAGGGCTTAACGAAACAGGGCCACCAC	qRT-PCR analysis
HSFA2 R	GATCCTTGCTGATTCACATTCTGCAAACC	
HSFA3 F	CTTGGGGACTGACCGGAGCTAGCTTCGTAG	qRT-PCR analysis
HSFA3 R	GCTAGTGCTACTGCAGCAAGTTTGGTTG	
HSFA4a F	ATGATTCTTCATCCGATTCTATCGTCTCTTGG	qRT-PCR analysis
HSFA4a R	TCATCATTCGCAAATTCCCATTGCTCAGG	
HSFA5 F	AGGAGCCGGAGGACCAGCGCCTTTCTTGG	qRT-PCR analysis
HSFA5 R	ACTCCCACCTCTCTGGATCAATCTTCCTAAACC	
HSFA6a F	AGAGGGTCTCAAAGAAACGCCACCAACG	qRT-PCR analysis
HSFA6a R	TGTTCTTAAGAAGATGCCTCTCTCCCTTCAG	
HSFA6b F	TCCATGGCTGAAGCAGCCATAAATGATCC	qRT-PCR analysis
HSFA6b R	TGCTTGAAGAATCTGGGAAGGAGAGTTACAG	
HSFA7a F	AACCCGTTTCTCCCGGAAGGCTGCGATC	qRT-PCR analysis
HSFA7a R	TGAGAAATTGCTGTGTTTGAAATGACGAGG	
HSFA7b F	ATGGACCCGTCGTCAAGCTCCAGAGCACG	qRT-PCR analysis
HSFA7b R	TGCTTGAAGTATAGAGGCAGAATAGTGGCCGAG	
HSFA8 F	ATGGAGTCCAAGTGCAGATAATAGCTTCG	qRT-PCR analysis
HSFA8 R	TGACCTCTCACAAACCCGTCATTCGCAAAC	
HSFA9 F	AGACGGCAACGGAGACCGTCACCGTTGAAAGAG	qRT-PCR analysis
HSFA9 R	TTGGGAAGTAGATTCTCTGAGAACTCGTAAGAATCC	
HSFB1 F	ATACGACGGCGTAAATCGGTGATTGC	qRT-PCR analysis
HSFB1 R	ACTCACTCTCTTCGTCAGACTCCACC	
HSFB2a F	GACGCATCAAACAGTTGTTGCTCCTTCGTC	qRT-PCR analysis
HSFB2a R	TCAGTGGGCTGAGATCCGACGTAATTCGAC	
HSFB2b F	CTCTCAGCCTGCTATGGCCGCGGCTG	qRT-PCR analysis
HSFB2b R	GTGCAGTGGTGCAGCTCGTTGTCCTCTG	
HSFB3 F	GACGGGGTTATATCTTGGAACGAATAC	qRT-PCR analysis
HSFB3 R	GTTGGCTCTTCCTTCTTCGGATATTGCTC	
HSFB4 F	CACAACAACACTCTCCGTTCATGTCACAC	qRT-PCR analysis
HSFB4 R	GTGTCAATTTGTTGTGGTATGACTCGTGGTC	
HSFC1 F	CTTCTCGCAACGAATCTTACCTGCTTATTTC	qRT-PCR analysis
HSFC1 R	CTTGACCGTACATCCCCCGCGCGTGTTTC	
DREB2A F	ATGGCAGTTTATGATCAGAGTGGAGATAGAAAC	qRT-PCR analysis
DREB2A R	TCATACAACCCTTCTTCGACCCTTTCGCAGGTAC	

DREB2B F	GAGAGAAACCGAAACGCAAAGTTCCTGC	qRT-PCR analysis
DREB2B R	TAAGCGGAAGCAGCTTTTTCCGCGGTAG	
DREB2C F	CTTCTTCGACTGCTGCCACTGCCACTGTGT	qRT-PCR analysis
DREB2C R	TCTTTTCCTTTCAGCTCCTCTTTAATACAC	
HSP17.6 F	ACAGGCGAATCAACAACAACATATTCG	qRT-PCR analysis
HSP17.6 R	AAGACCCAGAGAGAACTCAAATCAAGC	
HSP18 F	AGCAACGAACAATGTCTCTCATTCCAAGC	qRT-PCR analysis
HSP18 R	AACCTTGACTTCTTCCTTCTTCAGGCCTG	
HSP25.3 F	ATGGCTTCTACACTCTCATTTGCTGCATCGGCTC	qRT-PCR analysis
HSP25.3 R	AGAGACGTCCATGGTTAAGCGTTGTTGAGGTC	
HSP70B F	AGCTATTGGTATCGATCTCGGCACTAC	qRT-PCR analysis
HSP70B R	AAGCCTCAGCGACTTCCTTCATCTTCAC	
HSP90.1 F	TTGCGTTGAATCAAAGTTCGTTGC	qRT-PCR analysis
HSP90.1 R	TGTCCTATCATGCTTACATCAGCTCC	
HSP101 F	ACGAGACAATTGCTACAGCTCATGAGC	qRT-PCR analysis
HSP101 R	AGAAGACCCATAATCAACTGGTCAACAGC	
rcf3-2 qPCR F	CCACAACTGGCCCTCTCGAAGGTGTTGCAG	qRT-PCR analysis
rcf3-2 qPCR R	GTGGTACCGCCATTCTGCTTGTCGTGACAG	
RCF3 qPCR F	ACCAGAGGCGGTTGTTCCTAAGCTCG	qRT-PCR analysis
RCF3 qPCR R	GGTCCATCCTCTTGTATGCTCAAAATGA	
CBF2 qPCR F	TGTCGAGGGAGATGATGACGTGTCC	qRT-PCR analysis
CBF2 qPCR R	TCTGCACTCAAAAACATTTGCATTTGACAAC	
CBF3 qPCR F	ACTAGAACAGAAAGAGAGAGAAACTATTATTTCAG	qRT-PCR analysis
CBF3 qPCR R	TACGACCCGCCGGTTTCTTGGGGCAGCTGCTC	
CBK3 qPCR F	AACTCGGACTAGGGCCATCA	qRT-PCR analysis
CBK3 qPCR R	CTCATCTAACAATGGCGTTACTCTAAGCT	
CaM3 qPCR F	ACTCGAGGTATGTTTTCTGCTTGTTTAAGACG	qRT-PCR analysis
CaM3 qPCR R	ACACACCACACCACGTTTTGACC	
HSBP qPCR F	TGACATGGGAGGCAGAATCAATGAGCTGG	qRT-PCR analysis
HSBP qPCR R	TCCTTCGGACATGTCAATGAACACCACATTCC	
TUB8 F	ATAACCGTTTCAAATTCTCTCTCTC	qRT-PCR analysis as a reference gene
TUB8 R	TGCAAATCGTTCTCTCCTTG	

Appendix C1. Primers Used in This Study.

Primer name	Sequence (5' to 3')	Purpose
SALK_025986 LP	TCAGGGCCTTTGAATTCTGCTAC	Genotyping
SALK_025986 RP	AAGCCGCAAAAACTGAAGAAGCAAG	
SALK_024857 LP	ATGAACCCCGAGTTACCAGAG	Genotyping
SALK_024857 RP	TTGCAGTTTTGAACAGCAGTG	
HSFA1e F	ATGGGAACGGTTTGCGAATCTGTAGCGAC	qRT-PCR analysis
HSFA1e R	AGCTGGAGAAATTGTTGTGCTTGAAATACTTTGG	
HSFA2 F	GAAGGGCTTAACGAAACAGGGCCACCAC	qRT-PCR analysis
HSFA2 R	GATCCTTGCTGATTCACATTCTGCAAACC	
HSFA3 F	CTTGGGGACTGACCGGAGCTAGCTTCGTAG	qRT-PCR analysis
HSFA3 R	GCTAGTGCTACTGCAGCAAGTTTGGTTG	
HSFA7b F	ATGGACCCGTCGTCAAGCTCCAGAGCACG	qRT-PCR analysis
HSFA7b R	TGCTTGAAGTATAGAGGCAGAATAGTGGCCGAG	
HSP17.6 F	ACAGGCGAATCAACAACAACATATTCG	qRT-PCR analysis
HSP17.6 R	AAGACCCAGAGAGAACTCAAATCAAGC	
HSP70B F	AGCTATTGGTATCGATCTCGGCACTAC	qRT-PCR analysis
HSP70B R	AAGCCTCAGCGACTTCCTTCATCTTCAC	
HSP90.1 F	TTGCGTTGAATCAAAGTTCGTTGC	qRT-PCR analysis
HSP90.1 R	TGTCCTATCATGCTTACATCAGCTCC	
COX5b-1 qPCR F	CGTCGCTGCTTCTCCTCGTCGATCGATAGC	qRT-PCR analysis
COX5b-1 qPCR R	TGTCCAGTCGCAATGGGCATTACATCCTCC	
CCS qPCR F	TGCAGTAGCAGAATTCAAAGGCCCTGACATTTTCG	qRT-PCR analysis
CCS qPCR R	TCCGTTTTTGTCTGCCTCTAGTGTTCCCAGGTC	
CSD1 qPCR F	TGGTAGTTGTGTGTATCTTCTGGTGTGTG	qRT-PCR analysis
CSD1 qPCR R	TGAAAGTACCATATCCAGGACTCTTGTTACC	
CSD2 qPCR F	ATGTCTACTGTGTTGATCTTGTCTG	qRT-PCR analysis
CSD2 qPCR F	ACGCATGATTCATCACAATCTTGAAC	
miR398a qPCR F	AGAAGAAGAGAAGAACAACAGGAGGTG	qRT-PCR analysis
miR398a qPCR R	ATTAGTAAGGTGAAAAAATGGAACAGG-3	
miR398b qPCR F	CATGAAGGTAGTGGATCTCGACAG	qRT-PCR analysis
miR398b qPCR R	GGTAAATGAGTAAAAGCCAGCC	
miR398c qPCR F	TCTCAGCAGATTTGAAGGAT	qRT-PCR analysis
miR398c qPCR R	GGTAAATGAATAGAAGCCACGG	
TUB8 F	ATAACCGTTTCAAATTCTCTCTCTC	qRT-PCR analysis as an internal control
TUB8 R	TGCAAATCGTTCTCTCCTTG	
miR398b Pro F	GGGGACAAGTTTGTACAAAAAAGCAGGCTTCCATGTAACAATTTATCAGCATGGGCCTTC	pMDC164-miR398b
miR398b Pro R	GGGGACCACTTTGTACAAGAAAGCTGGGTCCAACCCTGTCGAGATCCACTACCTTCATG	
miR398c Pro F	GGGGACAAGTTTGTACAAAAAAGCAGGCTTCGATACATTCTCATAGCAGCAACCTGTATA	pMDC164-miR398c
miR398c Pro R	GGGGACCACTTTGTACAAGAAAGCTGGGTCACTACCTTAACAATATTTATCTATC	pMDC164-miR398c
CSD1 m F	GCTCAAGCACTTGATTCTTTCCAAAAGCTTTTCGCGAGGTATGTTTG	For pMDC99-mCSD1 by site-directed mutagenesis
CSD1 m R	CAAAAAGGAAAGCAAACATACCTCGCGAAAAGCTTTTGGAAAGAATC	
CSD1 Pro attB1 F	GGGGACAAGTTTGTACAAAAAAGCAGGCTTCCTGAGATTCAGAGATGGTGAATATC	pMDC99-CSD1
CSD1 attB2 3UTR	GGGGACCACTTTGTACAAGAAAGCTGGGTCCTCATCAAGAAACGTTTCAAATATC	
CSD2 attB1 F	GGGGACAAGTTTGTACAAAAAAGCAGGCTTCCCAAGGTCACGCAAGAGTCTTGCGATC	pMDC99-CSD2
CSD2 attB2 3UTR	GGGGACCACTTTGTACAAGAAAGCTGGGTCTGCTCAATACTACTAGTTTATTTCG	

CSD2 m F	AGATGAGTGCCGTCATGCCGGAGATTTAGGCAATATAAATGCCAATGCCGATGG	For pMDC99-mCSD2 by site-directed mutagenesis
CSD2 m R	GCATTGGCATTTATATTGCCTAAATCTCCGGCATGACGGCACTCATCTTCTGGAGC	
CCS m F	CCATTGGGAGACCTCGGTACCCTAGAGGCAGAC	For pMDC99-mCCS by site-directed mutagenesis
CCS m R	TGTCTGCGTCTGCCTCTAGGGTACCGAGGTCTCC	
CCS1 Pro attB1 F	GGGGACAAGTTTGTACAAAAAAGCAGGCTTCGGAAGTTGTAGAGAAGCTTAAGG	pMDC99-CCS
CCS1 attB2 3UTR	GGGGACCACTTTGTACAAGAAAGCTGGGTCGTTGAACATTGATTAGATACACACAATAT	
HSFA7b attB1 F	GGGGACAAGTTTGTACAAAAAAGCAGGCTGATTCCCCTCGACAGTTAATCACCAGGAAG	HSFA7b-PearleyGate 302
HSFA7b attB2 R	GGGGACCACTTTGTACAAGAAAGCTGGGTCCTAATCTTGCTTCACATTCGCCTCTTCTTC	
HSFA1b attB1 F	GGGGACAAGTTTGTACAAAAAAGCAGGCTTCCACTGTAAGAATGAATTGACTCAGCCTATG	HSFA1b-PearleyGate 302
HSFA1b attB2 R	GGGGACCACTTTGTACAAGAAAGCTGGGTCTTTCCTCTGTGCTTCTGAGGAAAGCAGTC	
HSFA1a attB1 F	GGGGACAAGTTTGTACAAAAAAGCAGGCTTCCTGTACACTTGAACCAGGCCATTCAAGATC	HSFA1a-PearleyGate 302
HSFA1a attB2 R	GGGGACCACTTTGTACAAGAAAGCTGGGTCGTGTTCTGTTTCTGATGTGAGAAGACCCA	
HSF A7a attB1 F	GGGGACAAGTTTGTACAAAAAAGCAGGCTGTGGACCGTGGACCGGTTATTGTTTGCTAG	HSFA7a-PearleyGate 302
HSF A7a attB2 R	GGGGACCACTTTGTACAAGAAAGCTGGGTCGGAGGTGGAAGCCAAACTCTCATCAC	
HSFB2a attB1 F	GGGGACAAGTTTGTACAAAAAAGCAGGCTCACAAGCAGGGAATTGCACTTGGCCGTTC	HSFB2a-PearleyGate 302
HSFB2a attB2 R	GGGGACCACTTTGTACAAGAAAGCTGGGTCATTACAAACTCTCTGATTGGTTCG	HSFB2a-PearleyGate 302
miR398b ChIP A 5'	CAGCATGGGCCTTCATTGTCCGATC	ChIP-qPCR. Amplify region from -2189 to -2073 upstream of stem-loop start site, including *cis* element: gaaggttc.
miR398b ChIP A 3'	CAGAGTTATGGCTCTATGGACTCTC	
miR398b ChIP B 5'	AGGCGTATGCCGCTTGGTACGACAAGCAC	ChIP-qPCR. Amplify region from -679 to -458 upstream of stem-loop start site, including *cis* element: gaattttc.
miR398b ChIP B 3'	CCATATTCTTTGTGACAAAAGAGAGCGCGT	
miR398b ChIP C 5'	AGAATATGGGGACTAGGGACCATAGAG	ChIP-qPCR. Amplify region from -343 to -190 upstream of stem-loop start site, including *cis* element: gaaagttc.
miR398b ChIP C 3'	CTTCGGACATGTGTACTGCAAACTTG	
miR398b ChIP D 5'	GTCATGCTCTTTGCCCTCTAACAAGATAG	ChIP-qPCR. Amplify region from +221 to +363 down-stream of stem-loop start site (no *cis* element included), and serve as negative control.
miR398b ChIP D 3'	GTTCACTCGTCCCGCCGCTCTCCGCCT	
miR169	CCGGCAAGTCATCCTTGGCTG	For small RNA Northern as a probe
miR393	GGATCAATGCGATCCCTTTGGA	
miR398	CAGGGGTGACCTGAGAACACA	
U6	TCATCCTTGCGCAGGGGCCA	
Zm-miR398	CGGGGGCGACCTGAGAACACA	

SPL7 F	CCTCTTGTTAGATATTGCATGGTCGGTG	qRT-PCR analysis
SPL7 R	GAAGCCTCACGTCGCAGTCACAGGTAC	
HSFA1a F	GTGTTACCGGCGGAGGAACGAATATC	qRT-PCR analysis
HSFA1a R	TGTTCGTCGGACTCCATGAGACAATCG	
HSFA1b F	TGAGCAGGAGAATCGTGGTGACAATGTG	qRT-PCR analysis
HSFA1b R	CTCTACTTGAAGGGTTCCCATTGTCTAC	
HSFA7a F	AACCCGTTTCTCCCGGAAGGCTGCGATC	qRT-PCR analysis
HSFA7a R	TGAGAAATTGCTGTGTTTGAAATGACGAGG	
HSFB2a F	GACGCATCAAACAGTTGTTGCTCCTTCGTC	qRT-PCR analysis
HSFB2a R	TCAGTGGGCTGAGATCCGACGTAATTCGAC	

Appendix D1. Genes with Increased Expression Levels in *rsa3-1* under Salt Stress as Determined by Microarray Analysis.

AGI ID	Fold Change	P Value	Description
At2g46600	2.18	0.0032	Calcium-binding EF-hand family protein
At2g47550	2.58	0.0024	Plant invertase/pectin methylesterase inhibitor superfamily
At1g43910	3.69	0.0058	P-loop containing nucleoside triphosphate hydrolases superfamily protein
At3g20470	2.09	0.0100	glycine-rich protein
At4g30430	2.67	0.0021	Member of TETRASPANIN family
At2g43570	2.79	0.0024	chitinase, putative" (CHI)
At2g43620	4.96	0.0006	Chitinase family protein
At3g03640	3.23	0.0015	beta-glucosidase (GLUC)
At3g14620	2.18	0.0082	putative cytochrome P450
At4g25000	2.63	0.0265	alpha-amylase - like protein alpha-amylase
At4g30280	2.66	0.0093	a xyloglucan endotransglucosylase/hydrolase
At5g47330	2.14	0.0050	alpha/beta-Hydrolases superfamily protein
At1g24140	2.04	0.0066	Matrixin family protein
At4g23140	2.41	0.0273	CYSTEINE-RICH RLK (RECEPTOR-LIKE PROTEIN KINASE) 6, CRK6
At4g23220	2.85	0.0126	a cysteine-rich receptor-like protein kinase, CRK14
At5g10760	16.47	0.0001	Eukaryotic aspartyl protease family protein
At5g25440	2.08	0.0097	Protein kinase superfamily protein
At1g15010	2.46	0.0021	unknown protein
At1g21250	12.04	0.0004	cell wall-associated kinase (WAK1)
At1g33960	5.97	0.0002	AIG1, exhibits RPS2- and avrRpt2-dependent induction early after infection with Pseudomonas
At1g67865	2.25	0.0083	unknown protein
At1g74710	2.50	0.0046	a protein with isochorismate synthase activity, isochorismate synthase (icsI)
At2g04450	3.45	0.0066	a protein with NADH pyrophosphatase activity
At2g41100	9.66	0.0001	calmodulin-like protein
At3g50480	2.06	0.0050	Homolog of RPW8
At3g56400	5.61	0.0004	member of WRKY Transcription Factor; Group III
At3g57260	14.01	0.0001	beta-1,3-glucanase 2 (BG2) (PR-2)
At4g02330	3.16	0.0008	a pectin methylesterase
At4g11890	2.49	0.0471	a receptor-like cytosolic kinase ARCK1
At4g12720	2.53	0.0045	a protein with ADP-ribose hydrolase activity.
At5g06320	2.45	0.0052	harpin-induced protein-like
At5g06720	2.05	0.0096	PEROXIDASE 53, with diverse roles in the wound response, flower development, and syncytium formation
At5g10380	4.74	0.0007	a RING finger domain protein with E3 ligase activity
At5g13320	4.94	0.0024	an enzyme capable of conjugating amino acids to 4-substituted benzoates
At5g20230	7.86	0.0021	blue copper binding protein
At5g24530	2.00	0.0109	a putative 2OG-Fe(II) oxygenase that is defense-associated but required for susceptibility to downy mildew.
At5g26920	2.23	0.0429	calmodulin-binding protein CBP60g
At5g55450	3.11	0.0024	Bifunctional inhibitor/lipid-transfer protein/seed storage 2S albumin superfamily protein
At1g13340	2.21	0.0126	Regulator of Vps4 activity in the MVB pathway protein
At1g19610	2.94	0.0096	Predicted to encode a PR (pathogenesis-related) protein
At1g21520	3.89	0.0024	unknown protein
At1g57630	2.48	0.0030	Toll-Interleukin-Resistance (TIR) domain family protein
At5g41740	2.04	0.0109	Disease resistance protein (TIR-NBS-LRR class) family

AGI ID	Fold Change	P Value	Description
At1g35710	2.17	0.0067	Protein kinase family protein with leucine-rich repeat domain
At3g50770	3.26	0.0030	calmodulin-like 41 (CML41)
At2g17040	3.10	0.0008	NNAC transcription factor family, NAC036
At3g22910	7.05	0.0001	calmodulin-stimulated calcium-ATPase E1-E2 type family protein
At5g52750	3.29	0.0018	Heavy metal transport/detoxification superfamily protein
At1g10340	3.20	0.0006	Ankyrin repeat family protein
At1g56060	3.95	0.0020	unknown protein
At1g74440	2.02	0.0058	unknown protein
At1g76960	2.11	0.0101	unknown protein
At2g18690	4.23	0.0004	unknown protein
At2g25510	13.98	0.0004	unknown protein
At2g32190	2.75	0.0282	unknown protein
At2g32210	3.69	0.0050	unknown protein
At3g47480	4.96	0.0007	Calcium-binding EF-hand family protein
At3g56710	2.16	0.0053	SIB1 (SIGMA FACTOR BINDING PROTEIN 1)
At5g03350	4.23	0.0096	Legume lectin family protein
At5g10695	2.05	0.0050	unknown protein
At5g39670	5.20	0.0052	Calcium-binding EF-hand family protein
At5g64870	2.11	0.0170	SPFH/Band 7/PHB domain-containing membrane-associated protein

Appendix D2. Genes with Reduced Expression Levels in *rsa3-1* under Salt Stress as Determined by Microarray Analysis.

AGI ID	Fold Change	P Value	Description
At1g72100	2.38	0.046	late embryogenesis abundant domain-containing protein
At2g36640	2.72	0.031	a putative phosphotyrosine protein belonging to late embryogenesis abundant (LEA) protein in group 3 (AtECP63)
At3g15670	3.30	0.051	Late embryogenesis abundant protein (LEA) family protein
At3g17520	2.65	0.007	Late embryogenesis abundant protein (LEA) family protein
At3g51810	3.31	0.032	embryonic abundant protein AtEm1
At5g44120	2.87	0.001	Encodes a 12S seed storage protein
At5g44310	2.01	0.007	Late embryogenesis abundant protein (LEA) family protein
At1g19530	2.24	0.029	unknown protein
At1g04560	3.04	0.034	AWPM-19-like family protein
At1g05510	2.01	0.018	Unknown protein;tyrosine is phosphorylated and its phosphorylation state is modulated in response to ABA in seeds
At1g48660	2.36	0.021	Auxin-responsive GH3 family protein
At2g47780	3.14	0.002	Rubber elongation factor protein (REF)
At3g01570	4.30	0.018	Oleosin family protein
At3g19920	2.44	0.034	unknown protein
At5g51210	2.83	0.002	oleosin 3, a protein found in oil bodies, involved in seed lipid accumulation
At1g02700	2.97	0.012	unknown protein
At1g27990	2.01	0.048	unknown protein
At1g43800	2.15	0.011	Plant stearoyl-acyl-carrier-protein desaturase family protein
At1g65090	3.78	0.006	unknown protein
At1g68250	2.17	0.025	unknown protein
At2g21820	2.27	0.004	unknown protein
At2g28490	2.35	0.017	RmlC-like cupins superfamily protein, functions in seed storage protein.
At2g28780	2.00	0.024	unknown protein
At1g32900	2.14	0.005	UDP-Glycosyltransferase superfamily protein
At1g48470	3.04	0.001	Encodes cytosolic glutamine synthase isozyme
At3g21370	2.13	0.012	beta glucosidase 19 (BGLU19)
At3g21720	3.85	0.007	Encodes a glyoxylate cycle enzyme isocitrate lyase (ICL)
At3g48700	2.90	0.001	carboxyesterase 13 (CXE13)
At5g01670	2.02	0.048	NAD(P)-linked oxidoreductase superfamily protein
At5g03860	3.96	0.015	malate synthase -like protein
At5g42800	2.08	0.028	dihydroflavonol 4-reductase
At3g20210	4.09	0.006	vacuolar processing enzyme/asparaginyl endopeptidase
At3g54940	2.29	0.013	Papain family cysteine protease
At5g22470	2.29	0.012	NAD+ ADP-ribosyltransferases
At1g32560	3.84	0.025	late-embryogenesis abundant protein, LEA4-1
At1g35310	2.13	0.006	MLP-like protein 168 (MLP168)
At1g48130	2.25	0.005	Similar to antioxidant (1-CYSTEINE PEROXIREDOXIN 1, ATPER1, PER1)
At1g61800	2.67	0.010	glucose-6-phosphate/phosphate-translocator
At2g21490	2.75	0.037	dehydrin LEA (LEA)
At2g35300	3.17	0.007	late embryogenesis abundant protein (LEA18)
At3g50980	2.27	0.011	dehydrin xero 1 (XERO1)
At4g25140	2.26	0.005	oleosin 1, a protein found in oil bodies, involved in seed lipid accumulation
At5g10120	4.00	0.002	Ethylene insensitive 3 family protein
At5g40420	2.06	0.041	Encodes oleosin2, involved in seed lipid accumulation
At5g62490	2.83	0.008	Part of the AtHVA22 family
At5g66400	2.33	0.006	ABA- and drought-induced glycine-rice dehydrin protein, RAB18.
At1g52040	2.96	0.005	Encodes myrosinase-binding protein expressed in flowers

AGI ID	Fold Change	P Value	Description
At2g15010	3.66	0.001	Belongs to the plant thionin (PR-13) family
At3g11050	2.44	0.010	ferritin 2 (FER2); functions in oxidoreductase activity
At5g36910	2.32	0.002	thionin Thi2.2, belongs to the plant thionin (PR-13) family
At1g27470	2.46	0.007	transducin family protein / WD-40 repeat family protein
At1g03790	2.18	0.038	SOMNUS (SOM), a nucleus-localized CCCH-type zinc finger protein
At5g67060	2.30	0.010	sequence-specific DNA binding transcription factor, HECATE 1 (HEC1)
At1g73190	2.25	0.008	ALPHA-TONOPLAST INTRINSIC PROTEIN, TIP3;1; Moves to the Protein Storage Vacuole in a Golgi independent manner
At1g73220	3.06	0.001	organic cation/carnitine transporter1 (1-Oct)
At2g04040	2.16	0.034	detoxifying efflux carrier for plant-derived antibiotics and other toxic compounds, including CD2+(AtDTX1)
At4g16160	2.88	0.009	a member of Arabidopsis OEP16 family
At5g07330	2.25	0.044	unknown protein
At5g66780	4.57	0.008	unknown protein

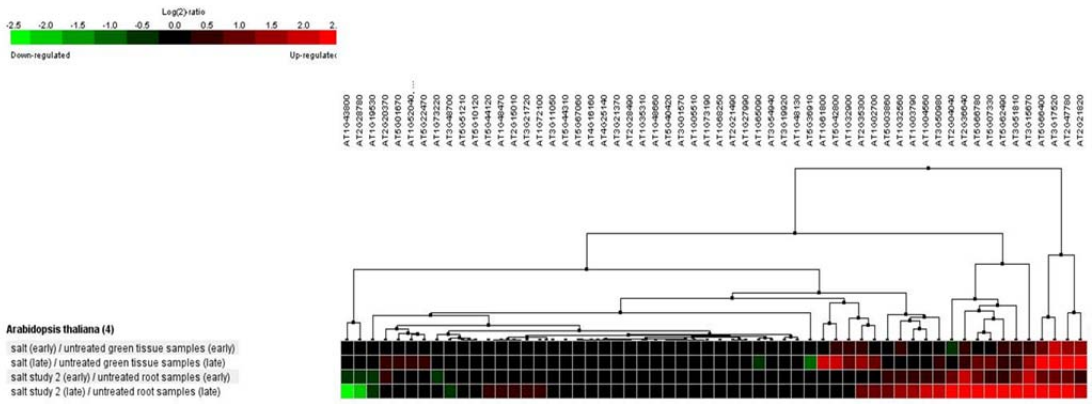

Appendix D3. Hierarchical Clustering Analysis of Genes in Wild Type Plants in Response to Salt Stress treatments Using Publically Available Gene Expression Data, and These Genes Showed Increased Expression in *rsa3-1* by Our Microarray Analysis under Salt Stress. Hierarchical clustering analysis was performed in Genevestigator with Hierarchical Clustering Tool (https://www.genevestigator.com/gv/user/gvLogin.jsp) (Hruz et al., 2008). Scale bar at the top indicates relative expression level (green, repression; red, induction) of a gene compared to non-stressed condition.

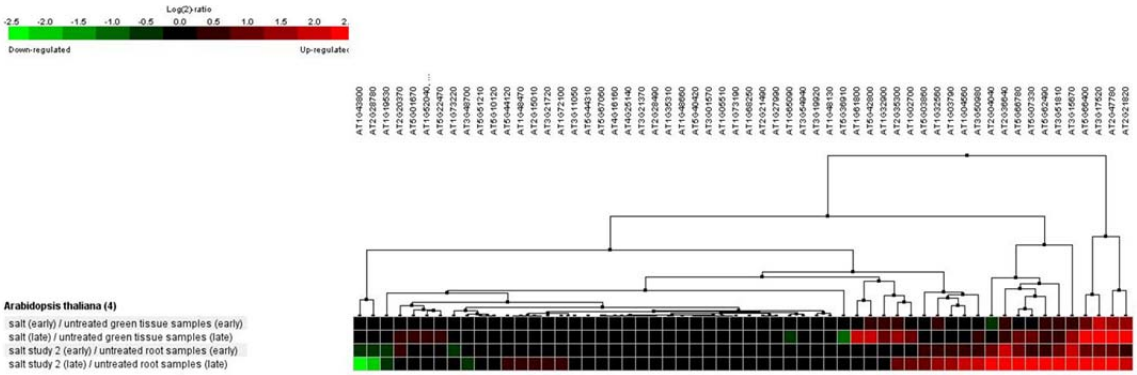

Appendix D4. Hierarchical Clustering Analysis of Genes in Wild Type Plants in Response to salt stress treatments Using Publically Available Gene Expression Data, and These Genes Showed Reduced Expression in *rsa3-1* by Our Microarray Analysis under Salt Stress. Hierarchical clustering analysis was performed in Genevestigator with Hierarchical Clustering Tool

(https://www.genevestigator.com/gv/user/gvLogin.jsp) (Hruz et al., 2008). Scale bar at the top indicates relative expression level (green, repression; red, induction) of a gene compared to non-stressed condition.

Appendix D5. Primers Uused inThis Study.

Primer Name	Primer Sequence (5' to 3')	Purpose
RSA3 G-F	cagtGAGCTCGGACAAACGACGTGACGATA	Construction of pCMBIA1303-RSA3
RSA3 G-R	gtcaGGTACCTTGCTTTGTAGGATGATGGT	
RSA3 P-F	cagtGAATTCGGACAAACGACGTGACGATA	Construction of *RSA3:GUS* in
RSA3 P-R	cagtGTCGACTGTACGAAGATCACAACATC	
RSA3 qPCR F	GTGGGGATACAATATCTCGAGAAGGGATGC	qRT-PCR
RSA3 qPCR R	CCTTTGCTGGGTGGAAGTAGGTTGGGTAC	
At5g10760 qPCR F	TCTCAATTGGTGTTTTGCTGAAGGAGCTG	qRT-PCR
At5g10760 qPCR R	CTTGATCGCGTCTGATGATTTCGTCATG	
At1g21250 qPCR F	GAAATCAGACATGCGAGCAAGTTGGAAGC	qRT-PCR
At1g21250 qPCR R	ATGCAAACTCTTTACGCTTGCAGCTCATAGT	
At5g06720 qPCR F	CAACATTTTACTCTGGGACTTGTCCCAACG	qRT-PCR
At5g06720 qPCR R	AACGTTGAATCCTCTAGCTGAGTTTAC	
At5g66400 qPCR F	TGGCGTCTTACCAGAACCGTCCAGGAG	qRT-PCR
At5g66400 qPCR R	AGCCTTCAGTCCCGGTCCCGGTTCC	
At5g01670 qPCR F	GTCTCAAGCCGCCCACGCCGTTGTC	qRT-PCR
At5g01670 qPCR R	ACTCTCTCAGGAGATAACTCAGTGCACct	
At3g11050 qPCR F	AGTTCTCCGACGATTCTGAATCTGCCATC	qRT-PCR
At3g11050 qPCR R	TGATCAAACTCAGAGACGGGCATC	
At1g32560 qPCR F	GATAAGCGATATGGCTAGTACAGCCAAG	qRT-PCR
At1g32560 qPCR R	CATGATCAGTAACATGGTAGTGAGATTGCT	
At1g48130 qPCR F	TGCGATGGCCAAATACGCTCATGAGTTC	qRT-PCR
At1g48130 qPCR R	ACAATATGAAGGGCACGAGACGGTCCGTTC	
At2g35300 qPCR F	GAAACTCAACATCGGTGGCGCAAAGGCAC	qRT-PCR
At2g35300 qPCR R	CTGTCCCGGCGGGTAATTAGCTCCGGTG	
At5g67060 qPCR F	ACCAACGAACCAGGTTTCCGCTACGGTTC	qRT-PCR
At5g67060 qPCR R	TGAGGATCTTTAGAGATCCTGACGTTC	
TUB8 qPCR-F	ATAACCGTTTCAAATTCTCTCTCTC	qRT-PCR
TUB8 qPCR-R	TGCAAATCGTTCTCTCCTTG	

Bibliography

Agarwal, M., Hao, Y., Kapoor, A., Dong, C.H., Fujii, H., Zheng, X., and Zhu, J.-K. (2006). A R2R3 type MYB transcription factor is involved in the cold regulation of CBF genes and in acquired freezing tolerance. J. Biol. Chem. 281: 37636-37645.

Apel, K., and Hirt, H. (2004). Reactive oxygen species: metabolism, oxidative stress, and signal transduction. Annu. Rev. Plant Biol. 55: 373-399.

Baker, C.C., Sieber, P., Wellmer, F., and Meyerowitz, E.M. (2005). The early extra petals1 mutant uncovers a role for microRNA miR164c in regulating petal number in Arabidopsis. Curr. Biol. 15:303-315.

Baniwal, S.K., Bharti, K., Chan, K.Y., Fauth, M., Ganguli, A., Kotak, S., Mishra, S.K., Nover, L., Port, M., Scharf, K.D., Tripp, J., Weber, C., Zielinski, D., and von Koskull-Döring, P. (2004). Heat stress response in plants: a complex game with chaperones and more than twenty heat stress transcription factors. J Biosci. 29: 471-487.

Bartel, D.P. (2004). MicroRNAs: Genomics, Biogenesis, Mechanism, and Function. Cell 116: 281-297.

Beauclair, L., Yu, A., and Bouché, N. (2010). microRNA-directed cleavage and translational repression of the copper chaperone for superoxide dismutase mRNA in Arabidopsis. Plant J. 62: 454-462.

Bell, C.J., and Ecker, J.R. (1994). Assignment of 30 Microsatellite Loci to the Linkage Map of *Arabidopsis*. Genomics 19: 137–144.

Scherf, U., and Speed, T.P. (2003). Exploration, normalization, and summaries of high density oligonucleotide array probe level data. Biostatistics 4: 249–264.

Ishitani, M., Xiong, L., Lee, H.J., Stevenson, B., and Zhu, J.-K. (1998). HOS1, a genetic locus involved in cold-responsive gene expression in *Arabidopsis*. Plant Cell 10**:** 1151-1161.

Ishitani, M., Xiong, L., Stevenson, B., and Zhu, J.-K. (1997). Genetic analysis of osmotic and cold stress signal transduction in *Arabidopsis thaliana*: Interactions and convergence of abscisic acid-dependent and abscisic acid-independent pathways. Plant Cell 9: 1935-1949.

Jaglo-Ottosen, K.R., Gilmour, S.J., Zarka, D.G., Schabenberger, O., and Thomashow, M.F. (1998). *Arabidopsis* CBF1 overexpression induces COR genes and enhances freezing tolerance. Science 280: 104-106.

Jander, G., Norris, S.R., Rounsley, S.D., Bush, D.F., Levin, I.M., and Last, R.L. (2002). *Arabidopsis* map-based cloning in the post-genome era. Plant Physiol. 129: 440-450.

Jefferson, R.A. (1987). Assaying Chimeric Genes in Plants: The GUS Gene Fusion System. Plant Mol. Biol. Rep. 5: 387-405.

Jefferson, R.A., Kavanagh, T.A., and Bevan, M.W. (1987). GUS fusions: beta-glucuronidase as a sensitive and versatile gene fusion marker in higher plants. EMBO J. 6: 3901-3907.

Jia, X., Wang, W.X., Ren, L., Chen, Q.J., Mendu, V., Willcut, B., Dinkins, R.,

Tang, X., and Tang, G. (2009). Differential and dynamic regulation of miR398 in response to ABA and salt stress in Populus tremula and Arabidopsis thaliana. Plant Mol. Biol. 71: 51-59.

Jiang, Y., and Huang, B. (2001). Drought and heat stress injury to two cool season turfgrasses in relation to antioxidant metabolism and lipid peroxidation. Crop Sci. 41: 436–442.

Jonak, C., O¨ kresz, L., Bo¨gre, L., and Hirt, H. (2002). Complexity, cross talk and integration of plant MAP kinase signaling. Curr. Opin. Plant Biol. 5: 415-424.

Jones-Rhoades, M.J., and Bartel, D.P. (2004). Computational identification of plant microRNAs and their targets, including a stress induced miRNA. Mol. Cell 14: 787-799.

Jones-Rhoades, M.J., Bartel, B., and Bartel, D.P. (2006). MicroRNAs and their regulatory roles in plants. Annu. Rev. Plant Biol. 57**:** 19-53.

Katiyar-Agarwal, S., Zhu, J., Kim, K., Agarwal, M., Fu, X., Huang, A., and Zhu, J.K. (2006). The plasma membrane Na+/H+ antiporter SOS1 interacts with RCD1 and functions in oxidative stress tolerance in Arabidopsis. Proc. Natl. Acad. Sci. U S A. 103:18816-18821.

Khraiwesh, B., Zhu, J.-K., and Zhu, J. (2012). Role of miRNAs and siRNAs in biotic and abiotic stress responses of plants. Biochim. Biophys. Acta 1819: 137-148.

Kilian, J., Whitehead, D., Horak, J., Wanke, D., Weinl, S., Batistic, O., D'Angelo, C., Bornberg-Bauer, E., Kudla, J., and Harter, K. (2007). The AtGenExpress global stress expression data set: protocols, evaluation and model data analysis of UV-B light,

drought and cold stress responses. Plant J. 50: 347-363.

Kim, J.S., Jung, H.J., Lee, H.J., Kim, K.A., Goh, C.H., Woo, Y., Oh, S.H., Han, Y.S., and Kang, H. (2008). Glycine-rich RNA-binding protein7 affects abiotic stress responses by regulating stomata opening and closing in Arabidopsis thaliana. Plant J. 55: 455-466.

Kim, J.Y., Park, S.J., Jang, B., Jung, C.H., Ahn, S.J., Goh, C.H., Cho, K., Han, O., and Kang, H. (2007b). Functional characterization of a glycine-rich RNA-binding protein 2 in Arabidopsis thaliana under abiotic stress conditions. Plant J. 50: 439–451.

Kim, Y.J., Björklund, S., Li, Y., Sayre, M.H., and Kornberg, R.D. (1994). A multiprotein mediator of transcriptional activation and its interaction with the C-terminal repeat domain of RNA polymerase II. Cell 77: 599-608.

Kim, Y.-O., and Kang, H. (2006). The role of a zinc finger-containing glycine-rich RNA-binding protein during the cold adaptation process in *Arabidopsis thaliana*. Plant Cell Physiol. 47: 793-798.

Kim, Y.-O., Kim, J.S., and Kang, H. (2005). Cold-inducible zinc finger-containing glycine-rich RNA-binding protein contributes to the enhancement of freezing tolerance in *Arabidopsis thaliana*. Plant J. 42: 890-900.

Kim, Y.-O., Pan, S., Jung, C.H., and Kang, H. (2007a). A zinc finger-containing glycine-rich RNA-binding protein, atRZ-1a, has a negative impact on seed germination and seedling growth of Arabidopsis thaliana under salt or drought stress conditions. Plant Cell Physiol. 48: 1170-1181.

Kliebenstein, D.J., Monde, R.A., and Last, R.L. (1998). Superoxide dismutase in Arabidopsis: An eclectic enzyme family with disparate regulation and protein localization. Plant Physiol. 118: 637–650.

Knight, H., Mugford, N., Garton, S.G., Ulker, B. Gao, D., Thorlby, G., and Knight, M.R. (2009). Identification of SFR6, a key component in cold acclimation acting posttranslationally on CBF function. Plant J. 58: 97-108.

Konieczny, A. and Ausubel, F.M. (1993). A procedure for mapping Arabidopsis mutations using co-dominant ecotype-specific PCR-based markers. Plant J. 4: 430-410.

Kotak, S., Larkindale, J., Lee, U., von Koskull-Döring, P., Vierling, E., and Scharf, K.D. (2007). Complexity of the heat stress response in plants. Curr. Opin. Plant Biol. 10: 310-316.

Kovtun, Y., Chiu, W.-L., Tena, G., and Sheen J. (2000). Functional analysis of oxidative stress-activated mitogen-activated protein kinase cascade in plants. Proc. Natl. Acad. Sci. USA 97: 2940-2945.

Kwak, K.J., Kim, Y.O., and Kang, H. (2005). Characterization of transgenic Arabidopsis plants overexpressing GR-RBP4 under high salinity, dehydration or cold stress. J. Exp. Bot. 56: 3007-3016.

Lafta, A.M., and Lorenzen, J.H. (1995). Effect of High Temperature on Plant Growth and Carbohydrate Metabolism in Potato. Plant Physiol. 109: 637-643.

Larkindale, J., and Huang, B. (2004). Thermotolerance and antioxidant systems in Agrostis stolonifera: involvement of salicylic acid, abscisic acid, calcium, hydrogen

peroxide, and ethylene. J. Plant Physiol. 161: 405-413.

Larkindale, J., Hall, J.D., Knight, M.R., and Vierling, E. (2005). Heat stress phenotypes of Arabidopsis mutants implicate multiple signaling pathways in the acquisition of thermotolerance. Plant Physiol. 138: 882-897.

Lauter, N., Kampani, A., Carlson, S., Goebel, M., and Moose, S.P. (2005). microRNA172 down-regulates glossy15 to promote vegetative phase change in maize. Proc. Natl. Acad. Sci. USA 102: 9412-9417.

Law, R.D., and Crafts-Brandner, S.J. (1999). Inhibition and acclimation of photosynthesis to heat stress is closely correlated with activation of ribulose-1,5-bisphosphate carboxylase/oxygenase. Plant Physiol. 120: 173–181.

Lee, B.H., Kapoor, A., Zhu, J., and Zhu, J.-K. (2006). STABILIZED1, a stress-upregulated nuclear protein, is required for pre-mRNA splicing, mRNA turnover, and stress tolerance in *Arabidopsis*. Plant Cell 18: 1736-1749.

Lee, B.-H., Lee, H., Xiong, L., and Zhu, J.-K. (2002). A mitochondrial complex I defect impairs cold-regulated nuclear gene expression. Plant Cell 14, 1235-1251.

Lee, H., Xiong, L., Gong, Z., Ishitani, M., Stevenson, B., and Zhu, J.-K. (2001). The *Arabidopsis* HOS1 gene negatively regulates cold signal transduction and encodes a RING finger protein that displays cold-regulated nucleo-cytoplasmic partitioning. Genes Dev. 15: 912-924.

Lee, R.C., Feinbaum, R.L., and Ambros, V. (1993). The C. elegans heterochronic gene lin-4 encodes small RNAs with antisense complementarity to lin-14. Cell 75: 843-

854.

Lee, Y.C., and Kim, Y.J. (1998). Requirement for a functional interaction between mediator components Med6 and Srb4 in RNA polymerase II transcription. Mol Cell Biol. 18: 5364-5370.

Li, R., Yu, C., Li, Y., Lam,T.W., Yiu, S.M., Kristiansen K, and Wang J. (2009). SOAP2: an improved ultrafast tool for short read alignment. Bioinformatics 25: 1966-1967.

Lichtenthaler, H.K., and Wellburn, A.R. (1983). Determinations of total carotenoids and chlorophyll a and b of leaf extracts in different solvents. Biochem. Soc. Trans. 603: 591-592.

Lim, L.P., Glasner, M.E., Yekta, S., Burge, C.B., and Bartel, D.P. (2003). Vertebrate microRNA genes. Science 299: 1540.

Liu, H.C., Liao, H.T., and Charng, Y.Y. (2011). The role of class A1 heat shock factors (HSFA1s) in response to heat and other stresses in Arabidopsis. Plant Cell Environ. 34: 738-751.

Liu, Q., Kasuga, M., Sakuma, Y., Abe, H., Miura, S., Yamaguchi-Shinozaki, K., and Shinozaki, K. (1998). Two transcription factors, DREB1 and DREB2, with an EREBP/AP2 DNA binding domain separate two cellular signal transduction pathways in drought- and low-temperature-responsive gene expression, respectively, in *Arabidopsis*. Plant Cell 10: 1391-1406.

Liu, S.G., Zhu, D.Z., Chen, G.H., Gao, X.Q., and Zhang, X.S. (2012). Disrupted

actin dynamics trigger an increment in the reactive oxygen species levels in the Arabidopsis root under salt stress. Plant Cell Rep. 31: 1219-1226.

Llave, C., Xie, Z., Kasschau, K.D., and Carrington, J.C. (2002). Cleavage of Scarecrow-like mRNA targets directed by a class of Arabidopsis miRNA. Science 297: 2053-2056. (317.15 KB)

Lorković, Z.J. (2009). Role of plant RNA-binding proteins in development, stress response and genome organization. Trends Plant Sci. 14: 229-236.

Lorković, Z.J., and Barta, A. (2002). Genome analysis: RNA recognition motif (RRM) and K homology (KH) domain RNA-binding proteins from the flowering plant Arabidopsis thaliana. Nucleic Acids Res. 30: 623-635.

Madson, M., Dunand, C., Li, X., Verma, R., Vanzin, G.F., Caplan, J., Shoue, D.A., Carpita, N.C. and Riter, W.-D. (2003). The *MUR3* Gene of Arabidopsis Encodes a Xyloglucan Galactosyltransferase That Is Evolutionarily Related to Animal Exostosins. Plant Cell, 15: 1662-1670.

Mahajan, S., Pandey, G.K. and Tuteja, N. (2008). Calcium- and salt-stress signaling in plants: Shedding light on SOS pathway. Arch. Biochem. Biophys, 471:146-158.

Manavella, P.A., Hagmann, J., Ott, F., Laubinger, S., Franz, M., Macek, B., Weigel, D. (2012) Fast-forward genetics identifies plant CPL phosphatases as regulators of miRNA processing factor HYL1. Cell. 151:859-870.

Medina, J., Bargues, M., Terol, J., Perez-Alonso, M., and Salinas, J. (1999). The *Arabidopsis* CBF gene family is composed of three genes encoding AP2 domain-containing proteins whose expression is regulated by low temperature but not by

abscisic acid or dehydration. Plant Physiol. 119**:** 463-470.

Miller, G., and Mittler, R. (2006). Could heat shock transcription factors function as hydrogen peroxide sensors in plants? Ann. Bot. 98: 279-288.

Mishra, S.K., Tripp, J., Winkelhaus, S., Tschiersch, B., Theres, K., Nover, L., and Scharf, K.D. (2002). In the complex family of heat stress transcription factors, HsfA1 has a unique role as master regulator of thermotolerance in tomato. Genes Dev. 16: 1555-1567.

Mizoguchi, T., Wheatley, K., Hanzawa, Y., Wright, L., Mizoguchi, M., Song, H.R., Carré, I.A., and Coupland, G. (2002). LHY and CCA1 are partially redundant genes required to maintain circadian rhythms in *Arabidopsis*. Dev. Cell 2: 629–641.

Mockler, T.C., Yu, X., Shalitin, D., Parikh, D., Michael, T.P., Liou, J., Huang, J., Smith, Z., Alonso, J.M., Ecker, J.R., Chory, and J., Lin, C. (2004). Regulation of flowering time in Arabidopsis by K homology domain proteins. Proc. Natl. Acad Sci. USA. 101: 2759-2764.

Møller, I.M., Jensen, P.E., and Hansson, A. (2007). Oxidative modifications to cellular components in plants. Annu. Rev. Plant Biol. 58: 459-481.

Murashige, T., and Skoog, F. (1962). A revised medium for rapid growth and bioassays with tobacco tissue cultures. Physiol. Plant. 15: 473-497.

Nadimpalli, R., **Yalpani, N., Johal, G.S., and Simmons, C.R.** (2000). Prohibitins, stomatins, and plant disease response genes compose a protein superfamily that controls cell proliferation, ion channel regulation, and death. J. Biol. Chem. 275:

29579-29586.

Nakamichi, N., Kusano, M., Fukushima, A., Kita, M., Ito, S., Yamashino, T., Saito, K., Sakakibara, H., and Mizuno, T. (2009). Transcript profiling of an *Arabidopsis* PSEUDO RESPONSE REGULATOR arrhythmic triple mutant reveals a role for the circadian clock in cold stress response. Plant Cell Physiol. 50: 447-462.

Nanda, A.K., Andrio, E., Marino, D., Pauly, N., and Dunand, C. (2010). Reactive oxygen species during plant-microorganism early interactions. J. Integr. Plant Biol. 52: 195-204.

Nicol, J.W., Helt, G.A., Blanchard, S.G. Jr, Raja, A., and Loraine, A.E. (2009). The Integrated Genome Browser: free software for distribution and exploration of genome-scale datasets. Bioinformatics 25: 2730-2731.

Nishizawa-Yokoi, A., Nosaka, R., Hayashi, H., Tainaka, H., Maruta, T., Tamoi, M., Ikeda, M., Ohme-Takagi, M., Yoshimura, K., Yabuta, Y., and Shigeoka, S. (2011). HsfA1d and HsfA1e involved in the transcriptional regulation of HsfA2 function as key regulators for the Hsf signaling network in response to environmental stress. Plant Cell Physiol. 52: 933-945.

Nover, L., Bharti, K., Doring, P., Mishra, S.K., Ganguli, A. and Scharf, K.D. (2001). *Arabidopsis* and the heat stress transcription factor world: How many heat stress transcription factors do we need? Cell Stress Chaperones 6: 177-189.

Novillo, F., Alonso, J.M., Ecker, J.R., and Salinas, J. (2004). CBF2/DREB1C is a negative regulator of CBF1/DREB1B and CBF3/DREB1A expression and plays a central role in stress tolerance in *Arabidopsis*. Proc. Natl. Acad. Sci. USA 101: 3985-

3990.

Novillo, F., Medina, J., and Salinas, J. (2007). *Arabidopsis* CBF1 and CBF3 have a different function than CBF2 in cold acclimation and define different gene classes in the CBF regulon. Proc. Natl. Acad. Sci. USA 104: 21002-21007.

O'Neill, M.A., Eberhard, S., Albersheim, P., and Drvill, A.G. (2001). Requirement of Borate Cross-Linking of Cell Wall Rhamnogalacturonan II for *Arabidopsis* Growth. Science 294: 846-849.

Örvar, B.L., Sangwan, V., Omann, F., and Dhindsa, R.S. (2000). Early steps in cold sensing by plant cells: the role of actin cytoskeleton and membrane fluidity. Plant J. **23**,785-794.

Palatnik, J.F., Allen, E., Wu, X., Schommer, C., Schwab, R., Carrington, J.C., and Weigel, D. (2003). Control of leaf morphogenesis by microRNAs. Nature 425: 257-263.

Palva, E.T., Welin, B., Vahala, T., Olson, A., Nordin-Henriksson, K., Mantyla, E., and Lang, V. (1994). Regulation of low temperature-induced genes during cold acclimation of *Arabidopsis thaliana*. in Biochemical and Cellular Mechanisms of Stress Tolerance in Plants (eds. JH Cherry) pp. 527-542. Springer-Verlag, Berlin, Germany.

Peña, M.J., Ryden, P., Madson, M., Smith, A.C. and Carpita, N.C. (2004). The Galactose Residues of Xyloglucan Are Essential to Maintain Mechanical Strength of the Primary Cell Walls in Arabidopsis during Growth. Plant Physiol. 134: 443-451.

Pleskot, R., Potocký, M., Pejchar, P., Linek, J., Bezvoda, R., Martinec, J.,

Valentová, O., Novotná, Z., and Žárský, V. (2010). Mutual regulation of plant phospholipase D and the actin cytoskeleton. Plant J. 62: 494-507.

Qiu, Q.S., Guo, Y., Quintero, F.J., Pardo, J.M., Schumaker, K.S., and Zhu, J.-K. (2004). Regulation of vacuolar Na^+/H^+ exchange in Arabidopsis thaliana by the salt-overly-sensitive (SOS) pathway. J. Biol. Chem. 279: 207-215.

Rasmussen, I., Pedersen, L.H., Byg, L., Suzuki, K., Sumimoto, H., and Vilhardt, F. (2010). Effects of F/G-actin ratio and actin turn-over rate on NADPH oxidase activity in microglia. BMC Immunol. 11: 44.

Reinhart, B.J., Weinstein, E.G., Rhoades, M.W., Bartel, B., and Bartel, D.P. (2002). MicroRNAs in plants. Genes Dev. 16: 1616-1626.

Reyes, J..L, and Chua, N.H. (2007). ABA induction of miR159 controls transcript levels of two MYB factors during Arabidopsis seed germination. Plant J. 49: 592-606.

Rhoades, M.W., Reinhart, B.J., Lim, L.P., Burge, C.B., Bartel, B., and Bartel, D.P. (2002). Prediction of plant microRNA targets. Cell 110: 513-20.

Ripoll, J.J., Rodríguez-Cazorla, E., González-Reig, S., Andújar, A., Alonso-Cantabrana, H., Perez-Amador, M.A., Carbonell, J., Martínez-Laborda, A., and Vera, A. (2006). PEPPER, a novel K-homology domain gene, regulates vegetative and gynoecium development in Arabidopsis. Dev. Biol. 289: 346-359.

Ristic, Z., and Ashworth, E.N. (1993). Changes in leaf ultrastructure and carbohydrates in *Arabidopsis thaliana* (*Heynh*) *cv. Columbia* during rapid cold acclimation. Protoplasma 172: 111-123.

Rivera-Milla, E., Stuermer, C.A.O., and Málaga-Trillo, E. (2006). Ancient origin of reggie (flotillin), reggie-like, and other lipid-raft proteins: convergent evolution of the SPFH domain. Cell Mol. Life Sci. 63: 343-357.

Rizhsky, L., Liang, H., and Mittler, R. (2003). The Water-Water Cycle Is Essential for Chloroplast Protection in the Absence of Stress. J. Biol. Chem. 278: 38921-38925.

Rocak, S., and Linder, P. (2004). DEAD-box proteins: the driving forces behind RNA metabolism. Nat. Rev. Mol. Cell Biol. 5: 232-241.

Ruelland, E.V.M., Zachowski, A., and Vaughn, H. (2009). Cold signaling and cold acclimation in plants. Adv. Bot. Res. 49: 36-54.

Sakuma, Y., Maruyama, K., Qin, F., Osakabe, Y., Shinozaki, K., and Yamaguchi-Shinozaki, K. (2006). Dual function of an Arabidopsis transcription factor DREB2A in water-stress-responsive and heat-stress-responsive gene expression. Proc. Natl. Acad. Sci. USA. 103: 18822-18827.

Savin, R., and Nicolas, M.E. (1996). Effects of short periods of drought and high temperature on grain growth and starch accumulation of two malting barley cultivars. *J.* Plant Physiol. 23: 201–210.

Schaffer, R., Ramsay, N., Samach, A., Corden, S., Putterill, J., Carré, I.A., and Coupland, G. (1998). The late elongated hypocotyl mutation of *Arabidopsis* disrupts circadian rhythms and the photoperiodic control of flowering. Cell 93: 1219–1229.

Schramm, F., Larkindale, J., Kiehlmann, E., Ganguli, A., Englich, G., Vierling, E., and von Koskull-Döring, P. (2008). A cascade of transcription factor DREB2A and

heat stress transcription factor HsfA3 regulates the heat stress response of Arabidopsis. Plant J. 53: 264-274.

Shi, Y., Tian, S., Hou, L., Huang, X., Zhang, X., Guo, H., and Yang, S. (2012). Ethylene Signaling Negatively Regulates Freezing Tolerance by Repressing Expression of CBF and Type-A ARR Genes in *Arabidopsis*. Plant Cell. 24: 2578-2595.

Shoji, T., Suzuki, K., Abe, T, Kaneko, Y., Shi, H., Zhu, J.-K., Rus, A., Hasegawa, P.M., and Hashimoto, T. (2006). Salt stress affects cortical microtubule organization and helical growth in Arabidopsis. Plant Cell Physiol. 47: 1158-1168.

Stockinger, E.J., Gilmour, S.J., and Thomashow, M.F. (1997). *Arabidopsis thaliana CBF1* encodes an AP2 domain-containing transcriptional activator that binds to the C-repeat/DRE, a cis-acting DNA regulatory element that stimulates transcription in response to low temperature and water deficit. Proc. Natl. Acad. Sci. USA 94: 1035-1040.

Sukumaran, N.P., and Weiser, C.J. (1972). An excised leaflet test for evaluation potato frost tolerance. Hort. Science 7: 467-468.

Sunkar, R., and Zhu, J.-K. (2004). Novel and stress-regulated microRNAs and other small RNAs from Arabidopsis. Plant Cell 16: 2001-2019.

Sunkar, R., Kapoor, A., and Zhu, J.-K. (2006). Posttranscriptional induction of two Cu/Zn superoxide dismutase genes in Arabidopsis is mediated by downregulation of miR398 and important for oxidative stress tolerance. Plant Cell 18, 2051-2065.

Sunkar, R., Chinnusamy, V., Zhu, J., and Zhu, J.-K. (2007). Small RNAs as big

players in plant abiotic stress responses and nutrient deprivation. Trends Plant Sci. 12:301-309.

Tamura, K., Shimada, T., Kondo, M., Nishimura, M. and Hara-Nishimura, I. (2005). KATAMARI1/MURUS3 Is a Novel Golgi Membrane Protein That Is Required for Endomembrane Organization in *Arabidopsis*. Plant Cell, 17: 1764-1776.

Tamura, K., Takahashi, H., Kunieda, T., Fuji, K., Shimada, T. and Hara-Nishimura, I. (2007). *Arabidopsis* KAM2/GRV2 Is Required for Proper Endosome Formation and Functions in Vacuolar Sorting and Determination of the Embryo Growth Axis. Plant cell, 19: 320-332.

Tavernarakis, N., Driscoll, M., and Kyrpides, N.C. (1999). The SPFH domain: implicated in regulating targeted protein turnover in stomatins and other membrane-associated proteins. Trends Biochem. Sci. 24: 425-427.

Thomashow, M.F. (1994). Arabidopsis thaliana as a model for studying mechanisms of plant cold tolerance. in *Arabidopsis* (eds. EM Meyerowitz and CR Somerville), pp. 807-834. Cold Spring Harbor Laboratory Press, Cold Spring Harbor, NY.

Thomashow, M.F. (1999). Plant cold acclimation: freezing tolerance genes and regulatory mechanisms. Annu. Rev. Plant Physiol. Plant Mol. Biol. 50: 571-599.

Thomashow, M.F. (2000). Molecular basis of plant cold acclimation: insights gained from studying the CBF cold response pathway. Plant Physiol. 154:571-577.

Trent, J.D. (1996). A review of acquired thermotolerance, heat-shockproteins and molecular chaperones in Archaea. Fems Microbiol.Rev. 18: 249-258.

Trindade, I., Capitão, C., Dalmay, T., Fevereiro, M.P., and Santos, D.M. (2010). miR398 and miR408 are up-regulated in response to water deficit in Medicago truncatula. Planta 231: 705-716.

Tusher, V.G., Tibshirani, R., and Chu, G. (2001). Significance analysis of microarrays applied to the ionizing radiation response. Proc. Natl. Acad. Sci. USA 98: 5116-5121.

Tuteja, N. (2007). Abscisic Acid and Abiotic Stress Signaling. Plant Signal. Behav. 2: 135-138.

Vacca, R.A., de Pinto, M.C., Valenti, D., Passarella, S., Marra, E., and De Gara, L. (2004). Production of reactive oxygen species, alteration of cytosolic ascorbate peroxidase, and impairment of mitochondrial metabolism are early events in heat shock induced programmed cell death in tobacco bright-yellow 2 cells. Plant Physiol. 134: 1100-1112.

Vandenabeele, S., Van Der Kelen, K., Dat, J., Gadjev, I., Boonefaes, T., Morsa, S., Rottiers, P., Slooten, L., Van Montagu, M., Zabeau, M., Inze, D., Van Breusegem, F. (2003). A comprehensive analysis of hydrogen peroxide-induced gene expression in tobacco. Proc. Natl. Acad. Sci. USA 100: 16113-16118.

Vierling, E. (1991). The role of heat shock proteins in plants. Annu.Rev. Plant Physiol. Plant Mol. Biol. 42: 579-620.

Vogel, J.T., Zarka, D.G., Van Buskirk, H.A., Fowler, S.G., and Thomashow, M.F. (2005). Roles of the CBF2 and ZAT12 transcription factors in configuring the low

temperature transcriptome of *Arabidopsis*. Plant J. 41: 195-211.

Voinnet, O., Rivas, S., Mestre, P., and Baulcombe, D. (2003). An enhanced transient expression system in plants based on suppression of gene silencing by the p19 protein of tomato bushy stunt virus. Plant J. 33: 949-956.

Volkov, R.A., Panchuk, I.I., Mullineaux, P.M., and Schöffl, F. (2006). Heat stress-induced H_2O_2 is required for effective expression of heat shock genes in Arabidopsis. Plant Mol. Biol. 61: 733-746.

Wang, C., Zhang, L., Yuan, M., Ge, Y., Liu, Y., Fan, J., Ruan, Y., Cui, Z., Tong, S., and Zhang S. (2010). The microfilament cytoskeleton plays a vital role in salt and osmotic stress tolerance in Arabidopsis. Plant Biol. 12: 70-78.

Wang, X. (2002). Phospholipase D in hormonal and stress signaling. Curr. Opin. Plant Biol. 5: 408-414.

Wang, X., Devaiah, S.P., Zhang, W. and Welti, R. (2006). Signaling functions of phosphatidic acid. Prog. Lipid Res. 45: 250-278.

Wang, X., Zhu, L., Liu, B., Wang, C., Jin, L., Zhao, Q., Yuan, M. (2007). Arabidopsis MICROTUBULE-ASSOCIATED PROTEIN18 functions in directional cell growth by destabilizing cortical microtubules. Plant Cell 19: 877-889.

Wang, Z., and Huang, B. (2004). Physiological recovery of Kentucky bluegrass from simultaneous drought and heat stress. Crop Sci. 44: 1729–1736.

Wang, Z.Y, and Tobin, E.M. (1998). Constitutive expression of the CIRCADIAN CLOCK ASSOCIATED 1 (CCA1) gene disrupts circadian rhythms and suppresses its

own expression. Cell 93: 1207–1217.

Warren, G., McKown, R., Marin, A., and Teutonico, R. (1996). Isolation of mutations affecting the development of freezing tolerance in *Arabidopsis thaliana* (*L.*) *Heynh.* Plant Physiol. 111: 1011-1019.

Wasteneys, G.O., and Yang, Z. (2004) New views on the plant cytoskeleton. Plant Physiol. 136: 3884-3891.

Winder, S.J. and Ayscough, K.R. (2005). Actin-binding proteins. J. Cell Sci. 118: 651-654.

Wu, S.-J., Ding, L. and Zhu, J.-K. (1996). *SOS1*, a Genetic Locus Essential for Salt Tolerance and Potassium Acquisition. Plant Cell 8: 617-627.

Xin, Z., and Browse, J. (1998). *eskimo1* mutants of *Arabidopsis* are constitutively freezing-tolerant. Proc. Natl. Acad. Sci. USA **95:** 7799-7804.

Xiong, L., Ishitani, M., Lee, H., and Zhu, J.-K. (2001). The *Arabidopsis LOS5/ABA3* locus encodes a molybdenum cofactor sulfurase and modulates cold stress– and osmotic stress–responsive gene expression. Plant Cell **13:** 2063-2083.

Yamaguchi-Shinozaki, K., and Shinozaki, K. (1994). A novel cis-acting element in an *Arabidopsis* gene is involved in responsiveness to drought, low-temperature, or high-salt stress. Plant Cell **6:** 251-264.

Yamasaki, H., Abdel-Ghany, S.E., Cohu, C.M., Kobayashi, Y., Shikanai, T., and Pilon, M. (2007). Regulation of Copper Homeostasis by Micro-RNA in *Arabidopsis.* J. Biol. Chem. 282: 16369-16378.

Yamasaki, H., Hayashi, M., Fukazawa, M., Kobayashi, Y., and Shikanai, T. (2009). SQUAMOSA Promoter Binding Protein-Like7 Is a Central Regulator for Copper homeostasis in Arabidopsis. Plant Cell 21: 347-361.

Yang, L., Wu, G., and Poethig, R.S. (2012). Mutations in the GW-repeat protein SUO reveal a developmental function for microRNA-mediated translational repression in Arabidopsis. Proc. Natl. Acad. Sci. USA 109: 315-320.

Yoshida, T., Ohama, N., Nakajima, J., Kidokoro, S., Mizoi, J., Nakashima, K., Maruyama, K., Kim, J.M., Seki, M., Todaka, D., Osakabe, Y., Sakuma, Y., Schöffl, F., Shinozaki, K., and Yamaguchi-Shinozaki, K. (2011). Arabidopsis HsfA1 transcription factors function as the main positive regulators in heat shock-responsive gene expression. Mol. Genet. Genomics 286: 321-332.

Yu, B., and Wang, H. (2010). Translational inhibition by microRNAs in plants. Prog. Mol. Subcell. Biol. 50: 41-57.

Yu, X., Wang, H., Lu, Y., de Ruiter, M., Cariaso, M., Prins, M., van Tunen, A., and He, Y. (2012). Identification of conserved and novel microRNAs that are responsive to heat stress in Brassica rapa. J. Exp. Bot. 63: 1025-1038.

Zhang, W., Zhou, R.G., Gao, Y.J., Zheng, S.Z., Xu, P., Zhang, S.Q., and Sun, D.Y. (2009). Molecular and genetic evidence for the key role of AtCaM3 in heat-shock signal transduction in Arabidopsis. Plant Physiol. 149: 1773-1784.

Zhang, X., **Chen, Y., Wang, Z.-Y., Chen, Z., Gu, H., and Qu, L.-J.** (2007). Constitutive expression of CIR1 (REV2) affects several circadian-regulated processes

and seed germination in *Arabidopsis*. Plant J. 51: 512-525.

Zhou, G.K., Kubo, M., Zhong, R., Demura, T., and Ye, Z.H. (2007). Overexpression of miR165 affects apical meristem formation, organ polarity establishment and vascular development in Arabidopsis. Plant Cell Physiol. 48: 391-404.

Zhu, J., Dong, C.H., and Zhu, J.- K.(2007). Interplay between cold-responsive gene regulation, metabolism and RNA processing during plant cold acclimation. Curr Opin Plant Biol. 10:290-295.

Zhu, J., Gong, Z., Zhang, C., Song, C.-P., Damsz, B., Inan, G., Koiwa, H., Zhu, J.-K., Hasegawa, P.M, and Bressan, R.A. (2002). OSM1/SYP61: A syntaxin protein in Arabidopsis controls abscisic acid–mediated and non-abscisic acid–mediated responses to abiotic stress. Plant Cell 14: 3009-3028.

Zhu, J., Jeong, J.C., Zhu, Y., Sokolchik, I., Miyazaki, S., Zhu, J.-K., Hasegawa, P.M., Bohnert, H.J., Shi, H., Yun, D.J., and Bressan, R.A. (2008). Involvement of *Arabidopsis* HOS15 in histone deacetylation and cold tolerance. Proc. Natl. Acad. Sci. USA 105: 4945-4950.

Zhu, J., Lee, B.-H., Dellinger, M., Cui, X., Zhang, C., Wu, S., Nothnagel, E.A., and Zhu, J.-K. (2010). A cellulose synthase-like protein is required for osmotic stress tolerance in *Arabidopsis*. Plant J. 63: 128-140.

Zhu, J., Shi, H., Lee, B.H., Damsz, B., Cheng, S., Stirm, V., Zhu, J.-K, Hasegawa, P.M., and Bressan, R.A. (2004). An *Arabidopsis* homeodomain transcription factor gene, HOS9, mediates cold tolerance through a CBF-independent pathway. Proc. Natl.

Acad. Sci. USA 101: 9873-9878.

Zhu, J.-K. (2003). Regulation of ion homeostasis under salt stress. Curr. Opin. Plant Biol. 6: 441-445.

Zhu, J.-K. (2010). A cellulose synthase-like protein is required for osmotic stress tolerance in *Arabidopsis*. Plant J. 63: 128-140.